

The Role of Bacterial Peptide Transporters in Intrinsic  
Resistance to Beta-lactam Antibiotics

Max Stafford

MSc (by research)

University of York

Biology

May 2023

## Abstract

Bacteria utilise peptides for a variety of biological functions. For bacteria to acquire peptides from the extracellular environment, they must pass the normally impermeable plasma membrane. For this purpose, a series of peptide transport proteins have evolved which facilitate the uptake of peptides into the cytoplasm. Despite peptide uptake being their primary function, peptide transporters have also been shown to facilitate the uptake of various drug molecules. One example is the beta-lactam antibiotics, the transport of which can be rationalised due to the presence of a peptide bond within their structure. The beta-lactam antibiotics exert their effect through binding to penicillin-binding proteins found within the periplasmic space, therefore the ability of peptide transporters to translocate beta-lactam antibiotics from the periplasmic space into the cytoplasm (and thus outside of their site of action) may contribute to the basal level of resistance to these drugs – a novel and previously untested hypothesis. These initial results described in this study document the creation by previous lab members of two mutant *E. coli* strains (known as  $\Delta$ DB1 or  $\Delta$ DB50) which lack either of the two peptide transporter classes present in *E. coli* (ABC and POT respectively). The comprehensive account of the creation of these strains, combined with confirmation of their genotype conducted in this work, allows these strains to now be used to investigate the role of these peptide transporters. To examine the role of peptide transporters in antibiotic resistance, growth of  $\Delta$ DB50 was compared with that of wild type *E. coli* in the presence of various beta-lactam antibiotics with differing structural modifications. This revealed a consistently higher susceptibility in the mutant strain, an observation which was not present when exposed to antibiotics lacking a peptide bond, revealing a previously undescribed mechanism of antibiotic resistance. Phylogenetic analysis performed in this study demonstrates that POT transporters have significant diversity and are widely distributed across pathogenic bacterial species against which antibiotics are primarily used. Meanwhile, growth comparisons of  $\Delta$ DB1 and  $\Delta$ DB50 in the presence of aminoglycoside antibiotics revealed increased resistance in  $\Delta$ DB1 but not  $\Delta$ DB50, demonstrating a difference in antibiotic affinity of the two transporter types. Toxic peptide assays also revealed differences in transport specificity between the two classes depending on the stereoisomerism of the oligopeptide. The findings of this study therefore highlight the importance of understanding peptide transport in pathogenic bacteria and provide a potential insight into the nature of *E. coli* resistance to antibiotics which could be used to inform future strategies to combat this growing threat, alongside revealing additional differences in the transport specificities of peptide transporter classes.

## Table of Contents

<b>Abstract</b> .....	<b>2</b>
<b>Table of Contents</b> .....	<b>3</b>
<b>List of Figures</b> .....	<b>5</b>
<b>List of Tables</b> .....	<b>7</b>
<b>Authors Declaration:</b> .....	<b>8</b>
<b>1 Introduction</b> .....	<b>9</b>
<b>1.1 Bacterial metabolism and nutrition</b> .....	<b>9</b>
<b>1.2 Molecular transport in bacteria</b> .....	<b>10</b>
1.2.1 Secondary active transporters .....	11
1.2.2 Group Translocation .....	12
1.2.3 ABC Transport Systems.....	12
1.2.4 Peptide Transport.....	13
<b>1.3 Proton Dependent Oligopeptide Transporters (POTs)</b> .....	<b>15</b>
1.3.1 Structure.....	15
1.3.2 Mechanism of Action .....	15
<b>1.4 Peptide Specific ATP-binding Cassette (ABC) Transporters</b> .....	<b>17</b>
1.4.1 Structure.....	17
1.4.2 Mechanism of Action .....	18
<b>1.5 <math>\beta</math>-lactam antibiotics</b> .....	<b>20</b>
1.5.1 Structure and Classification.....	20
1.5.2 Mechanism of Action .....	21
1.5.3 Resistance.....	24
<b>1.6 Illicit Drug Transport</b> .....	<b>25</b>
1.6.1 B-lactam antibiotics.....	25
1.6.2 Illicit transport of non- $\beta$ -lactam antibiotics .....	25
<b>1.7 Intrinsic Resistance Hypothesis</b> .....	<b>26</b>
<b>1.8 Project Background: Generation of <math>\Delta</math>DB1 and <math>\Delta</math>DB50</b> .....	<b>28</b>
<b>1.9 Project Aims</b> .....	<b>33</b>
<b>2 Materials and Methods</b> .....	<b>34</b>
<b>2.1 Chemicals and Strains</b> .....	<b>34</b>
2.1.1 Antibiotics.....	34
2.1.2 Bacterial Strains and Plasmids .....	35
2.1.3 Oligonucleotide Primers.....	36
2.1.4 Bacterial Growth Media .....	37
2.1.5 Amino Acids and Peptides.....	39
<b>2.2 Molecular and Biochemical Techniques</b> .....	<b>40</b>
2.2.1 Genomic DNA Isolation .....	40
2.2.2 Plasmid Mini Prep .....	40
2.2.3 Polymerase Chain Reaction (PCR) .....	40
2.2.4 Agarose gel electrophoresis .....	41
2.2.5 Generation of Knockout Strains (Dr Daniel Bawdon & Emmanuele Severi) .....	41
2.2.6 Preparation of competent <i>E. coli</i> cells.....	42

2.2.7	Transformation of competent <i>E. coli</i> with plasmid DNA.....	42
<b>2.3</b>	<b>Microbiological Techniques .....</b>	<b>42</b>
2.3.1	Bacterial growth .....	42
2.3.2	Antibiotic Susceptibility Experiments.....	43
2.3.3	Analysis of Growth Phenotype .....	44
2.3.4	Toxic Peptide Inhibition Assays .....	46
<b>2.4</b>	<b>Bioinformatics .....</b>	<b>47</b>
<b>3</b>	<b>Results.....</b>	<b>48</b>
<b>3.1</b>	<b>Antibiotic susceptibility experiments .....</b>	<b>48</b>
3.1.1	Growth comparison of $\Delta$ DB50 wild type <i>E. coli</i> in LB.....	48
3.1.2	Comparison of wild type <i>E. coli</i> and $\Delta$ DB50 susceptibility to Ampicillin.....	49
3.1.3	Comparison of wild type <i>E. coli</i> and $\Delta$ DB50 susceptibility to Amoxicillin .....	53
3.1.4	Comparison of wild type <i>E. coli</i> and $\Delta$ DB50 susceptibility to Carbenicillin.....	54
3.1.5	Comparison of wild type <i>E. coli</i> and $\Delta$ DB50 susceptibility to Cefalexin and Cefadroxil.....	56
<b>3.2</b>	<b>Comparison of wild type <i>E. coli</i> and <math>\Delta</math>DB50 susceptibility to Kanamycin.....</b>	<b>59</b>
3.2.1	Growth comparison of $\Delta$ DB51 and wild type <i>E. coli</i> in LB.....	61
3.2.2	Comparison of wild type <i>E. coli</i> and $\Delta$ DB50/ $\Delta$ DB1 susceptibility to Blastocidin S and Kasugamycin.....	62
<b>3.3</b>	<b>Toxic Peptide Inhibition Assay .....</b>	<b>65</b>
3.3.1	Dr Daniel Bawdon's Thesis Results.....	66
3.3.2	Wild Type <i>E. coli</i> .....	69
3.3.3	$\Delta$ DB50 and $\Delta$ DB5 .....	71
3.3.4	$\Delta$ DB1.....	74
3.3.5	$\Delta$ dppC and $\Delta$ oppC.....	76
<b>3.4</b>	<b>Phylogenetic Analysis of POT transporters in pathogenic bacteria.....</b>	<b>78</b>
<b>4</b>	<b>Discussion:.....</b>	<b>82</b>
<b>4.1</b>	<b>Creation of <math>\Delta</math>DB5: .....</b>	<b>82</b>
<b>4.2</b>	<b>Antibiotic Susceptibility Comparison .....</b>	<b>83</b>
4.2.1	Growth comparisons in the absence of antibiotic: .....	83
4.2.2	Susceptibility to penam beta-lactam antibiotics:.....	85
4.2.3	Susceptibility to cephalosporin beta-lactam antibiotics:.....	87
4.2.4	Non-specific transport of antibiotics:.....	87
4.2.5	Susceptibility to aminoglycoside antibiotics: .....	88
4.2.6	Implications for antibiotic resistance: .....	89
4.2.7	Limitations:.....	90
<b>4.3</b>	<b>Determination of peptide transporter specificities: .....</b>	<b>91</b>
<b>4.4</b>	<b>Phylogenetic analysis: .....</b>	<b>93</b>
<b>5</b>	<b>Conclusion .....</b>	<b>96</b>
<b>6</b>	<b>Supplementary Information .....</b>	<b>97</b>
6.1	Supplementary Methods:.....	97
6.2	Supplementary Data: .....	99
<b>7</b>	<b>References .....</b>	<b>109</b>

## List of Figures

<b>Figure 1.1</b> – The structure and formation of a peptide bond. ....	6
<b>Figure 1.2</b> - Mechanism of simple transporter proteins. ...	10
<b>Figure 1.3</b> - Mechanism of the phosphotransferase system of <i>E. coli</i> . ....	11
<b>Figure 1.4</b> - Mechanism of ABC transporters (in a Gram-negative bacterium). .	12
<b>Figure 1.5</b> – Alternating access mechanism of POT transporters. ....	15
<b>Figure 1.6</b> – The basic structure of a bacterial ABC transporter (in a gram-negative bacterium). ....	17
<b>Figure 1.7</b> - Figure 1.7– Mechanism of action of an ABC importer.....	18
<b>Figure 1.8</b> – Molecule structure of (A) 7-aminopenicillanic acid, (B) 7-aminocephalosporanic acid. ....	20
<b>Figure 1.9</b> – Peptide bond within the $\beta$ -lactam ring.. ....	20
<b>Figure 1.10</b> – Mechanism of $\beta$ -lactam antibiotic action.. ....	22
<b>Figure 1.11</b> – Structure of non- $\beta$ -lactam antibiotics implicated in illicit drug transport. ....	25
<b>Figure 1.12</b> – Schematic diagram of the intrinsic resistance hypothesis.....	26
<b>Figure 1.13</b> – Generation of $\Delta$ DB1 .....	27
<b>Figure 1.14</b> – Generation of $\Delta$ DB5. ....	28
<b>Figure 1.15</b> – Diagnostic PCR for $\Delta$ DB5.....	29
<b>Figure 1.16</b> – Alternative $\Delta$ DB5 clones.. ....	30
<b>Figure 1.17</b> – Diagnostic PCR for $\Delta$ DB50.....	31
<b>Figure 1.18</b> – Full lineage of $\Delta$ DB50.. ....	31
<b>Figure 3.1</b> – Comparison of POT deletion mutants and wild type <i>E. coli</i> growth dynamics in LB. ....	48
<b>Figure 3.2</b> – Growth comparison in ampicillin.. ....	50
<b>Figure 3.3</b> – Growth comparison in amoxicillin. ....	52
<b>Figure 3.4</b> – Growth comparison in carbenicillin. ....	54
<b>Figure 3.5</b> – Growth phenotype comparison in cefalexin or cefadroxil.. ....	56
<b>Figure 3.6</b> – Growth comparison in kanamycin. ....	59
<b>Figure 3.7</b> – Growth dynamics of $\Delta$ DB1 and wild type <i>E. coli</i> . ....	60
<b>Figure 3.8</b> – Growth phenotype comparison of $\Delta$ DB50 and $\Delta$ DB1 in kasugamycin and blasticidin S. ....	63
<b>Figure 3.9</b> – Toxic peptide inhibition assay performed by Dr Daniel Bawdon. ....	66
<b>Figure 3.10</b> - Toxic peptide inhibition assay (wild type <i>E. coli</i> ). ....	69

<b>Figure 3.11</b> – Toxic peptide inhibition assay ( $\Delta$ DB5 and $\Delta$ DB50). .....	72
<b>Figure 3.12</b> - Toxic peptide inhibition assay ( $\Delta$ DB1). .....	74
<b>Figure 3.13</b> – Toxic peptide inhibition assay ( $\Delta$ DB5 and $\Delta$ DB50). .....	77
<b>Figure 3.14</b> – Phylogenetic tree displaying the relationship between POT transporters present in a selection pathogenic bacterial species.....	79
<b>Figure 3.15</b> – Number of putative POT transporters identified in the genomes of the bacteria included in the phylogenetic analysis (supplementary table 1).....	81
<b>Supplementary Figure 1</b> – Growth comparison in 2.5 $\mu$ g/ml carbenicillin. ....	103
<b>Supplementary Figure 2</b> – Growth comparison in 12.5 $\mu$ g/ml amoxicillin. ....	104
<b>Supplementary Figure 3</b> – Growth comparison in 12.5 $\mu$ g/ml cephalexin. ....	105
<b>Supplementary Figure 4</b> – Growth comparison in kanamycin.....	106
<b>Supplementary Figure 5</b> – Growth comparison in $\Delta$ DB50 and wild type <i>E. coli</i> in Kasugamycin and Blastidicin S. ....	107
<b>Supplementary Figure 6</b> – Growth comparison in $\Delta$ DB1 and wild type <i>E. coli</i> in Kasugamycin and Blastidicin S. ....	108

## List of Tables

<b>Table 2.1</b> – Antibiotics used in this work.....	33
<b>Table 2.2</b> – Bacterial strains used in this work. ....	34
<b>Table 2.3</b> – Plasmids used within this work. ....	35
<b>Table 2.4</b> – Oligonucleotide primers used within this work. ....	35
<b>Table 2.5</b> - Table 2.5 – Suppliers of media components used in this work.....	37
<b>Table 2.6</b> – $\Delta$ DB50 genotyping PCR cycling parameters. ....	38
<b>Table 2.7</b> – Concentrations of antibiotics tested.. ....	42
<b>Table 2.8</b> - Amino Acids and Peptides Used in the Toxic Peptide Inhibition Assay.....	39
<b>Supplementary Table 1</b> – Pathogenic bacterial species examined for their POT complement. ....	97-98
<b>Supplementary Table 2</b> – POT transporter proteins identified from TransportDB.....	99-101

## Authors Declaration:

*I declare that this thesis is a presentation of original work and I am the sole author. This work has not previously been presented for an award at this, or any other, University. All sources are acknowledged as References.*

Max Stafford



# 1 Introduction

## 1.1 Bacterial metabolism and nutrition

Bacterial cells are made up of various macronutrients, all of which are required in differing quantities. Carbon makes up 50% of the cells dry weight, followed by oxygen and hydrogen (both 25%) and finally nitrogen (13%). In addition to these, the remainder of the cells weight is made up of various essential elements present in much smaller quantities (>5%) such as phosphorous, sulphur, potassium, and magnesium along with several trace elements known as micronutrients. These macronutrients are used to produce essential macromolecules such as proteins, nucleic acids, lipids, and polysaccharides. These compounds are made up of amino acids, nucleotides, fatty acids and sugars respectively.

In order to survive and grow the bacteria must therefore acquire these various macronutrients. Carbon can be acquired from the breakdown of monomeric compounds (such as sugars), which can be acquired by direct uptake or from the breakdown of the polymeric compounds they make up (such as polysaccharides). Meanwhile, nitrogen can be acquired directly from the environment (primarily in the form of ammonia –  $\text{NH}_3$ ) or alternatively from organic sources such as peptides, which again can be taken up directly or acquired from the breakdown of existing macromolecules (such as proteins).

The production and subsequent breakdown of these macromolecules occurs through a series of biochemical reactions catalysed by enzymes, the sum of which within the cell is known as metabolism. One primary function of bacterial metabolism is to generate the energy required for these biochemical reactions. This is stored in the form of chemical energy, which is conserved through the formation of high energy compounds such as adenosine diphosphate (ADP) and adenosine triphosphate (ATP). These compounds contain a high energy phosphate bond, which in the presence of certain enzymes can be broken to release the required energy to drive biochemical reactions (Peter Jurtshuk 1996).

The enzymes which both drive the breakdown of ATP, and later utilise the energy released to catalyse chemical reactions are made up of proteins. Proteins are made up of individual peptides which are linked via peptide bonds (Figure 1.1), in a polymer known as a polypeptide. Peptides which consist of two amino acids are known as dipeptides, with three they are known as a tripeptide and with upwards of three they are known as oligopeptides. A molecule containing between two and fifty amino acids is said to be a peptide, whereas molecules more than fifty amino acid residues are classed as a protein (Sato, A.K. et al. 2006). Depending on the amino acid residues which make up the peptide, the polypeptide (and thus protein) formed will have different properties. When combined with further folding processes and post-translational modifications, a core series of 20 amino acids can form the peptides required to generate a diverse range of proteins with differing functions (Boyle 2005). In addition to acting as the building blocks for proteins, peptides can also act directly as a source of both carbon and nitrogen, alongside as an energy source through breakdown into their amino acid constituents which can be directly fermented.

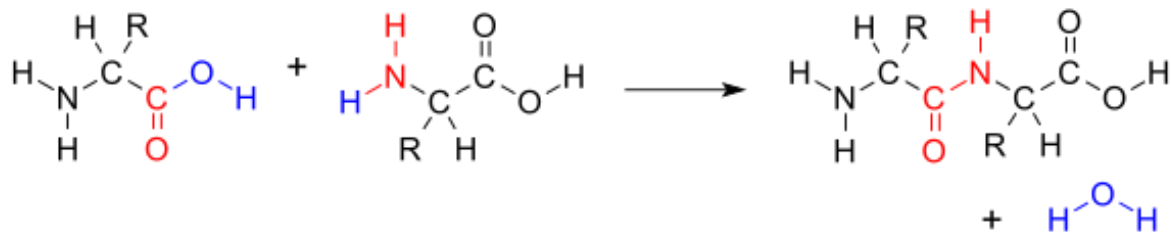


**Figure 1.1** – The structure and formation of a peptide bond. The (amide) bond is formed through a dehydration condensation reaction. Groups which are maintained within the bond are shown in red, groups which are lost (in the form of a water molecule) are shown in blue.

Peptides therefore play a central role in all aspects of bacterial growth and metabolism, and thus bacteria have developed the ability acquire peptides from various sources. One such source is the breakdown of existing proteins orchestrated by the use of peptidase enzymes, which catalyse the process of proteolysis. Proteases can be found within the cell, orchestrating the catabolism of old proteins, but can also be secreted into the extracellular environment, allowing individual peptides to be released and subsequently taken up into the cell.

Peptides play an important role in the virulence of pathogens which inhabit the human intestine. For example, bacteria of the genus *Vibrio* which encompasses many human pathogens (such as *Vibrio cholerae*) are known to utilise extracellular peptidases to obtain peptides from the environment (Miyoshi, S.-I. and Ceccarelli 2013). A second bacterial species which can inhabit the human gut is *Escherichia coli*. Despite not excreting extracellular peptidases, *E. coli* is able to exploit the high availability of peptides within the intestine, present as a result of human peptidases with a role in digestion and subsequent amino acid absorption (Chalova et al. 2009). The success *E. coli* finds in this environmental niche has been exploited in laboratory settings in the development of Lysogeny Broth (LB) media, which contains a large number of peptides (alongside other required micronutrients) and provides conditions in which rapid growth of *E. coli* can occur (Sezonov, Joseleau-Petit and D’Ari 2007).

## 1.2 Molecular transport in bacteria

As discussed in section 1.1.1, it is essential for the bacterial cell to acquire a range of molecules from their environment, this requires the cell to continuously import substances into the cell. In order to do this, these substances must pass through the normally impermeable cytoplasmic membrane, which serves as a barrier to solute leakage into or out of the cell. To overcome this, several transport systems have evolved which reside in the cytoplasmic membrane and facilitate the translocation of solutes through various mechanisms.

The process by which solutes are translocated against their concentration gradient (for example from the extracellular environment into the cytoplasm) is known as active transport. This mechanism of transport is inherently endergonic, requiring the energy from a

high energy molecule such as ATP, or alternatively from an electrochemical gradient such as the proton motive force (PMF).

The basic structure of membrane transporters consists of a polypeptide of multi-spanning domains which weave through the inner membrane, forming a channel through which the solute can pass. This process is usually linked to conformational changes within the transmembrane protein, initiated by solute binding, which results in the movement of the solute across the membrane into the cytoplasm (Madigan et al. 2017).

### 1.2.1 Secondary active transporters

The most basic form of membrane transporters are known as secondary active transporters, in which the energy required for transport is provided by the proton motive force (PMF). PMF refers to the force which promotes the movement of protons downwards along an electrochemical gradient, providing a source of potential energy which can drive solute translocation (Montville and Bruno 1994). The transport event can be considered a symport reaction (in which the solute and proton are co-transported in the same direction) or an antiport reaction (in which the solute and proton are co-transported in opposite directions).

Two well studied examples of simple transporters include the sodium-proton antiporter system (Beck and Rosen 1979), and the lactose permease symporter of *Escherichia coli* (Figure 1.2).

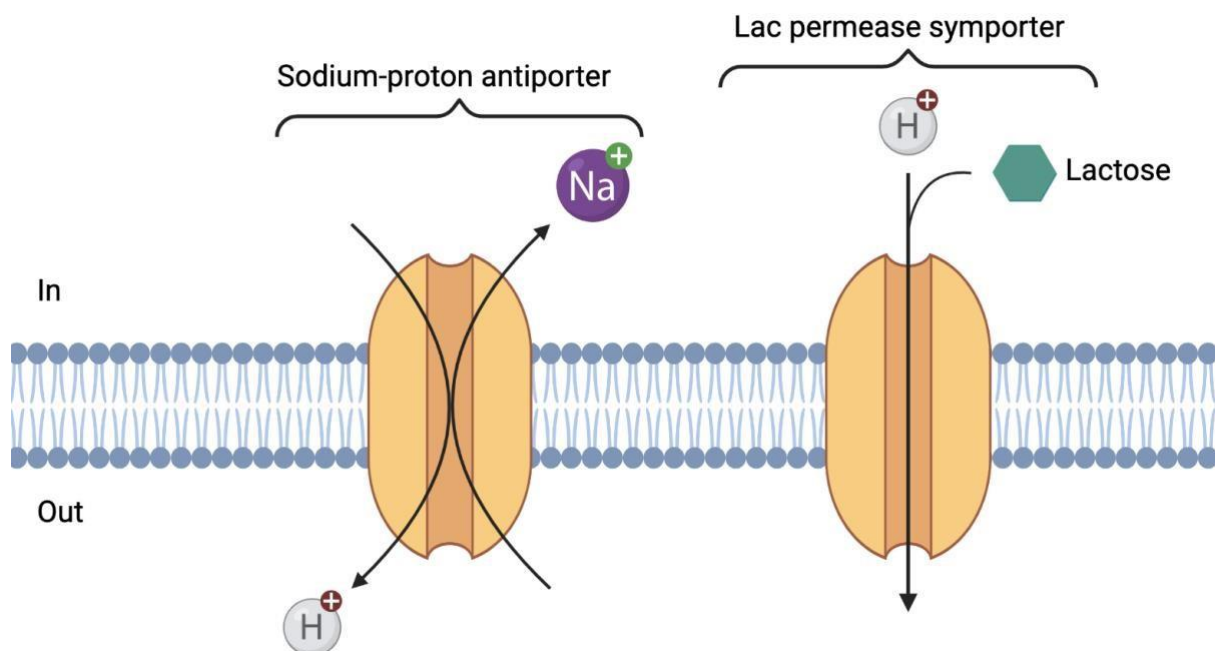


**Figure 1.2** - Mechanism of simple transporter proteins. Shown here are examples of both an antiport (sodium-proton antiporter) and a symport (lac permease) transport event. The oval shape represents a protein made up of 12 transmembrane  $\alpha$ -helices that form a membrane channel (simplified). In both cases, the energy required for transport is provided by coupling with the movement of a proton, utilising the proton motive force to facilitate transport.

### 1.2.2 Group Translocation

A second series of membrane transporters are known to employ a “group translocation” system. This mechanism utilises an energy rich organic molecule (rather than the PMF) to drive translocation across the membrane and characteristically involves modification to the chemical structure of the substrate during transport.

The best studied example is the sugar phosphotransferase system in bacteria (Figure 1.3). Before sugar translocation occurs, the proteins in the phosphotransferase system undergo alternate phosphorylation and dephosphorylation, culminating in the phosphorylation of the transported sugar as it enters the cytoplasm through the transport channel (chemical modification). The energy required to initiate the phosphorylation cascade is provided by the breakdown of phosphoenolpyruvate into pyruvate, releasing the required phosphate group (Erni 1992; Jeckelmann and Erni 2019). The specific components of the system differ between bacterial species and the sugar transported, but the core mechanism remains the same.

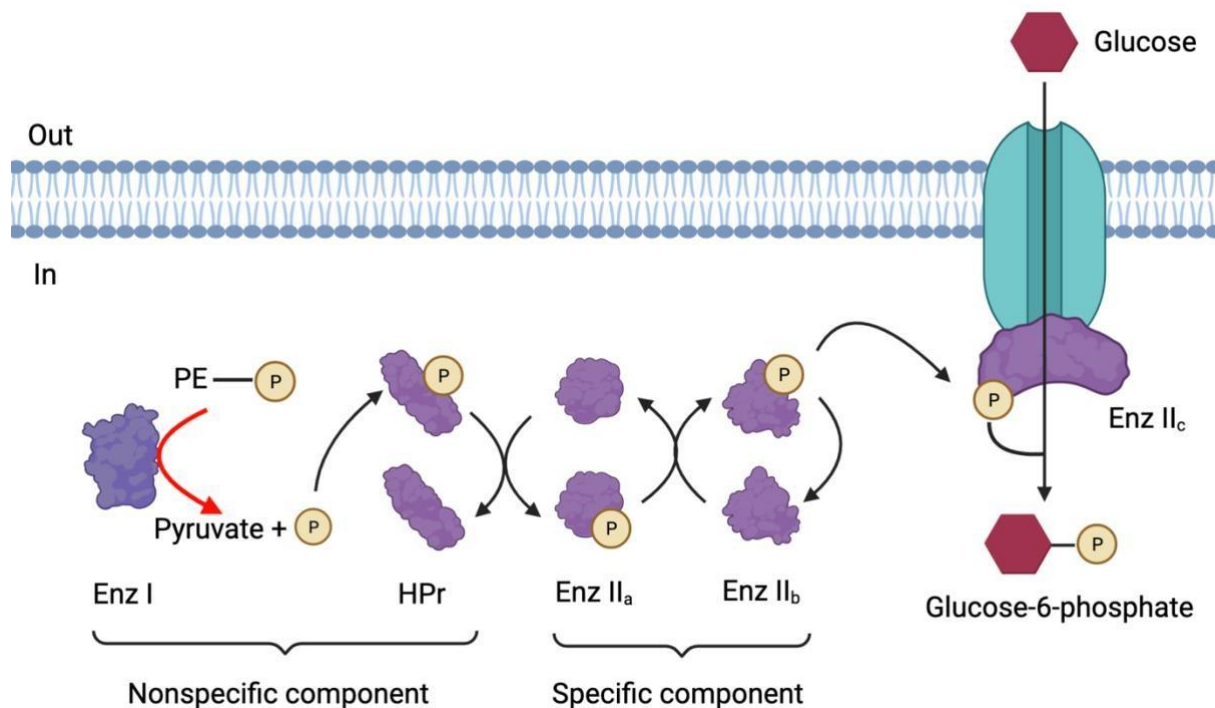


**Figure 1.3** - Mechanism of the phosphotransferase system of *E. coli*. In the example glucose transport, the system utilises 5 proteins: *Enz I*, *Enz II<sub>a</sub>*, *Enz II<sub>b</sub>*, and *Enz II<sub>c</sub>*, and *HPr*. A phosphate cascade is initiated using the energy provided from the breakdown of phosphoenolpyruvate (PE-P) into pyruvate and a free phosphate group, and culminates in the phosphorylation of glucose by *Enz II<sub>c</sub>* (chemical modification). Proteins *HPr* and *Enz I* are nonspecific and participate in the transport of any sugar, while the three components of *Enz II* are specific for a particular sugar.

### 1.2.3 ABC Transport Systems

The final type of transporters are known as “ABC” transporters – with the term ABC referring to an “ATP-binding cassette”. These transporters are extremely diverse, transporting a wide range of organic and inorganic substances within both prokaryotes and eukaryotes. Alongside the core transport channel, ABC transporters employ a periplasmic binding protein together with a transmembrane ATP-hydrolysing domain.

In gram-negative bacteria, the function of the periplasmic binding proteins is to bind to the transport substrate within the periplasmic space (which lies between the outer and cytoplasmic membrane). Once the substrate is bound, the binding protein interacts with the transmembrane domain of the transporter, after which translocation is driven by the binding and later hydrolysis of ATP to ADP (Figure 1.4).

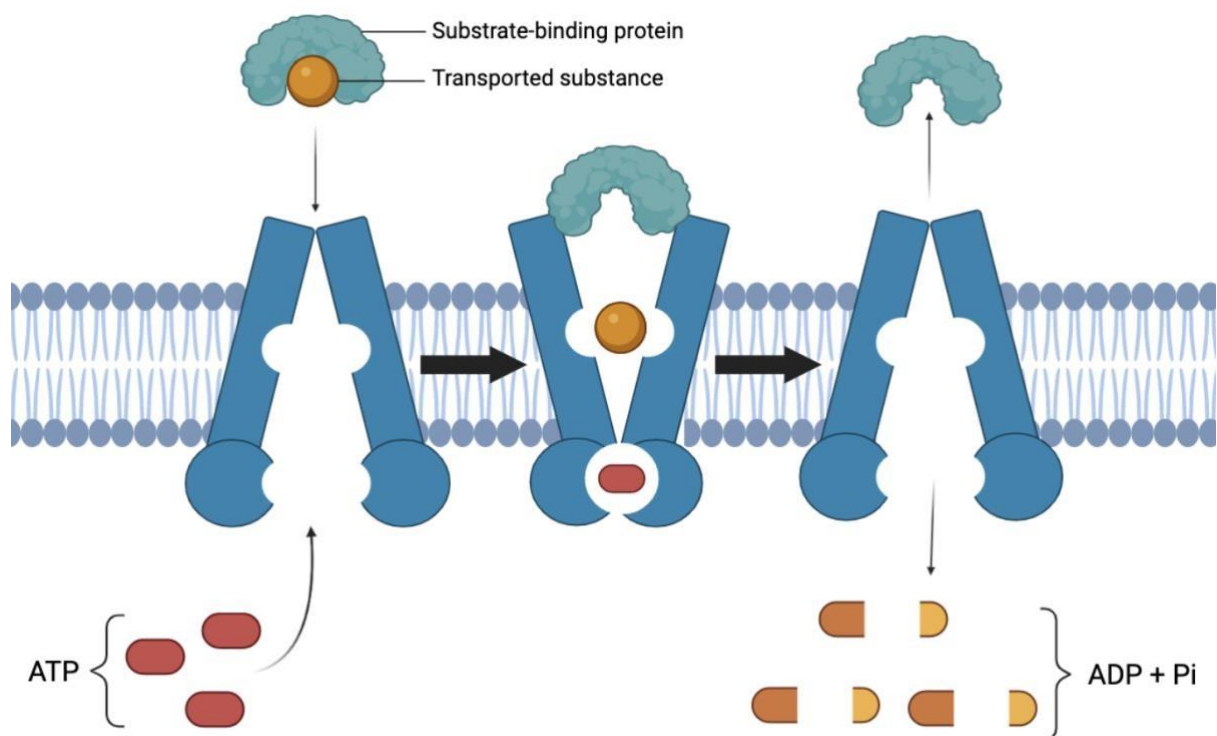


**Figure 1.4 - Mechanism of ABC transporters (in a gram-negative bacterium).** The substrate binding protein binds to the transport substrate, allowing for translocation of the transport substrate across the membrane using energy released from ATP hydrolysis by the ATP hydrolysis protein. Simplified ABC transporter structure is shown.

In gram-positive bacteria which lack a periplasm, the periplasmic binding protein is replaced with a functionally equivalent substrate binding protein, which is attached to the external surface of the cytoplasmic membrane. After binding is achieved, transport can occur through an identical mechanism. For clarity, the term “substrate-binding protein” is now used to describe the component both gram-positive and gram-negative bacteria.

#### 1.2.4 Peptide Transport

As discussed in section 1.1.2, peptides play a central role in bacterial metabolism, acting as both a potential energy source, and as a potential source of nitrogen or amino acids. However, the peptides must first be broken down into their individual amino acid residues. Whilst extracellular peptidases are known to exist, alongside several amino acid transporters, it is more energetically favourable to transport a single peptide into the cell, rather than multiple amino acids individually (Piperno et al., 1968; Nguyen et al., 2019). These peptides can then be digested into their amino acid substituents within the cytoplasm and used to generate new proteins or used in respiration directly as an energy source following deamination (Fernández and Zúñiga 2006). Alternatively, the imported peptides may be left intact and used as signalling molecules in various contexts (Sturme et al., 2002; Thoendel and Horswill, 2010; Verbeke et al., 2017). It is therefore essential for bacteria to have the ability to transport peptides through the cell membrane into the cytoplasm, this is achieved through the activity of a class of membrane proteins known as peptide transporters. Peptide transporters are located within the plasma membrane of gram-positive bacteria, and the cytoplasmic membrane of gram-negative bacteria - allowing peptides to be obtained from the environment or periplasm respectively.

The success of *E. coli* in the human intestine is in part due to the large number of available peptides found in the environment, thus it is of particular importance for this species to be able to uptake peptides (section 1.1). Since its discovery in 1884, *E. coli* rapidly rose to prominence within the field of microbiology, due to factors such as its ubiquitous nature and ease of cultivation - leading to *E. coli* being considered a “model organism” (Blount 2015). In *E. coli*, peptide transporters come in two forms, one of which is proton driven (Proton-dependent oligopeptide transporter: POT) as discussed in section 1.2.1 and another which is driven by the hydrolysis of ATP (ABC transporters) as described in section 1.2.3 (Steiner et al., 1995; Detmers et al., 2001).

The field of ABC transporter research in *E. coli* emerged in the 1970s, with the characterisation of a new type of substrate-binding protein (SBP)-dependent transport system energized directly by hydrolysis of ATP. Two of the early ABC transporters studied were the peptide specific systems Dpp and Opp (referring to a di- and oligo- peptide permease respectively) (Berger and Heppel, 1974). The first POT transporter was not identified until 1995, as a distinct class of peptide transport proteins with a different mode of action to the ABCs with a specificity for di- and tripeptides (Steiner et al., 1995). For many years the majority of POT transporter research focussed on the human PEPT1 transporter, which is responsible for peptide absorption in the intestine, until an equivalent gene was identified in *E. coli* through homology with the *Salmonella enterica* serovar Typhimurium *tppB* gene – this gene was termed *ygdR* (Goh et al., 2004). *ygdR* was initially studied in isolation, until analysis of the full genome sequence of *E. coli* revealed the existence of three additional POT transporters within the *E. coli* genome, termed *yhiP*, *yjdL* and *ybgH* (Blattner et al. 1997; Harder et al. 2008; Ernst et al. 2009; Zhao, Y. et al. 2014). The nomenclature of these genes was later standardised to reflect their function as di- and tripeptide permeases (dtp). Under this classification *ygdR* was renamed *dtpA*, *yhiP* to *dtpB*, *yjdL* to *dtpC* and *ybgH* to *dtpD* (Harder 2008).



Our understanding of the biology of *E. coli* has been aided significantly by the development of the KEIO collection - a library of single-gene deletions of non-essential genes within *E. coli*. This collection includes strains with single gene deletions amongst both the individual POT transporters, and subunits of the ABC transporters, providing an invaluable resource in studying the biology of peptide transport (Baba, T. et al. 2006).

### 1.3 Proton Dependent Oligopeptide Transporters (POTs)

The POT transporters, also known as the PTR (peptide transporter) family, are a family of secondary active transporter proteins found across both prokaryotes and eukaryotes (Daniel et al. 2006). The POTs are members of the Major Facilitator Superfamily (MFS), transporting solutes across the membrane using energy provided from an electrochemical proton gradient (section 1.2.1) (Pao et al., 1998). The primary substrate of the POT transporters is peptides, whilst they have also been reported to transport a range of drugs including antibiotics (Newstead 2011).

#### 1.3.1 Structure

As described in section 1.2.1, peptides are molecules made up of individual amino acids. There are 20 different amino acids, all with different individual chemical structures, thus there is a wide range of possible peptide structures. It is estimated that over 8000 di/tripeptides are recognised as ligands by the POT transporters (Ito et al. 2013), all whilst using a single mechanism of transport. To maintain such a high level of polyspecificity, whilst operating within the limitations of existing proton coupling machinery, a sophisticated structure has evolved.

The POT transporters as members of the MFS superfamily are integral membrane proteins consisting of twelve transmembrane helices, which fold into two distinct bundles of 6 domains, to form a V-shaped structure within the membrane. The two bundles are connected exclusively through side chain interactions between the domains, without any crossing over of the backbone chain. The POT transporters operate through an “alternating access mechanism”, during which the substrate binds to an exposed ligand binding site within the V-shape to facilitate transport, access to which is controlled by various “gating” helices. The mechanism also requires the binding and release of protons, this is facilitated through the interaction of salt bridges located at either end of the transmembrane domains, which enable the various conformational changes required for this process (Solcan et al. 2012; Doki et al. 2013).

#### 1.3.2 Mechanism of Action

Secondary active transporters utilise the energy stored in a secondary ion gradient across the membrane to drive the translocation of a ligand. With regards to the POT transporters, protons provide the electrochemical gradient required, through the inward flow of ions into the cytoplasm. To fulfil the function of the transporter, this process must result in the

transport of peptides across the membrane – this is explained through the aforementioned “alternating access” model.

As previously described (section 1.3.1), the POT structure is arranged in a V-shape, with a ligand binding site located within. This site can change orientation, based on the surrounding domains, to face the outside of the membrane (outward facing) or inside of the membrane (inward facing). The model begins with the transporter in the outward facing direction, in which the binding site is open to the outside of the cell allowing peptides and protons to bind within the structure. The transporter then undergoes a conformational change to wrap around the peptide and proton, forming an “occluded” state which prevents the release of the ligand. During this process, the bound proton moves from the extracellular salt bridge (on the outer membrane side) to the intracellular salt bridge (on the inner membrane side). This causes the disruption of the intracellular salt bridge interaction, causing the gate to open and release the proton and peptide from the binding site which is now facing the inside of the cell. The loss of the proton allows the intracellular salt bridge to reform, causing the transporter to return to the outward facing state (Solcan et al. 2012; Newstead 2017a, 2017c)(Figure 1.5).

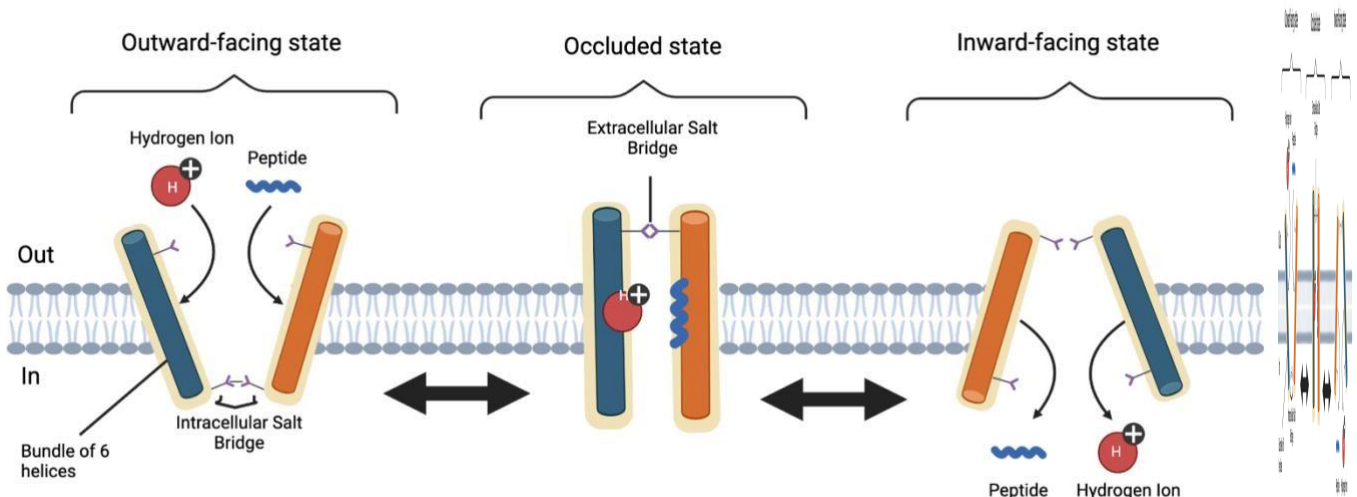


**Figure 1.5 – Alternating access mechanism of POT transporters.** Cylinders represent a simplified representation of the POT transporter domains, made up of six transmembrane helices each. The proton motive force is directed from the outside of the membrane to the inside of the membrane, which also represents the direction of transport. The initial sequence moves from left to right, after the transport event is complete the transporter then returns to the outward facing state through an occluded state intermediate.

In order to transport a diverse range of possible substrates, whilst remaining specific for di- and tripeptides the POT transporters require a sophisticated mechanism of peptide recognition. This was originally thought to be achieved exclusively through interactions between the wider binding site structure and the amino and carboxy termini of the substrate (Meredith, D. et al. 2000; Newstead et al. 2011). However, crystal structures of bacterial POT transporters in complex with peptides revealed the importance of regions within the binding site which allow a diverse range of peptides to be accommodated



(Guettou et al., 2014; Lyons et al., 2014). This led to the identification of distinct regions within the binding site including a polar pocket, a hydrophobic pocket and an acidic patch. Depending on the side chains present within the amino acids which make up the peptide, different regions will be involved in the interaction with the peptide substrate (Newstead, 2017). Electrostatic interactions between the peptide and these regions allow for the orientation of the peptide, and a later clamping movement which holds the peptide within the pocket as transport commences (Boggavarapu et al. 2015).

## 1.4 Peptide Specific ATP-binding Cassette (ABC) Transporters

ABC transporters are integral membrane proteins that actively transport substances across the membrane against a concentration gradient, providing either an import or an export function. The full substrate range of the ABCs is extremely diverse, with individual ABCs able to transport a wide range of substrates such as ions, sugars, and amino acids alongside those which transport peptides (Moussatova et al. 2008). This diversity is maintained within the *E. coli* genome, with the ABCs forming the largest transporter family, making up 5% of the total genome content (Moussatova et al. 2008). Whilst the function of peptide transport is shared with the POT transporters, the mechanism of action is entirely different, utilising the energy released from ATP hydrolysis rather than the PMF (Jones, P.M. and George 2002).

### 1.4.1 Structure

Despite their varied substrate specificities, all ABC transporters share a common basic structure.

ABC transporters are made up of two integral membrane proteins known as transmembrane domains (TMDs). These domains form the transport channel the substrate passes through and are formed from several membrane-spanning  $\alpha$ -helices which vary in number depending on the direction of transport (Locher 2004). The  $\alpha$ -helices are arranged to form a transmembrane pore which the transport substrate passes through. Depending on the orientation of the transporter, this pore can be either accessible from the cytoplasm (inward facing) or the outside of the cell (outward facing). Each of the TMDs are associated with a nucleotide binding domain (NBD). These domains are highly conserved within the ABC family and contain the Walker A and B motifs which are characteristic of all ATP-binding proteins, along with a signature motif which is specific to the ABC transporter family (Kerr 2002) (Figure 1.6).

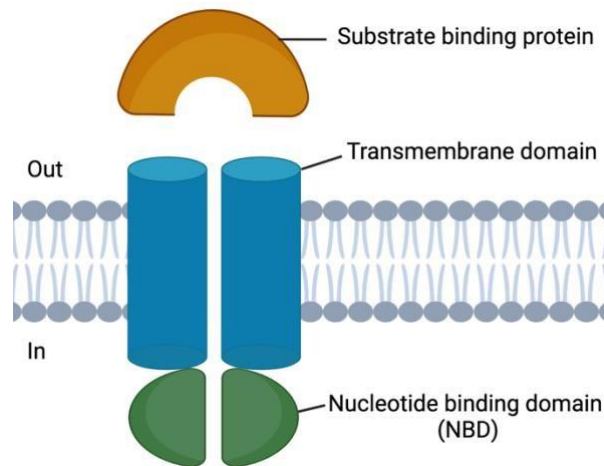


**Figure 1.6 – The basic structure of a bacterial ABC transporter (in a gram-negative bacterium). The transporter is formed from two integral transmembrane domains, which form the transport channel. Nucleotide binding domains are associated with both the transmembrane domains on the cytoplasmic side. The substrate is brought to the channel by a periplasmic binding protein, after which transport is driven by ATP hydrolysis.**

#### 1.4.2 Mechanism of Action

As active transporters, the ABCs move the transport substrate against a concentration gradient – this process requires energy. In the case of the ATP transporters, this energy is provided by the hydrolysis of ATP. This hydrolysis is orchestrated by the various motifs which make up the NBDs. The walker A-motif binds to ATP, whilst the walker-B motif directs the hydrolysis of the molecule (Oldham and Chen 2011).

The process of ATP hydrolysis drives several conformational changes within the transporter which occur in a “catalytic cycle”. During this process, the NBDs move into closer contact forming a dimer. This process also induces a conformational change within the TMDs via non-covalent interactions at the shared interfaces between the NBDs and TMDs (Hollenstein et al., 2007; Linton and Higgins, 2007). The overall result of this process is to switch between the “outward” and “inward” facing states, via an “occluded” state intermediate. The cycle repeats again with the release of the transport substrate into the cytoplasm, followed by the release of the ATP hydrolysis products. Switching between conformational states in this way prevents the backward movement of the substrate through the transport pore, and ensures transport is unidirectional (Wilkins 2015)(Figure 1.7).

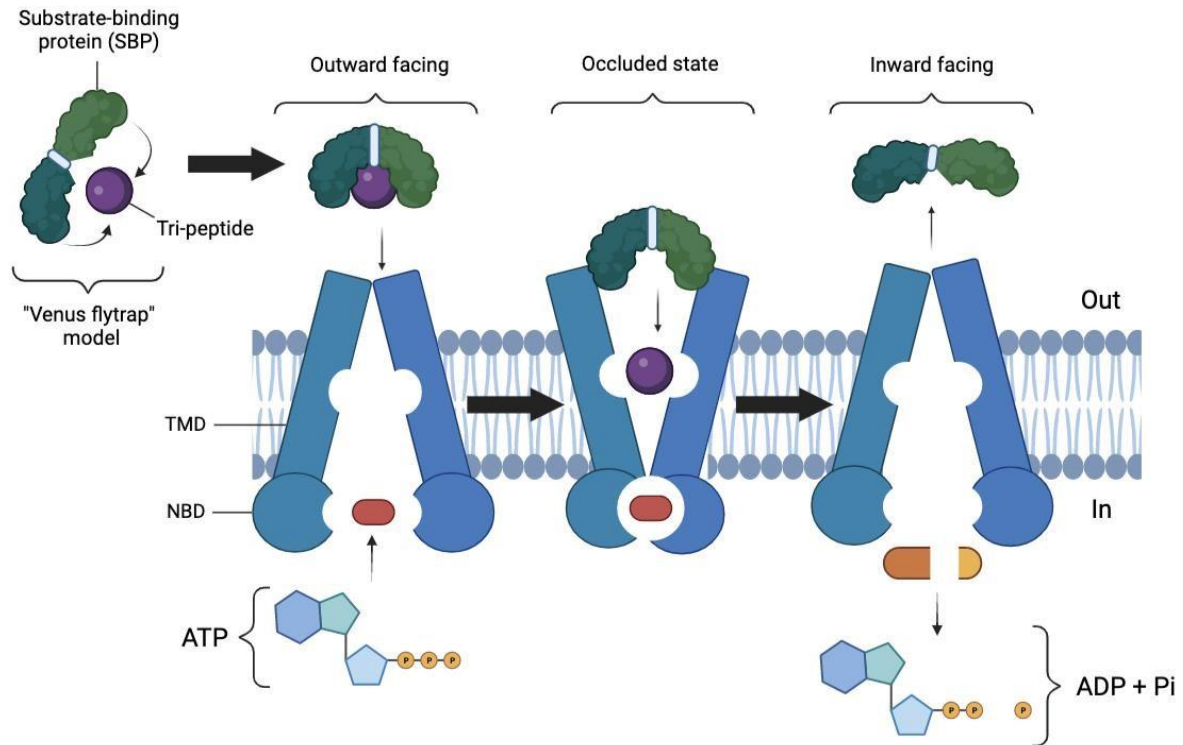


**Figure 1.7– Mechanism of action of an ABC importer.** *E. coli* Opp is used as an example. 3 conformational states (outward facing, occluded and inward facing) of a single transporter are shown. Energy required for the conformational changes between states is provided by the hydrolysis of ATP. The inward direction of transport is conferred by the substrate binding protein (SBP), which binds to the tri-peptide following the venus flytrap model, and initiates transport.

The substrate is first brought to the transporter by the substrate-binding protein (SBP). The structure of the SBP is formed from two domains which are linked by a flexible hinge connection at the base of the cleft. During transport, the hinge allows the domains to form a closed conformation around the ligand, allowing it to be captured within the SBP in a "venus flytrap" model (Mao, B. et al. 1982)(schematic shown in Figure 1.7). Usually, one SBP is specific to a single transporter, though there are examples of multiple SBPs which are located separately within the genome working with a single ABC transporter – these are known as "orphan SBPs"(Thomas 2010).

The ABC transporters are an extremely diverse family of transporters, with a number of diverse possible substrates. Early attempts to comprehend the diversity within the group based on structural data demonstrated that the SBPs of the transporters fall into distinct groups, that did not share extensive sequence homology (Tam and Saier 1993). These groups were later further divided into clusters based on structural similarity (Berntsson, R.P. et al. 2010). One of which is known as the "cluster C SBPs", amongst which the majority of members are peptide transporters – the transporters Opp and Dpp in *E. coli* being two examples.

Whilst the primary substrate of Dpp is dipeptides, Opp binds peptides between 3 and 5 amino acids. Previous studies investigating the equivalent Opp transporter in *Salmonella enterica* serovar Typhimurium revealed the mechanism by which SBP recognise peptides, through making contact exclusively with the backbone chain of the peptide, whilst not interacting with the side chains. During binding, the side chains occupy a water filled cavity, giving the transporter promiscuity required to bind peptides with any possible side chain (Tame, J.R. et al. 1995; Sleight et al. 1997, 1999). Despite this apparent promiscuity, later studies provided evidence of a preference for positively charged peptides, which was later explained by the identification of a negatively charged surface within the binding site (Klepsch et al. 2011).

## 1.5 $\beta$ -lactam antibiotics

In addition to the native substrate of peptides, both the ABC transporters and the POT transporters are known to transport a variety of drugs including anti-cancer (Song et al. 2005) and anti-viral drugs (Agarwal et al. 2008), but most importantly in the context of bacteria they are also known to transport antibiotics (Dantzig, 1997). Antibiotics are substances which kill or inhibit the growth of bacteria. There are many different classes of antibiotic, with differing structures and mechanisms of action. Antibiotics can be produced naturally (for example by another bacteria), semi-synthetic (such as a modified version of a natural molecule) or entirely synthetic. Penicillin is an example of a natural antibiotic produced by fungi of the genus *Penicillium*. The discovery of Penicillin in 1928 preceded a “golden age” of antibiotics with many new antibiotic classes developed. In the years since, there have been various modifications to the original penicillin structure to combat the development of resistance and improve efficacy, deriving a large repertoire of semisynthetic molecules known as the  $\beta$ -lactam antibiotics (Demain and Blander 1999).

### 1.5.1 Structure and Classification

The concept of modifying the core penicillin molecule dates to the initial phase of penicillin mass production in the 1940s, during which time it was discovered that differing fermentation conditions could produce penicillin molecules with differing side chain modifications (Behrens 1948).

Regardless of the side chain modifications, the new penicillin molecules maintained a core nucleus containing a “ $\beta$ -lactam ring” common to all penicillin derivatives known as 6-aminopenicillanic acid (6-APA) (Fig. 1.8A). The production of new  $\beta$ -lactam antibiotics with modified structures led to the development of a wide array of new drugs, increasing both the effectiveness of the original penicillin molecule and their spectrum of action. Antibiotics derived from the original 6-APA nucleus are known as the penams (Sheehan and HeneryLogan 1959).

Whilst the generation of semi-synthetic compounds from the original 6-APA nucleus proved productive, investigations into additional natural sources of antibiotics (such as that which led to the discovery of penicillin) continued. This led to the discovery of a second class of

$\beta$ -lactam molecules from a strain of the fungus *Cephalosporium acremonium*. This molecule contained a modified version of the original  $\beta$ -lactam ring, with a 7-aminocephalosporanic acid (7-APA) nucleus (figure 1.8B). This nucleus then underwent further modifications, expanding the repertoire further to form a second sub-class of  $\beta$ -lactams known as the cephalosporins (Sheehan and Henery-Logan 1959).

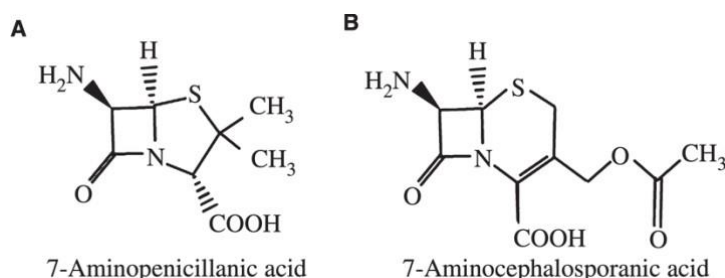


**Figure 1.8 – Molecule structure of (A) 7-aminopenicillanic acid, (B) 7-aminocephalosporanic acid. Figure adapted from (Kong et al., 2010).**

Within the  $\beta$ -lactam ring, there is an amide bond, in the form of a carbon double bond to an oxygen, adjacent to a nitrogen group within the ring (Fig 1.9). Therefore, the  $\beta$ -lactam antibiotics can be considered peptidomimetic drugs (peptide like), and thus may be expected to share some properties of peptides.

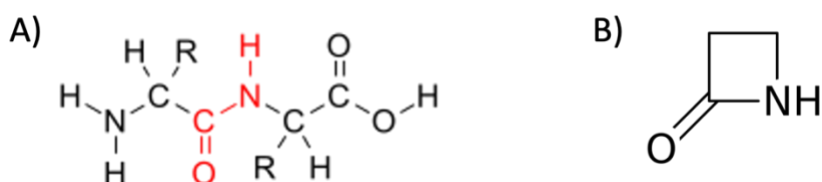


**Figure 1.9 – Amide bond within the  $\beta$ -lactam ring. A) The peptide bond (in red) within a typical peptide. B) The presence of the amide bond within the  $\beta$ -lactam ring structure (2Azetidinone shown here), formed from a carbon with a double bond oxygen and the nitrogen group.**

### 1.5.2 Mechanism of Action

Although the  $\beta$ -lactam antibiotics were first discovered in 1928, the mechanism of action was not elucidated until the 1970s. Blumberg and Strominger discovered the mechanism of action of penicillin after realising the structural similarity between penicillin and the D-AlaD-Ala ending of peptidoglycan. Peptidoglycan is the primary component of cell walls in both gram-positive and gram-negative bacteria, and thus it was proposed that the  $\beta$ -lactam antibiotics exerted their effect through inhibiting bacterial cell wall synthesis (Blumberg and Strominger 1974).

The bacterial cell wall is a structure which covers the cell membrane and is essential for the normal growth and survival of bacteria. The cell wall is a dynamic structure, which is

constantly undergoing repair and synthesis during the bacterial growth cycle. The primary component peptidoglycan is a heteropolymer which confers mechanical stability to the structure due to its rigidity, which is a result of its highly cross-linked structure. This structure is made up of two alternating monosaccharides, known as N-acetylglucosamine (NAG) and N-acetylmuramic acid (NAM), which form glycan chains which are cross-linked by short peptides (Izaki et al., 1968; Sharpe et al., 1974).

In gram-negative bacteria such as *E. coli* peptidoglycan synthesis occurs within the periplasmic space, the final step of which involves the formation of cross links between the glycan chains. This process involves a transpeptidation reaction catalysed by the transpeptidases within the periplasmic space. The purpose of this reaction is to form peptide bonds between the terminal D-Ala-D-Ala dipeptides found within the pentapeptide side chains which extend from the sides of the glycan polymers (Mainardi et al. 2008; van Heijenoort 2010; Typas et al. 2011). This process is targeted by the  $\beta$ -lactam antibiotics which inhibit the catalytic activity of the bacterial transpeptidases. Since these transpeptidases are targeted by  $\beta$ -lactam antibiotics such as penicillin, these enzymes are also known as the penicillin binding proteins or PBPs (Sauvage et al. 2008).

The ability of the  $\beta$ -lactam antibiotics to bind to the PBPs is based on the structural similarity between the amide bonds of the  $\beta$ -lactam ring (figure 1.9) and the transpeptidase substrate (D-Ala-D-Ala). This binding is irreversible, causing total inhibition of catalytic activity, and preventing cross-link formation between the glycan chains, resulting in weak peptidoglycan polymers (Figure 1.10).

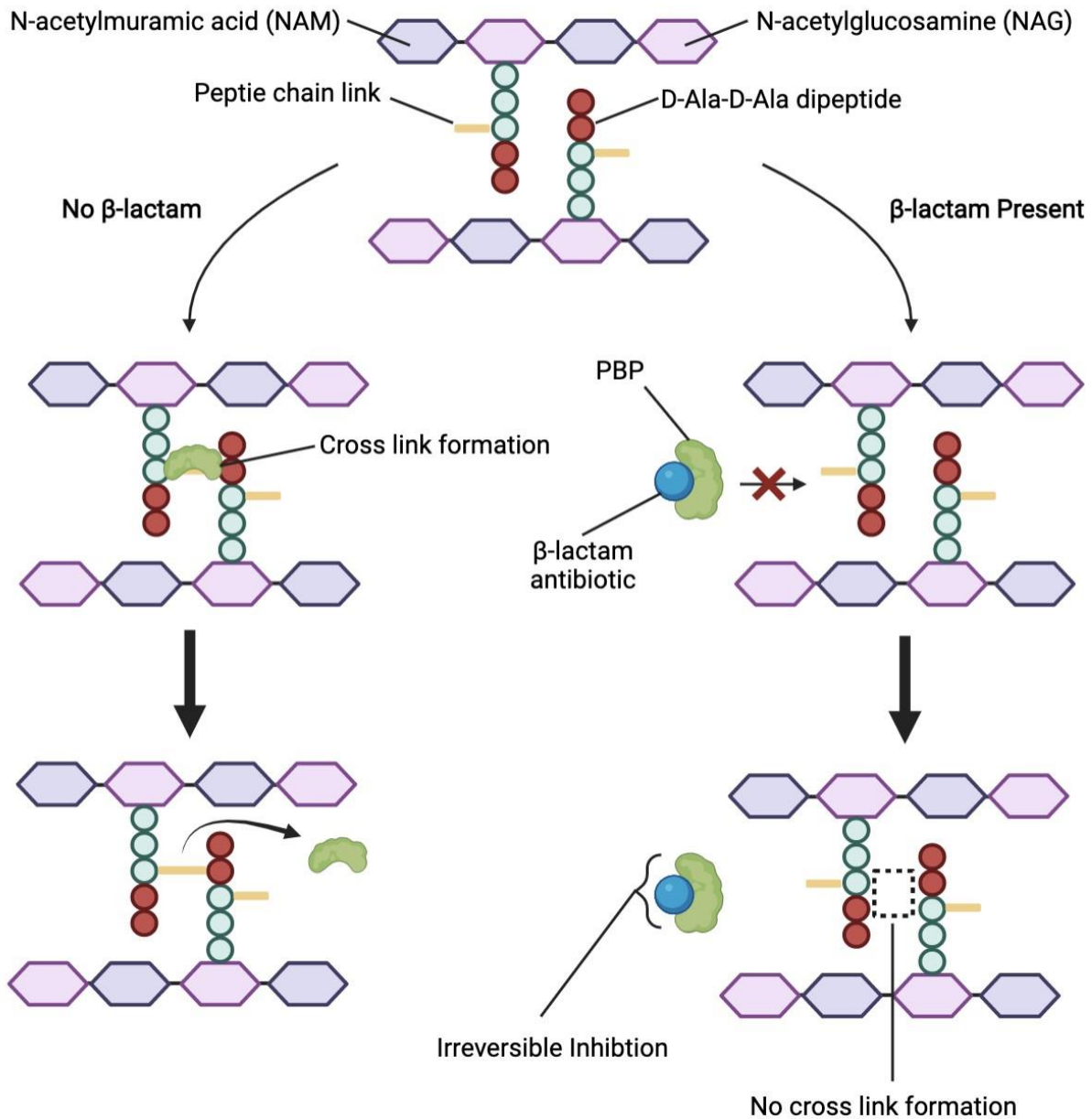


**Figure 1.10** – Mechanism of  $\beta$ -lactam antibiotic action. Peptidoglycan is a polymer of alternating NAM and NAG monomers, with individual layers linked by peptide chain links between the side chains which carry a terminal D-Ala-D-Ala dipeptide. The peptide bond links between the chains are formed by a transpeptidation reaction driven by the PBPs. Shown here is the activity of PBPs in the absence (left) and presence (right) of a  $\beta$ -lactam antibiotic.

This causes growing bacteria (which are continuously synthesising new peptidoglycan) to have increased lysis susceptibility leading to cell death – for this reason the  $\beta$ -lactam antibiotics are classed as bactericidal (Macheboeuf et al. 2006; Sauvage and Terrak 2016; Cochrane and Lohans 2020).



### 1.5.3 Resistance

Bacteria employ three main mechanisms of resistance against antibiotics. The first of which is through the production of enzymes which break down or modify the antibiotic before it reaches its target site, the second is through the modification of the target itself to render the antibiotic ineffective and the final is through prevention of antibiotic entry into the cell either through altered permeability or efflux. Bacteria employ a combination of all three mechanisms to confer resistance to  $\beta$ -lactam antibiotics. Despite this, resistance is not complete, and the extent of resistance varies between bacterial species. Furthermore, the  $\beta$ -lactams have been subject to various structural modifications to form new “generations” of antibiotic which can overcome previous resistances, and thus remain viable for the treatment of bacterial infections (Poole 2005).

#### 1.5.3.1 Antibiotic modifying enzymes

Bacteria possess a class of enzymes capable of breaking down  $\beta$ -lactam antibiotics known as  $\beta$ -lactamases. These enzymes are the primary defence mechanism against  $\beta$ -lactam antibiotics within gram-negative bacteria, with genes coding for  $\beta$ -lactamases spreading rapidly through mobile genetic elements such as plasmids or transposons. Once produced, the  $\beta$ -lactamases are secreted into the periplasmic space (in gram-negative bacteria) or excreted (in gram-positive bacteria). Upon contact with the antibiotic, the enzymes hydrolyse the amide bond within the  $\beta$ -lactam ring structure (Figure 1.9), causing degradation of the antibiotic (Weldhagen, 2004; Tooke et al., 2019)

#### 1.5.3.2 Altered antibiotic targets

An alternative mechanism by which resistance to  $\beta$ -lactam antibiotics is conferred is through the modification of the PBPs, which are an essential component within the  $\beta$ -lactam mechanism of action (Figure 1.10). One mechanism by which the PBPs can be modified is through the acquisition of a novel, less sensitive form of PBP with a modified structure that has a lower affinity for the  $\beta$ -lactam antibiotic whilst maintaining the transpeptidase activity (Chesnel et al. 2003; Pernot et al. 2004). The second mechanism is through the upregulation of PBP expression, increasing the overall number of uninhibited PBPs, and decreasing the impact of the antibiotic on peptidoglycan synthesis (Jiang et al. 2020).

#### 1.5.3.3 Altered antibiotic permeability and efflux

An alternative mechanism of resistance is through the removal of the antibiotic from the site of action. One system which can achieve this is the drug efflux pump MexAB–OprM - formed from the inner membrane RND transporter ‘pump’ MexB, the outer membrane porin OprM, and the soluble periplasmic Mex. This pump can act on a wide range of antibiotics, including both  $\beta$ -lactams and  $\beta$ -lactamase inhibitors. Through this action, the antibiotic is removed from the periplasmic space, thus preventing access to the PBP targets, and resulting in resistance (Poole 2005; Llarrull et al. 2010).



## 1.6 Illicit Drug Transport

Although peptides are the primary substrate of the PTRs, there is evidence that these transporters are also capable of translocating a variety of drug molecules. This fact has long been recognised, with many early studies demonstrating the capability of intestinal “H-coupled peptide transporters” (now known as POT transporters) to transport a variety of peptide-like drugs – including  $\beta$ -lactam antibiotics (Iseki et al., 1984; Okano et al., 1986; Tsuji et al., 1987). This is thought to be due to the high level of promiscuity observed within peptide transporters, a necessary attribute to allow for the transport of such a wide range of possible substrates (Lyons et al., 2014). Since these drugs are not the native substrate, this can be considered a form of “illicit transport” (Ames et al., 1973).

### 1.6.1 B-lactam antibiotics.

As discussed previously, the  $\beta$ -lactam antibiotics can be considered “peptide-like” due to the presence of an amide bond within the structure (Figure 1.9), allowing them to undergo illicit transport via peptide transporters. This has in part contributed to the success of  $\beta$ -lactam antibiotics, by conferring increased oral bioavailability through absorption via peptide transporters in the intestine (Dantzig 1997b). One such example is PEPT1, a human POT transporter which is primarily responsible for the absorption of dietary di- and tripeptides but is also known to transport various  $\beta$ -lactam antibiotics (Ganapathy, M.E. et al. 1995). This mechanism has been exploited in the design of new drugs for which intestinal absorption is beneficial (Adibi, 1997; Foley et al., 2010).

DtpA is the bacterial homologue of PEPT1 (Ural-Blimke et al., 2019), therefore it is logical to assume that DtpA might also be involved in the illicit transport of  $\beta$ -lactam antibiotics through a similar mechanism. This is demonstrated through the known transport of Ampicillin (a penam type  $\beta$ -lactam antibiotic – section 1.5.1) by both PEPT1 and DtpA (Prabhala et al. 2017). It has therefore been conceptually demonstrated that a bacterial POT transporter can transport a  $\beta$ -lactam antibiotic, however this is currently limited to a single bacterial POT transporter and a single  $\beta$ -lactam antibiotic. Whilst the ABC transporters are also known to contribute to illicit drug transport, with  $\beta$ -lactam antibiotics shown to be a substrate in various bacterial species, the affinity of *E. coli* ABC transporters for  $\beta$ -lactam antibiotics has not been investigated (Collins et al. 2010; Rismondo and Schulz 2021).

### 1.6.2 Illicit transport of non- $\beta$ -lactam antibiotics

The concept of illicit drug transport is not limited to the  $\beta$ -lactam antibiotics. There is also evidence that DtpA transports Chloramphenicol, a semi-synthetic antibiotic derived from *Streptomyces venequellae* (Prabhala et al., 2018). However, this evidence is limited to the POT transporters, and of those only DtpA was investigated. There is also evidence that *E. coli* ABC transporters Dpp and Opp translocate two additional antibiotics: Kasugamycin and Blastidicin S (Anthony L. Shiver et al., 2016). Both are aminoglycoside antibiotics, derived from *Streptomyces kasugaensis* and *Streptomyces griseochromogenes* respectively (Takeuchi et al., 1958; Umezawa et al., 1965).

Within the structure of both antibiotics there is a peptide bond but no  $\beta$ -lactam ring (Figure 1.11). This provides further evidence that the illicit transport of  $\beta$ -lactam antibiotics discussed previously (section 1.6.1) is driven by the presence of the peptide bond, rather than the beta-lactam ring.

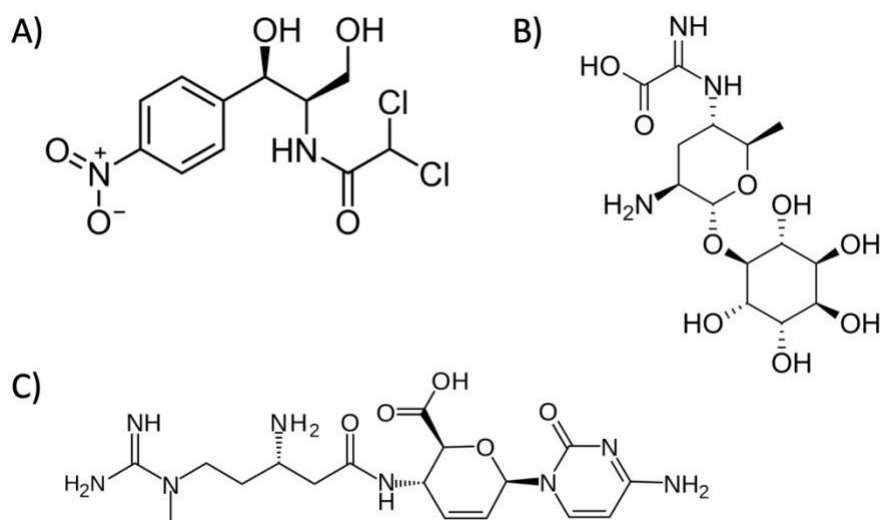


**Figure 1.11** – Structure of non- $\beta$ -lactam antibiotics implicated in illicit drug transport. A) Chloramphenicol B) Kasugamycin C) Blasacidin S.

## 1.7 Intrinsic Resistance Hypothesis

There is therefore evidence that both the POT and ABC transporters of *E. coli* are capable of transporting beta-lactam antibiotics in addition to the native substrate of di-/tripeptides. Since the peptide transporters are located within the inner membrane of bacteria, the antibiotics are translocated from the periplasmic space into the cytoplasm. To exert their bactericidal effect, the beta-lactam antibiotics need access to the PBPs which are located within the periplasmic space (section 1.5.2). Therefore, the translocation of beta-lactam antibiotics into the cytoplasm removes them from their site of action.

This leads to a hypothetical mechanism in which the activity of peptide transporters decreases the exposure of PBPs to beta-lactam antibiotics, which in turn would reduce the impact on peptidoglycan synthesis - thus reducing the effectiveness of the antibiotic. This represents a distinct mechanism of antibiotic resistance to those discussed previously (section 1.5.3), which is intrinsic to the bacteria through existing biological processes, rather than one which has evolved specifically to combat antibiotic pressure. Thus an “intrinsic resistance hypothesis” is proposed in which the bacterial peptide transporters contribute to the basal level of resistance to  $\beta$ -lactam antibiotics as a side effect of their peptide-like nature (Figure 1.12). This is a unique proposal which to date has not been explicitly described or investigated in the existing literature.

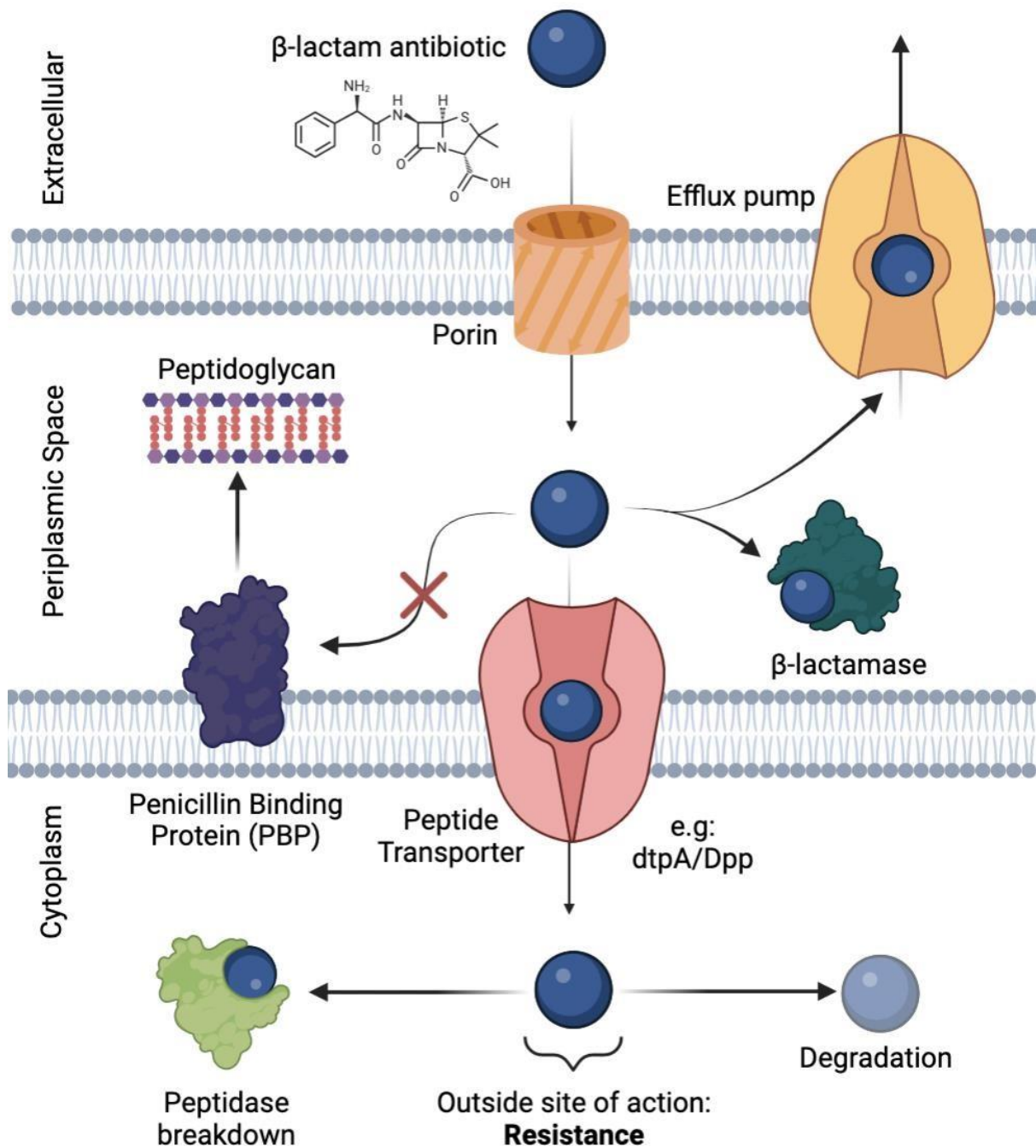


**Figure 1.12 – Schematic diagram of the intrinsic resistance hypothesis.** Under the proposed mechanism the beta-lactam antibiotic (penicillin shown here) enters the periplasmic space through porins. The concentration of beta-lactam antibiotics within the periplasm is limited through the known mechanisms of antibiotic resistance including export by efflux pumps (section 1.5.3.3) and breakdown by beta-lactamases (section 1.5.3.1). In addition to these, the hypothesis describes the role of peptide transporters in translocating the antibiotic into the cytoplasm. After the antibiotic has been removed from the periplasm, it can no longer bind to and inhibit the activity of PBPs, thus preventing the inhibition of peptidoglycan synthesis and contributing to the basal level of antibiotic resistance.

## 1.8 Project Background: Generation of $\Delta$ DB1 and $\Delta$ DB50

Prior to the start of this project, a significant amount of investigation had been conducted investigating peptide transport in *E. coli* by various lab members. This work spanned between 2011-2017 across multiple records. Thus, the first aspect of this project involved chronicling the process used to generate the strains that would later be used in this work and summarising the initial evidence for intrinsic resistance hypothesis.

### $\Delta$ DB1:

Dr Daniel Bawdon generated a double knockout *E. coli* BW25113 strain in which the genes encoding the inner membrane subunit of both the ABC type peptide transporters in *E. coli* (*dppC* and *oppC*) were deleted.

described by Datsenko and Wanner (2000), originating from a  $\Delta$ *dppC* strain from the KEIO collection (Baba, T. et al. 2006).

This strain is known as  $\Delta$ DB1 ( $\Delta$ *dppC*  $\Delta$ *oppC*) and was generated through deletion of the *oppC* gene, in a strain from the KEIO collection in which the *dppC* gene had previously been deleted – both utilising the method described in section 2.2.5. Successful deletion of both genes had been confirmed by PCR (Figure 1.13A), thus allowing the full lineage of  $\Delta$ DB1 to be understood (Figure 1.13B).

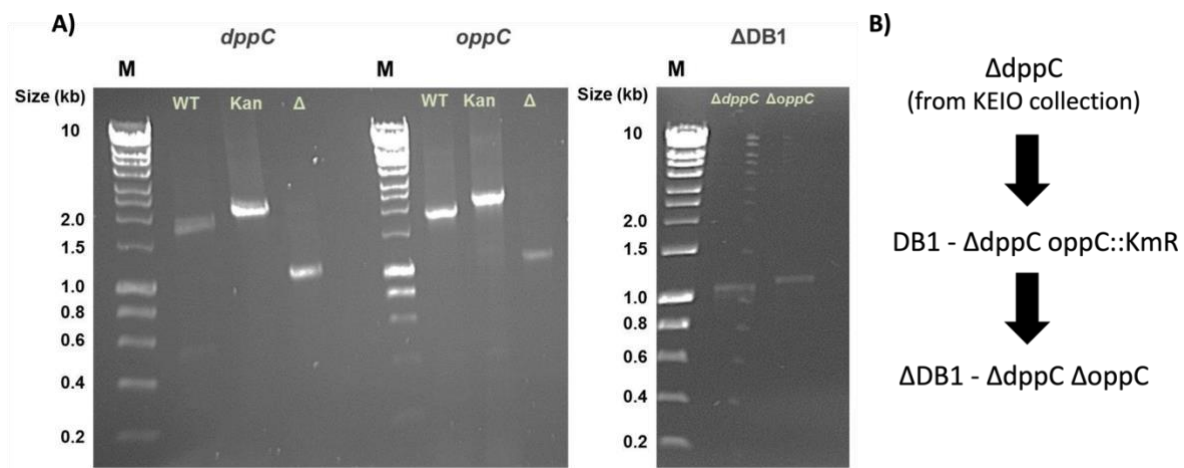


**Figure 1.13 – Generation of  $\Delta$ DB1.** A) Agarose gel (1%) stained with ethidium bromide showing colony PCR amplification products from  $\Delta$ DB1 at the *dppC* and *oppC* loci. Lane ‘M’ denotes DNA size marker, WT – wild type gene amplified from BW25113, Kan – kanamycin gene replacement amplified from respective Keio collection strain,  $\Delta$  – clean genetic deletion at respective locus. Expected band sizes (bp): *dppC* WT: 1885 Kan: 2239  $\Delta$ : 1052 *oppC* WT: 1969 Kan: 2317  $\Delta$ : 1130. ) Figure taken from Dr Daniel Bawdon’s PhD thesis (Bawdon 2014a). B) Lineage of  $\Delta$ DB1 chronicled by in this work based on lab records produced by Dr Daniel Bawdon in 2011. Black arrows denote steps in the methodology for gene deletion

In addition to  $\Delta$ DB1, Dr Daniel Bawdon also generated a quadruple deletion strain of *E. coli* BW25113 known as  $\Delta$ DB5, in which all 4 POT type peptide transporter genes are deleted ( $\Delta$ *dtpA*: $\Delta$ *dtpB*: $\Delta$ *dtpC*: $\Delta$ *dtpD*).

Similarly, to  $\Delta$ DB1,  $\Delta$ DB5 was generated through successive deletion steps originating from a single knockout KEIO collection strain ( $\Delta$ *dtpA*) and underwent successive deletions of the remaining POT genes (section 2.2.5). Due to the higher number of POT type peptide transporters compared to ABC type genes in *E. coli*, more deletion steps were required resulting in a series of intermediate strains being produced (figure 1.14B). After the final POT gene (*dtpC*) was deleted, the genotype of  $\Delta$ DB5 was confirmed by PCR, displaying the deletion of all 4 *dtp* genes (figure 1.14A).

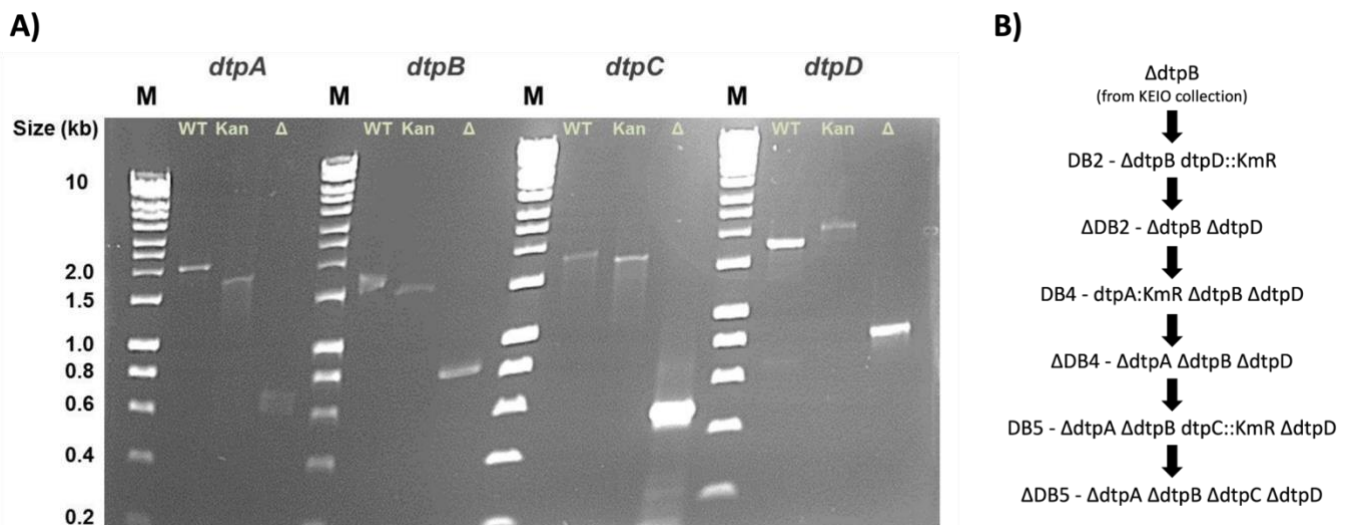


**Figure 1.14 – Generation of  $\Delta$ DB5.** **A)** Agarose gel (1%) stained with ethidium bromide showing colony PCR amplification products from single gene deletions at the loci of the 4 *dtp* genes in *E. coli*. Lane ‘M’ denotes DNA size marker, WT – wild type gene amplified from BW25113, Kan – kanamycin gene replacement amplified from respective Keio collection strain,  $\Delta$  – clean genetic deletion at respective locus. Expected band sizes (bp): *dtpA* WT: 2098 Kan: 1852  $\Delta$ : 689 *dtpB* WT: 1786 Kan: 1573  $\Delta$ : 810 *dtpC* WT: 1835 Kan: 1634  $\Delta$ : 447 *dtpD* WT: 1815 Kan: 1981  $\Delta$ : 804. Figure taken from Dr Daniel Bawdon’s PhD thesis (Bawdon 2014a). **B)** Lineage of  $\Delta$ DB5 chronicled in this work based on lab records produced by Dr Daniel Bawdon in 2012-2013. Black arrows denote steps in the methodology for gene deletion described by Datsenko and Wanner (2000), originating from a  $\Delta$ *dtpB* strain from the KEIO collection (Baba, T. et al. 2006).

$\Delta$ DB5 was later investigated by Emmanuele Severi, who first performed a diagnostic PCR to ensure the genotype of the strain was expected based on records from Dr Daniel Bawdon.

During this process, Emmanuele Severi found an anomalous PCR result. Whilst *dtpA* and *dtpD* showed results which would be expected based on the deletion of the genes compared to the wild type strain in which they were intact (figure 3. bands marked with x), *dtpB* did not undergo a successful PCR reaction (figure 1.15 bands marked with y) whilst the *dtpC*



gene appeared to still be intact (figure 1.15. bands marked with z). There is no evidence that  $\Delta DB1$  underwent a similar genomic inversion, this is logical due to the lower number of deletion events resulting in fewer FRT sites (Figure 1.13B), reducing the opportunity for such an inversion to occur.

The PCR performed by Dr Daniel Bawdon which previously showed successful deletions of the *ntp* genes (figure 1.14A) was performed with different PCR primer combinations to that performed by Emmanuele Severi. One possible explanation for this difference is that the primers used by Dr Daniel Bawdon targeted a sequence which was unchanged even after the genomic inversion, whereas the primers used by Emmanuele Severi targeted a sequence which was altered because of the genomic inversion, resulting in the unsuccessful diagnostic PCR (figure 1.15). Whilst this hypothesis was not tested due to time limitations, the genome sequencing data (now shown) is concurrent only with the findings of Emmanuele Severi.

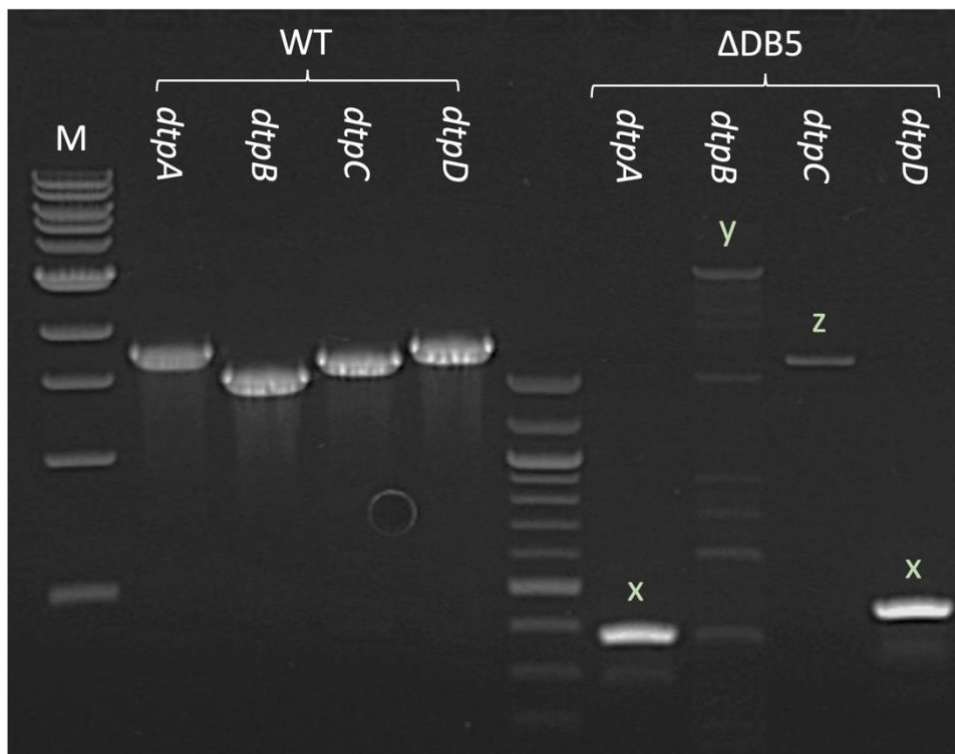


**Figure 1.15 – Diagnostic PCR for  $\Delta DB5$ .** Agarose gel (1%) electrophoresis comparing PCR products from WT and  $\Delta DB5$  targeting *ntp* gene loci using primers designed independently to those used by Dr Daniel Bawdon. 'M' denotes a DNA size marker, 'x', 'y', 'z' denote points of interest. Expected band sizes are unknown based on the records available. PCR performed by Emmanuele Severi, annotated by in this work.

Based on these findings, Emmanuele Severi performed a second diagnostic PCR using alternative clones generated from the same kanamycin curing step from which  $\Delta DB5$  was generated (Figure 1.14B), to find an alternative clone which had not undergone the genomic inversion.

This process revealed that of the 3 clones generated alongside  $\Delta$ DB5, 1 shared the anomalous genotype (figure 1.16 – clone 2), whilst one had successfully undergone deletion of both *ntpB* and *ntpC* (figure 1.16– clone 1) - this strain was later termed  $\Delta$ DB50.

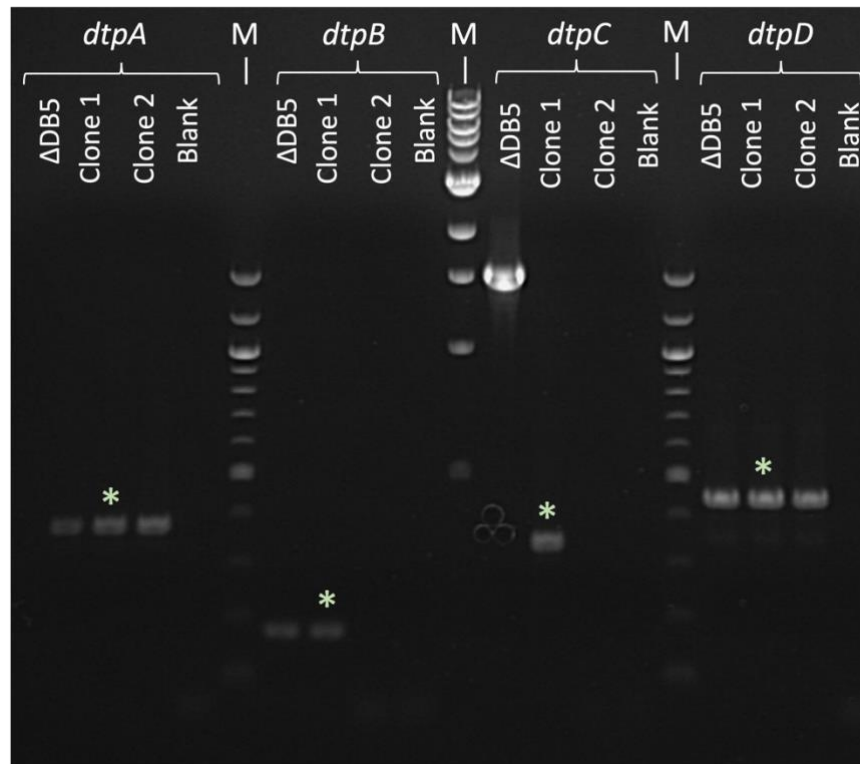


**Figure 1.16** – Alternative  $\Delta$ DB5 clones. Agarose gel (1%) electrophoresis showing colony PCRs targeting the 4 *ntp* genes in  $\Delta$ DB5 and two alternative clones (clone 1 and clone 2) isolated from the precursor step to DB5. One lane is left blank for each *ntp* gene, ‘M’ denotes a DNA size marker. \*Bands indicating successful deletion of *ntp* genes in clone 1. Expected band sizes are unknown based on the records available. PCR performed by Emmanuele Severi, annotated in this work.

At the start of this project,  $\Delta$ DB50 had been created but relatively little work had been performed using the strain. When combined with the complex lineage of  $\Delta$ DB50, it was deemed necessary to perform a final diagnostic PCR to ensure that the 4 POT genes in *E. coli* had been deleted in  $\Delta$ DB50.

The final diagnostic PCR confirmed  $\Delta$ DB50 had the expected genotype, with all 4 *ntp* genes deleted (figure 1.17), this agrees with genome sequencing data which confirms  $\Delta$ DB50 has not undergone a similar genomic inversion to  $\Delta$ DB5.

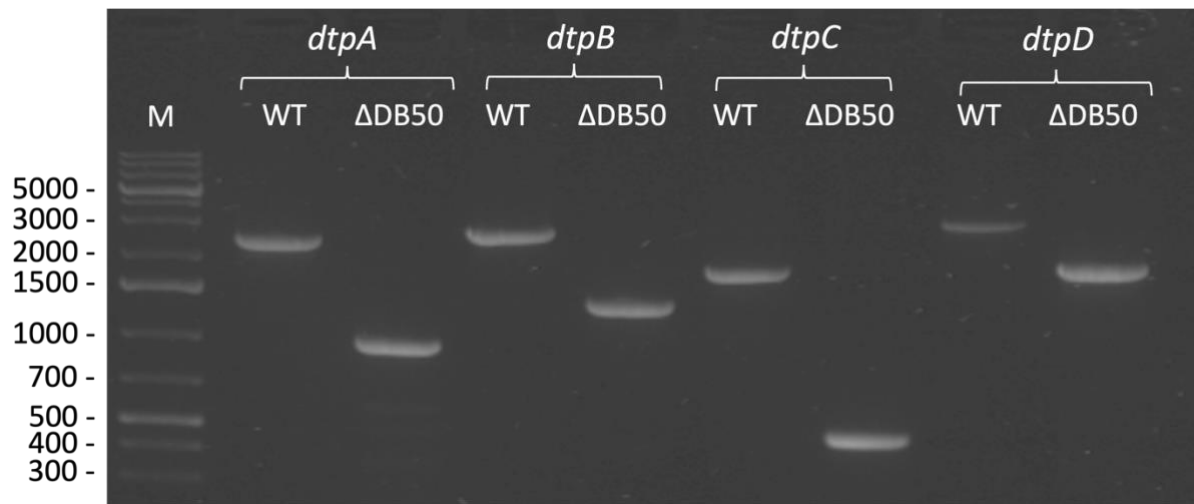


**Figure 1.17 – Diagnostic PCR for  $\Delta$ DB50.** Agarose gel (1%) electrophoresis comparing the *dtp* genes wild type *E. coli* and  $\Delta$ DB50. ‘M’ denotes a 1kb DNA size marker (band sizes shown in kb), ‘WT’ denotes wild type *E. coli* BW25113, ‘ $\Delta$ DB50’ denotes the strain previously known as “clone 1” (figure 1.16). Expected sizes (kb): *dtpA*: WT – 2347,  $\Delta$ DB50 – 844; *dtpB*: WT – 2712,  $\Delta$ DB50 – 1242; *dtpC*: WT – 1835,  $\Delta$ DB50 – 377; *dtpD*: WT – 3349,  $\Delta$ DB50 – 1867. PCR performed and annotated in this work, using independently designed primers (except for *dtpC*, which utilised primers designed by Emmanuele Severi).

With this conclusion, the full lineage of  $\Delta$ DB50 can now be understood (figure ), allowing this strain to be used in future experiments investigating the intrinsic resistance hypothesis.

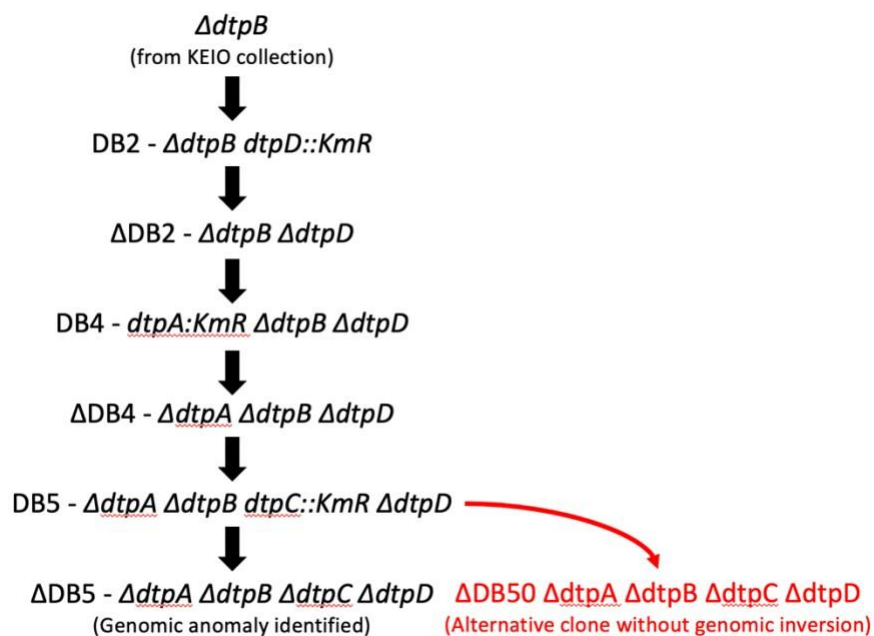


**Figure 1.18 – Full lineage of  $\Delta$ DB50.** The full processes which led to the creation of  $\Delta$ DB50 chronicled in this work based on lab records. The original  $\Delta dtpB$  strain originates from the KEIO collection (Baba, T. et al. 2006), black arrows indicate the successive introduction and deletion of kanamycin resistance genes resulting in the deletion of the target *dtp* genes via the



method outlined in Datsenko and Wanner, (2000). The red arrow denotes the process outlined in Figure 1.16. Black text indicates work performed by Dr Daniel Bawdon; red text indicates work performed by Emmanuele Severi.

## 1.9 Project Aims

The primary aim of this project is to assess the evidence for the proposed intrinsic resistance hypothesis. This will be conducted using an *E. coli* quadruple POT deletion mutant termed  $\Delta$ DB50 ( $\Delta dtpA:\Delta dtpB:\Delta dtpC:\Delta dtpD$ ) which was developed by a previous lab member (Dr Daniel Bawdon).  $\Delta$ DB50 is a successor to a previous strain called  $\Delta$ DB5, a previously developed quadruple POT deletion strain in which a genomic anomaly was identified. Thus, a preliminary aim of this project will be to confirm the genotype of  $\Delta$ DB50, along with repeating experiments related to the hypothesis which were performed exclusively using  $\Delta$ DB5. Since the POT transporters have been less extensively studied in comparison to the ABC peptide transporters in *E. coli*  $\Delta$ DB50 will form the basis of the investigation, however a secondary aim relates to investigating the potential role of ABC peptide transporters in the proposed mechanism - this will be done using a double ABC knockout strain termed  $\Delta$ DB1 ( $\Delta dppC:\Delta oppC$ ) (also created by Dr Daniel Bawdon). Despite substantial research conducted since the identification of peptide transporters in 1963 (Kessel and Lubin 1963), our understanding of this system remains incomplete, thus an overarching aim of this project is the further elucidation of the peptide transport system within *E. coli*.

## 2 Materials and Methods

### 2.1 Chemicals and Strains

#### 2.1.1 Antibiotics

A series of antibiotics were used in this work, encompassing a range of antibiotic classes. The antibiotics were obtained from a series of different suppliers and were stored in accordance with the manufacturer's instructions. All antibiotics stocks were filter sterilised using a 0.22 µm syringe filter and stored in 1ml aliquots at the specified temperature for no longer than one month (Table 2.1).

**Table 2.1 – Antibiotics used in this work.**

<b>Antibiotic</b>	<b>Supplier</b>	<b>Stock Concentration</b>	<b>Solute</b>	<b>Storage Temperature</b>
Amoxicillin (sodium salt)	Alfa Aesar	25 mg/ml	dH <sub>2</sub> O	-80°C
Ampicillin (sodium salt)	Melford	100 mg/ml	dH <sub>2</sub> O	-20°C
Blasticidin S(HCl)	Cambridge Bioscience	10 mg/ml	20mM HEPES	-20°C
Carbenicillin (sodium salt)	Melford	100 mg/ml	dH <sub>2</sub> O	-20°C
Cephalexin (monohydrate)	Apollo Scientific	1mg/ml	dH <sub>2</sub> O	-20°C
Cefadroxil (hydrate)	Cayman Chem	1mg/ml	dH <sub>2</sub> O	-20°C
Kanamycin (sulfate)	Sigma-Aldrich	50 mg/ml	dH <sub>2</sub> O	-20°C
Kasugamycin	TOKU-E	10 mg/ml	dH <sub>2</sub> O	-20°C

## 2.1.2 Bacterial Strains and Plasmids

Stocks of all bacterial strains used were stored in 50% glycerol stocks at -80°C throughout the course of this study. All strains used in this study are variations of *E. coli* BW25113, but the genotype and source differ between strains – information can be found in table 2.2.

**Table 2.2 – Bacterial strains used in this work.**

Species	Name	Background	Genotype	Source
<i>E. coli</i>	Wild Type*	BW25113	<i>dtpA:dtpB:dtpC:dtpD</i>	KEIO Collection (Baba et al., 2006)
	$\Delta dppC$		$\Delta dppC$	
	$\Delta oppC$		$\Delta oppC$	
	$\Delta DB50$	BW25113	$\Delta dtpA: \Delta dtpB: \Delta dtpC: \Delta dtpD$	Dr Daniel Bawdon
	$\Delta DB5$		$\Delta dtpA: \Delta dtpB: \Delta dtpC: \Delta dtpD$	
	$\Delta DB1$		$\Delta dppC:\Delta oppC$	
	N/A		pBADcLic-dtpA	
			pBADcLic-dtpB	
			pBADcLic-dtpC	
			pBADcLic-dtpD	
	$\Delta DB50$	pBADcLic-dtpA	This work	
		pBADcLic-dtpB		
		pBADcLic-dtpC		
		pBADcLic-dtpD		

\*Wild type refers to a BW25113 *E. coli* strain with intact POT transporters. The lab in which this work was conducted uses multiple BW25113 *E. coli* strains, the specific stock used in this study (designated number 397 at the time of writing) was obtained from the Keio collection single gene knockout library (Baba, T. et al. 2006).

A series of plasmids are referenced in this report, with some being used directly and some being only referenced in relation to previous work. Plasmids used directly in this work were designed and produced by Dr Daniel Bawdon, and later used in transformations conducted in this project. Plasmids only referenced in this work were utilised by Dr Daniel Bawdon in the production of knockout strains (later used in this project) but originate from outside sources. Details regarding these primers can be found in table 2.3.

**Table 2.3 – Plasmids used within this work.**

Plasmid	Backbone	Size (kb)	Antibiotic Resistance	Source
pBADcLIC2005	N/A	4.14	Amp (100)	Geertsma and Poolman (2007)
pKD46*	N/A	6.08		Datsenko and Wanner (2000)
pDtpA	pBADcLIC2005	5.64		Dr Daniel Bawdon
pDtpB	pBADcLIC2005	5.61		
pDtpC	pBADcLIC2005	5.60		
pDtpD	pBADcLIC2005	5.62		

\*pKD46 is discussed in relation to previous work, which is relevant to this project, but is not directly used at any point.

### 2.1.3 Oligonucleotide Primers

All oligonucleotide primers were supplied by Merk Life Sciences. The supplied material was reconstituted in sterile dH<sub>2</sub>O to a stock concentration of 500nM and then stored at -20°C. Primers in this work were utilised for the purpose of a diagnostic PCR to determine the genotype of ΔDB50. Primer sequences can be found in table 2.4.

**Table 2.4 – Oligonucleotide primers used within this work.**

Gene	Sequence (5' → 3')		Source
	Forward Primer	Reverse Primer	
<i>dtpA</i>	GATCACGATGCTGTCGCAAT	GGTGGCGATGTAATTCAGCC	This work
<i>dtpB</i>	GACCTCTCCCCGAAAGCAA	ATGCCACTGCAGGACTTGGG	
<i>dtpC</i>	GTGTGAAATCGGCGCTCACTATCCG	TAGCGTAGATAAAGAGACAGATCGG	DB*
<i>dtpD</i>	GAATGCCTGGCTGAAACGGC	CCACCTCAGGTCCGGTATCG	This work

\*Primers designed by Dr Daniel Bawdon were used in the diagnostic pcr performed for *dtpC*. This was used due to multiple unsuccessful PCR attempts using *dtpC* specific primers designed by myself (not shown), as part of a troubleshooting process.

#### 2.1.4 Bacterial Growth Media

Two different media types were used in this work: LB media and M9 Glucose minimal media. Each media was used in a liquid form (for production of liquid cultures) and a solid media form used in petri dishes in which agar was added. The solid form was used for the isolation of single colonies (LB – Section 2.3.1) or in toxic peptide assays (Section 2.1.5).

**Luria-Bertani (LB) medium** contained (per litre dH<sub>2</sub>O): 10 g tryptone, 5 g yeast Extract and 10 g NaCl. For **LB agar plates**, granulated agar was added to the mixture to a final concentration of 1.5% (suppliers in Table 2.5). Approximately 20ml of molten agar was then poured into Petri dishes and allowed to set at room temperature, then dried in a class II microbiology safety cabinet and stored at 4°C until use.

**M9 Glucose minimal medium** contained (per litre dH<sub>2</sub>O): 6g Sodium phosphate dibasic (Na<sub>2</sub>HPO<sub>4</sub>) (anhydrous), 3g Potassium phosphate monobasic (KH<sub>2</sub>PO<sub>4</sub>), 0.5g Sodium chloride (NaCl) and 1g Ammonium chloride (NH<sub>4</sub>Cl). This mixture was then autoclaved, followed by the addition of: 1ml 1M Magnesium sulfate (MgSO<sub>4</sub>), 1ml 0.1M Calcium chloride (CaCl<sub>2</sub>) and 10ml 10% (w/v) glucose (suppliers in Table 2.5).

**M9 Glucose minimal media plates** were formed from the combination of a solution of 16g agar dissolved within 500ml dH<sub>2</sub>O and a separate solution containing (per litre dH<sub>2</sub>O): 3g Sodium phosphate dibasic (Na<sub>2</sub>HPO<sub>4</sub>) (anhydrous), 1.5g Potassium phosphate monobasic (KH<sub>2</sub>PO<sub>4</sub>), 0.25g Sodium chloride (NaCl) and 0.5g Ammonium chloride (NH<sub>4</sub>Cl). The two solutions were autoclaved separately, allowed to cool until 55°C and then mixed. The following (sterile) components were then added to the mixture: 1ml 1M Magnesium sulphate (MgSO<sub>4</sub>), 1ml 0.1M Calcium chloride (CaCl<sub>2</sub>) and 10ml 10% (w/v) glucose was then added to the mixture (suppliers in Table 2.5). A serological pipette was then used to transfer 20ml of the solution to Petri dishes. The plates were then allowed to set at room temperature and subsequently dried in a class II microbiology safety cabinet and stored at 4°C until use. This methodology was adapted from a protocol developed by the Barrick lab (Barrick Lab, 2018).

**Table 2.5 – Suppliers of media components used in this work.**

<b>Media Component</b>	<b>Supplier</b>
Tryptone	Formedium
Yeast Extract	Oxoid
Granulated Agar	Formedium
Sodium phosphate dibasic (Na <sub>2</sub> HPO <sub>4</sub> )	ACROS Organics
Potassium phosphate monobasic (KH <sub>2</sub> PO <sub>4</sub> )	Fisher Scientific
Ammonium chloride (NH <sub>4</sub> Cl)	Fisher Scientific
Magnesium sulfate (MgSO <sub>4</sub> )	Fisher Scientific
Calcium chloride (CaCl <sub>2</sub> )	Sigma-Aldrich
Glucose	VWR Life Science

## 2.1.5 Amino Acids and Peptides

A series of amino acids and peptides were used in toxic peptide assays in this study. Some are used directly, whilst some are used in previous experiments performed by Dr Daniel Bawdon discussed in this work. Details of the amino acids and peptides discussed can be found in table 2.5.

**Table 2.5 – Amino acids and peptides used in this work.** All are stored at -20°C.

<b>Amino Acid/Peptide</b>	<b>Supplier</b>	<b>Stock Concentration</b>	<b>Solvent</b>
Alanine	Sigma-Aldrich	100 Mm	dH <sub>2</sub> O
Ala-Ala	Sigma-Aldrich	100 Mm	dH <sub>2</sub> O
Ala-Ala-Ala	Sigma-Aldrich	100 Mm	dH <sub>2</sub> O
Leucine	TCI (Tokyo Chemical Industry)	100 Mm	dH <sub>2</sub> O
Leu-Gly	FluoroChem	100 Mm	dH <sub>2</sub> O
Ala-Leu	Sigma-Aldrich	100 Mm	dH <sub>2</sub> O
Phe-Leu	FluoroChem	100 Mm	10% HCl
Valine	Thermo Scientific	100 Mm*	dH <sub>2</sub> O
Val-Tyr	Sigma-Aldrich	100 Mm	dH <sub>2</sub> O
DL-Val-Gly-Gly <sup>†</sup>	MP Biomedical	25Mm	dH <sub>2</sub> O
L-Val-Gly-Gly <sup>‡</sup>	Sigma-Aldrich	10µg/ml	dH <sub>2</sub> O
Met	Sigma-Aldrich	100 Mm	dH <sub>2</sub> O
Met-Gly	FluoroChem	100 Mm	dH <sub>2</sub> O

\*When used in Dr Daniel Bawdons work, the concentration of Valine used was 5µg/ml.

<sup>†</sup>A lower concentration of DL-Val-Gly-Gly is used in this study, due to limited remaining stocks available.

<sup>‡</sup>L-Val-Gly-Gly is referenced in relation to Dr Daniel Bawdon's work, in which it was used at the stated concentration, but is not directly used in this work.

## 2.2 Molecular and Biochemical Techniques

### 2.2.1 Genomic DNA Isolation

Genomic DNA was isolated from  $\Delta$ DB50 for use as template DNA in diagnostic PCR reactions, this was conducted using a Wizard<sup>®</sup> Genomic DNA Purification Kit (Promega). The strains were first grown overnight in LB media after which 1ml was harvested and transferred to a 1ml Eppendorf tube. The protocol was then conducted following instructions provided by the manufacturer.

### 2.2.2 Plasmid Mini Prep

Plasmid DNA was isolated from the strains carrying plasmids included in table 2.2, this was conducted using a GenElute Plasmid Miniprep Kit (Sigma-Aldrich). Strains of interest were grown overnight in LB media containing 100 $\mu$ g/ml Ampicillin (plasmid selective antibiotic – table 2.3), 1ml was then harvested and transferred to a 1ml Eppendorf tube. The protocol was then conducted following instructions provided by the manufacturer. The mini-prep product was then examined using a nanodrop spectrophotometer to ensure the procedure was successful, and then stored at -20 $^{\circ}$ C.

### 2.2.3 Polymerase Chain Reaction (PCR)

For the PCR described in this report, oligonucleotide primers were prepared as described in section 2.1.3. Template DNA consisted of isolated genomic (section 2.2.1) DNA for diagnostic PCRs for  $\Delta$ DB50.

The 50 $\mu$ l reaction mixture was prepared through the addition of the following components to a 0.5ml Eppendorf tube on ice: 10 $\mu$ l 5X Phusion HF buffer (NEB), 0.5 $\mu$ l 20mM dNTP mix (Thermo Scientific), 2.5 $\mu$ l 500nM forward primer, 2.5 $\mu$ l 500nM reverse primer, 2 $\mu$ l template DNA followed by the addition of dH<sub>2</sub>O to a final volume of 50 $\mu$ l. The PCR reaction was then conducted according to the conditions described in Table 2.6.



**Table 2.6 –  $\Delta$ DB50 genotyping PCR cycling parameters.**

Step	Temperature (°C)	Time
Initial Denaturation	98	30 seconds
Denaturation	98	10 seconds
Annealing	dtpA:	30 seconds
	dtpB:	
	dtpC:	
	dtpD:	
Extension	72	180 seconds
Final Extension	72	10 minutes
Hold	4	-

#### 2.2.4 Agarose gel electrophoresis

1% (w/v) agarose gels were created by melting 0.5g agarose (Melford) in 50ml 1X TBE buffer (Per litre dH<sub>2</sub>O: 10.8 g Tris HCl, 5.5 g Boric acid, 0.75 g EDTA). After cooling, 5 $\mu$ l 10,000X SYBR Safe DNA gel stain (Thermo Scientific) was added, following this the molten mixture was poured into a DNA electrophoresis gel tank. A comb was added to the still molten solution to create wells to create appropriately sized wells within the gel, which was then allowed to set at room temperature for 30 minutes.

DNA samples were prepared by combining the product of PCR reactions described in section 2.2.3 with 1 $\mu$ l DNA loading dye (NEB). The samples were then loaded into wells of the gel, and then electrophoresed at 100V for 30 minutes. After completion, the gels were visualised under a transilluminator within a Syngene GeneGenius Gel BioImaging Unit using Syngene GeneSnap software.

#### 2.2.5 Generation of Knockout Strains (Dr Daniel Bawdon & Emmanuele Severi)

To generate strains carrying deletions within genes coding for peptide transporters Dr Daniel Bawdon employed the protocol outlined by Datsenko and Wanner (2000). This methodology was used to induce successive gene deletions starting from a single KEIO collection strain ( $\Delta$ *dtpB* in the case of  $\Delta$ DB5,  $\Delta$ *dppC* in the case of  $\Delta$ DB1)(Baba et al., 2006). This led to the creation of a quadruple POT gene deletion strain known as  $\Delta$ DB5, alongside a double C-subunit ABC deletion strain known as  $\Delta$ DB1. The final genotypes can be found in Table 2.2. After the discovery of a genomic anomaly present within  $\Delta$ DB5 by Emmanuele Severi, the strain was later replaced with the otherwise equivalent strain  $\Delta$ DB50.

Records detailing the exact methodology used to generate  $\Delta$ DB5/ $\Delta$ DB1, and the subsequent decision to make  $\Delta$ DB50, were split across multiple sources. Using lab notebooks and other records the full history of  $\Delta$ DB50 and  $\Delta$ DB1 were chronicled in this report before lab work commenced.

### 2.2.6 Preparation of competent *E. coli* cells

The strain to be transformed (in this case,  $\Delta$ DB50) was grown in 5ml LB overnight at 37°C. The following day, 20ml of LB was inoculated with 1ml of the overnight culture, this was then incubated at 37°C for 2.5 hours, then separated into 1ml aliquots, which were incubated on ice for 50 minutes. These aliquots were then centrifuged for 5 minutes at 6000rpm at 4°C, after which the supernatant was discarded, and the pellet was resuspended in 100  $\mu$ l of ice cold 100 Mm CaCl<sub>2</sub> and left to incubate on ice for 50 minutes. The mixture was then centrifuged again at 6000 rpm at 4°C for 5 minutes, then resuspended in 50 $\mu$ l of ice-cold 100 Mm CaCl<sub>2</sub> and stored at -80°C until needed.

### 2.2.7 Transformation of competent *E. coli* with plasmid DNA

50 $\mu$ l aliquots of pre-prepared competent cells were thawed on ice for 30 minutes. 5 $\mu$ l of DNA was then added to the cells; in this case the plasmid DNA added was isolated from BW25113 strains carrying the individual pBADcLIC2005 based *ntp* genes (section 2.1.2) using a plasmid mini-prep method (section 2.2.2). The combined mixture was then gently inverted 5 times, then incubated on ice for 30 minutes. After incubation, the mixture was placed into a heat-block pre-heated to 42°C for 90 seconds, then placed back on ice and allowed to incubate for 2 minutes. 0.9ml of LB (pre-warmed to 37°C) was then added to the tube and mixed by inversion, then incubated at 37°C for 1 hour with shaking. After 1 hour, 100 $\mu$ l of the mixture was spread onto a selective LB plate (in this case containing 100 $\mu$ g/ml ampicillin) and incubated overnight at 37°C, after which a selection of colonies were then isolated from the plate and stocked in glycerol. In parallel to this process, a positive control in the form of commercially available competent cells (XL1 Blue – Agilent) and a negative control of pre-prepared competent cells without the addition of plasmid DNA were used to ensure the protocol was followed correctly.

Plasmid sequencing confirmed successful transformation of all 4 complementation strains, however these strains were not used further due to time limitations.

## 2.3 Microbiological Techniques

### 2.3.1 Bacterial growth

Bacteria were transferred aseptically from glycerol stocks onto LB agar plates using a sterile pipette tip, and then streaked out using standard technique. The plates were inverted and left at 37°C overnight, and then stored at 4°C for no longer than 2 weeks.

Liquid bacterial cultures were generated by transferring a single colony isolated from an agar plate to a 5ml solution of LB medium within a 50ml Falcon® conical centrifuge tube. This tube was then incubated at 37°C with shaking overnight.

Selective cultures were created by the addition of 5 $\mu$ l of Ampicillin (100mg/ml stock – table 2.1) to 5ml of LB creating a final working concentration of 100 $\mu$ g/ml. Selective agar plates

were created by the addition of 150µl Ampicillin (from the same stock) to 150ml of molten agar cooled to approximately 50°C, before pouring into Petri dishes as described in section 2.1.4.

### 2.3.2 Antibiotic Susceptibility Experiments

All growth experiments were conducted in a 96-well microplate (Nunc – ThermoFisher Scientific). Each well was first filled with 100µL LB except for wells in column 1 and column 12 which were filled with 200µL LB.

A pre-calculated volume of antibiotic was then added from the stock solution such that the final volume in all wells within column 1 was equivalent to double the concentration listed in table 2.7. Using a multi-channel pipette, the LB and antibiotic in column 1 wells were mixed, and then 100µL transferred to the subsequent column of wells and mixed by pipetting. This process was repeated until the final two columns remained (column 10 being the final column having antibiotic added), after which 100µL of the mixture was removed and discarded (leaving a final volume of 100µL in the wells. This served as a serial dilution, in which the wells of each subsequent column contained a concentration of antibiotic 50% lower to the previous column (Table 2.7). The range of concentrations tested was designed to include values both far above, approximately close to, and far below the MIC reported in the literature. This approach was utilized for all antibiotics, in order to ensure that any potential difference in susceptibility could be definitively identified.

**Table 2.7**– Concentrations of antibiotics tested. Numbers 1-10 represent columns within a 96 well plate used in this study.

Antibiotic	Concentrations (µg/ml)									
	1	2	3	4	5	6	7	8	9	10
Amoxicillin	320	160	80	40	20	10	5	2.5	1.25	0.63
Ampicillin	320	160	80	40	20	10	5	2.5	1.25	0.63
Carbenicillin	320	160	80	40	20	10	5	2.5	1.25	0.63
Kanamycin	320	160	80	40	20	10	5	2.5	1.25	0.63
Blastocidin S	500	250	125	62.5	31.3	15.6	7.8	4	2	1
Kasugamycin	500	250	125	62.5	31.3	15.6	7.8	4	2	1
Cephalexin	50	25	12.5	6.25	3.13	1.56	0.78	0.4	0.2	0.1
Cefadroxil	50	25	12.5	6.25	3.13	1.56	0.78	0.4	0.2	0.1

Overnights of bacterial strains to be tested were taken and diluted by a factor of 1:10, after which the optical density was measured using a Jenway 6305 spectrophotometer (OD<sub>650</sub>). This allowed for the calculation of the amount of liquid from the overnight culture to add to separate tubes of 10ml of LB to produce cultures of a standardised optical density (0.05). The deletion strains of bacteria tested were compared against an *E. coli* BW25113 wild type control strain (Table 2.2), with 100µL of the wild type strains transferred into all wells in rows 1-4, and 100µL of the strain of interest transferred into all wells in rows 5-8 (both from the standardised cultures) This methodology allows 4 technical repeats for each strain in the presence of each antibiotic concentration. **N.B:** This process doubles the volume in the wells,

and thus halves the concentration of antibiotic. Therefore, the final concentration of antibiotic in all wells is half the concentration before the addition of the culture. The final column (A12-H12) did not have culture added and served as a LB blank control.

The completed plate was then transferred to an Epoch microplate spectrophotometer set to continuously record the optical density of the wells at 650nm. The protocol used moved the plate in an orbital rotation at 37°C for 24 hours, with optical density readings taking place every 30 minutes.

This process was repeated 3 times on consecutive days using independent biological cultures generated from colonies within the same agar plate. Each data point therefore represents 12 individual datapoints (3 x biological repeats, each having 4 x technical repeats within a plate).

This methodology differs from that used by previous lab member Injae Chung to generate growth phenotype data. These experiments pre-date the microplate reader used in this work, and thus were conducted manually utilising a flask culture with periodic OD measurements. Although the resulting growth dynamics were similar between the two methodologies, the differing conditions resulted in different growth rates and maximum ODs between the two results, resulting in differing concentrations of antibiotics being needed in order to replicate the observed difference in susceptibility (see section 3.1).

### 2.3.3 Analysis of Growth Phenotype

All bacterial growth curve graphs were produced using R studio, utilising the “ggplot2” package (Wickham, 2016).

Growth metrics were calculated based on the combined data from all growth experiments for each individual antibiotic/condition using the “Growthcurver” R package (Sprouffske and Wagner 2016).

This package produces several outputs, three of which were used in this report.

**Intrinsic Growth Rate** – The growth rate that would occur if there were no restrictions imposed on total population size.

**Maximum OD** - The maximum possible population size in a particular environment (carrying capacity).

The intrinsic growth rate and maximum OD were calculated according to the following equation:

$$N_t = \frac{K}{1 + \left(\frac{K-N_0}{N_0}\right) e^{-rt}}$$

$N_t$  = number of cells at time  $t$

$N_0$  = population size at the start of the curve

$K$  = the maximum possible population size in a particular environment (maximum OD)

$r$  = intrinsic growth rate

Growthcurver finds the best values of  $K$ ,  $r$ , and  $N_0$  for the growth curve data using the implementation of the nonlinear least-squares Levenberg-Marquardt algorithm (Lin, O'Malley and Vesselinov 2016).

**Area under the curve** - Empirical AUC produced by summing the areas of the trapezoids made up by connecting consecutive data points of or absorbance measurements from time 0 to time  $t$ . This value allows incorporates the initial population size, growth rate and maximum OD into a single summary metric.

The three parameters are calculated automatically for each well within the plate, across all 3 repeats, and then combined into a single dataset. This method produced 12 data points for each strain & concentration combination at each time point, from this a value for each of the Growthcurver outputs can be calculated for each well. The mean ( $\bar{x}$ ) and standard deviation (SD) of each of these outputs was then calculated and is included in the figure legend of the growth curves displayed.

Preliminary analysis on the dataset using a Shapiro-Wilks test for normality determined that the dataset produced was not normally distributed (data not shown) and thus nonparametric tests were used throughout (Shapiro and Wilk, 1965; Kitchen, 2009). In order to compare the mean output for each parameter measured for the two strains, a Wilcoxon Rank Sum Test was used throughout. This is a commonly used non-parametric alternative to the two-sample T test, the output of which is included for each comparison referenced, and includes the following parameters:

**W** = the smaller of the rank totals of the two groups (the smaller the value, the less likely the result occurred by chance)

**p** = the probability that the true median value for the parameter tested is the same in the two groups.

The relevant output for the interpretation of the result is the  $p$ -value, on which the decision to reject the null hypothesis that "wild type *E. coli* and  $\Delta$ DB50/ $\Delta$ DB1 do not differ in the

parameter tested in the stated conditions” is based. In this study, a *p*-value of 0.05 or below is considered acceptable to reject this null hypothesis, leading to the conclusion of a statistically significant difference between the two groups.

#### 2.3.4 Toxic Peptide Inhibition Assays

Strains of interest were grown in M9 media (section 2.1.4) overnight until saturated, after which 400µL was transferred to a M9 media plate and evenly spread across the surface. These plates were then allowed to dry in a class II microbiology safety cabinet for 30 minutes.

5mm discs were cut from whatman filter paper using a handheld hole punch and autoclaved. 4 discs were then placed onto the surface of the plate in equidistant locations in each quadrant of the plate. A selection of di- and tripeptides were chosen which would be expected to be toxic to *E. coli* based on the literature (Table 2.8).

**Table 2.8** - Amino Acids and Peptides Used in the Toxic Peptide Inhibition Assay. \*L-ValGly-Gly was used in Dr Daniel Bawdon’s work but not in this study due to the original supplier discontinuing production. †A DL-stereoisomer mix was used as a substitute in this work but was not used in Dr Daniel Bawdon’s work.

Amino Acid/Peptide	Expected Result	Rationale
Alanine	Non-toxic (negative control)	Katsube, Ando and Yoneyama (2019)
Ala-Ala		
Ala-Ala-Ala		
Leucine	Non-Toxic	Tavori, Kimmel and Barak (1981)
Leu-Gly	Toxic	
Ala-Leu		
Phe-Leu		
Valine	Toxic (positive control)	Karkhanis, Mascarenhas and Martinis (2007)
Val-Tyr	Toxic	
DL-Val-Gly-Gly*		
L-Val-Gly-Gly <sup>†</sup>		
Met	Non-toxic	Vrajesh A. Karkhanis et al (2007)
Met-Gly		

10µL of the Amino Acid/Peptide of interest (directly from the stock – table 2.5) were dropped onto the filter paper discs, after which the plates were incubated (non-inverted) overnight at 37°C. Images were then taken and edited using the upper light function and camera within a Syngene GeneGenius Gel BioImaging Unit.

## 2.4 Bioinformatics

In order to examine the phylogenetic distribution of POT transporters across pathogenic bacteria, a series of pathogenic species were chosen for examination. The desired selection needed to include species which were representative of a range of biological attributes including gram-staining, shape, oxygen requirement and intra/extracellular niche. An appropriate list was found within the textbook 'Microbiology' (Harvey, Cornelissen and Fisher, B.D. 2007). Of the species included within the list, strains which are known to be pathogenic were then chosen resulting in a list of pathogenic strains which was then used for the subsequent analysis (supplementary table 1). The POT complement of the strains identified using TransportDB – a database of bacterial transporters (Elbourne et al. 2017). When a species was identified via TransportDB as having a predicted POT transporter within the genome, the protein name and amino acid sequence were recorded. Species which did not have POT transporters were also recorded as such. The primary sequences of the POT transporters identified were aligned using the programme Jalview (Waterhouse et al. 2009). The completed alignment was then used to infer a maximum likelihood tree using IQ-TREE (Trifinopoulos et al. 2016). This tree was then visualised and annotated using the Interactive Tree Of Life (iTOL) (Letunic and Bork 2021).

For each the species selected for use in the phylogenetic analysis, the number of POTs present in the genome was obtained via TransportDB. The species and their associated number of POTs were divided based on a number of factors including gram staining, oxygen requirement and environmental niche. The number of POTs identified in these species were then compared based on these characteristics. For simplicity, species classed as either 'Facultative Anaerobes' or 'Facultative Intracellular' were not included in the relevant analyses due to the potential confounding effect.

Comparisons of the number of POTs identified in the two groups were conducted using a Kruskal-Wallis, which was deemed appropriate due to the independent nature of the independent nature of the measurements within the groups. The output of the test includes the following parameters:

$\chi^2 (n) = y$ . Where  $\chi^2$  is the Chi-squared value (making  $y$ ) used to determine if the difference between the two groups is significant, and  $(n)$  is the degrees of freedom.

$p$  = the probability that the two groups in the comparison originate from statistically significantly different distributions.

## 3 Results

### 3.1 Antibiotic susceptibility experiments

#### 3.1.1 Growth comparison of $\Delta$ DB50 wild type *E. coli* in LB

According to the proposed intrinsic resistance hypothesis, peptide transporters contribute to the basal level of resistance to beta-lactam antibiotics observed in bacteria. Therefore, since all 4 POT transporters within  $\Delta$ DB50 have been deleted, the strain would be expected to have a higher susceptibility to beta-lactam antibiotics, since the contribution of the POT transporters to the level of resistance has been lost. This allows the hypothesis to be tested indirectly through comparing growth dynamics of wild type *E. coli* and  $\Delta$ DB50 in the presence of beta-lactam antibiotics, and antibiotics which have previously been demonstrated to be substrates of the POTs.

To compare the susceptibility of wild type *E. coli* and  $\Delta$ DB50 to antibiotics, their growth dynamics in the absence of an antibiotic must first be understood. Injae Chung previously found that  $\Delta$ DB5 displayed a growth defect compared to wild type *E. coli* in LB alone (Figure 3.1A). Since the discovery of the genomic inversion present in  $\Delta$ DB5, the newly developed strain  $\Delta$ DB50 was chosen for use in future growth phenotype experiments. Therefore, it was necessary to determine if  $\Delta$ DB50 shared the growth defect in LB seen in  $\Delta$ DB5.

Based on the observed growth dynamics of the two strains,  $\Delta$ DB50 appears to have a more similar growth phenotype to wild type *E. coli* than  $\Delta$ DB5 in LB (figure 3.1B). This is confirmed by analysis using the R package Growthcurver, the results of which can then undergo statistical examination (section 4.3.2). Under such an analysis, the two strains generate an equivalent area under the curve ( $p= 0.159$ ,  $W=2945$ ), reach the same maximum OD ( $p= 0.098$ ,  $W=3007$ ) and have a comparable intrinsic growth rate ( $p= 0.718$ ,  $W=2683$ ). The lack of a statistically significant difference between the two strains based on all three parameters examined implies that any difference in growth in the presence of an antibiotic is likely due to the presence of the antibiotic itself, rather than any intrinsic difference in growth between the two strains.



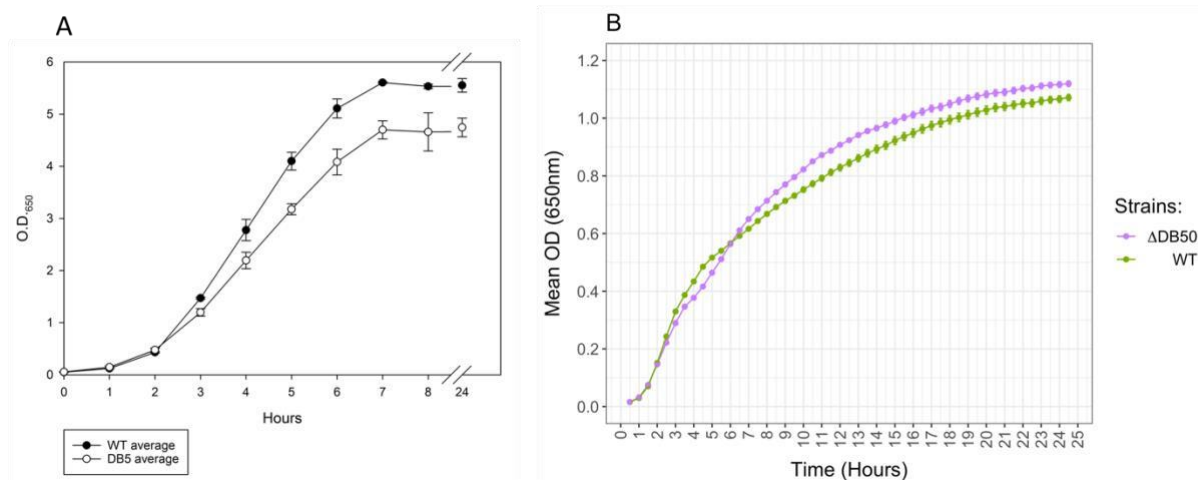


**Figure 3.1 – Comparison of POT deletion mutants and wild type *E. coli* growth dynamics in LB.** **A)** Comparison of growth dynamics of  $\Delta$ DB5 and wild type BW25113 *E. coli* in LB without antibiotic present. Data points represent a mean of 3 OD measurements from independent biological samples taken hourly for a period of 8 hours, and once at 24 hours from the start of growth. Error bars denote standard deviation. Data produced by Injae Chung. **B)** Comparison of growth dynamics of  $\Delta$ DB50 and wild type BW25113 *E. coli* (see table 2.2 for provenance) in LB without antibiotic present. Data points represent a mean of 80 OD measurements, with readings taken at 30-minute intervals for a 24.5-hour period. Each mean is calculated from 20 sets of 4 technical repeats, in which each set originated from a single biological sample. Error bars denote standard error. Area under the curve (WT:  $\bar{x}$  = 681.5, SD=43.5, n=80 | DB50:  $\bar{x}$  = 726.2, SD=47.3, n=80), maximum OD (WT:  $\bar{x}$  = 0.81, SD=0.03, n=80 | DB50:  $\bar{x}$  = 0.87 SD=0.02, n=80), intrinsic growth rate (WT:  $\bar{x}$  = 0.01, SD=5.0  $\times 10^{-4}$ , n=80 | DB50:  $\bar{x}$  = 0.01 SD=8.0  $\times 10^{-4}$ , n=80) – **n.b:** the equivalent data for Injae Chung’s work is unavailable. Data produced in this study.

### 3.1.2 Comparison of wild type *E. coli* and $\Delta$ DB50 susceptibility to Ampicillin

The first antibiotic examined in relation to the intrinsic resistance hypothesis was ampicillin - a semi-synthetic penam type  $\beta$ -lactam antibiotic (section 1.5.1). The structure of ampicillin is formed from a penicillin molecule in which the substituent group at position 6 of the penam ring is a 2-amino-2-phenylacetamido group, classifying it as an aminopenicillin (Figure 3.2A)(PubChem, 2004).

Ampicillin was previously investigated by Injae Chung in relation to  $\Delta$ DB5, in which context, wild type *E. coli* displayed a stronger growth phenotype than  $\Delta$ DB5 in the presence of Ampicillin. This phenotype manifested in the form of growth inhibition at a concentration of ampicillin in which wild type *E. coli* can grow (Figure 3.2B) or a slower growth rate and maximum OD in conditions in which growth is possible for both strains (Figure 3.2C).

However, as discussed previously this weaker growth phenotype was also seen to be present in the absence of the antibiotic (Figure 3.7A), thus it was impossible to definitively attribute the difference in growth phenotype to a difference in antibiotic susceptibility. Furthermore, at the time this experiment was performed, the genomic anomaly present in  $\Delta$ DB5 was not

known. It was therefore necessary to perform the same test in using  $\Delta$ DB50 in place of  $\Delta$ DB5, alongside using the wild type *E. coli* BW25113 strain demonstrated in this study to have equivalent growth dynamic (Figure 3.7B).

In the presence of 20 $\mu$ g/ml ampicillin, wild type and  $\Delta$ DB50 initially grow similarly but begin to diverge at approximately the 2-hour time point. At this stage the wild type strain continues to grow (albeit at a slower rate than in the absence of the antibiotic), whilst growth of  $\Delta$ DB50 slows significantly, and appears delayed compared to the wild type. Through the remainder of the time course, the wild type strain recovers from the initial prolonged lag phase, reaching an equivalent growth rate to in the absence of the antibiotic ( $p= 0.178$ ,  $W= 96$ ). Meanwhile,  $\Delta$ DB50 is unable to fully recover from the initial loss in growth, entering a premature stationary phase which is both much lower than the same strain in the absence of the antibiotic, and the wild type strain in the same conditions (Figure 3.2D). This growth dynamic results in a significantly lower area under the curve ( $p= 0.001$ ,  $W= 16$ ) and maximum OD ( $p= 0.019$ ,  $W= 31$ ) generated by  $\Delta$ DB50 compared to wild type *E. coli*.

This difference in growth phenotype is further demonstrated in 10 $\mu$ g/ml ampicillin, with the wild type strain being unaffected by the antibiotic for longer, with less restricted growth afterwards, whilst  $\Delta$ DB50 appears to be similarly affected to in 20 $\mu$ g/ml ampicillin. After the initial loss in growth, both strains are able to recover and follow a similar growth pattern with an equivalent growth rate ( $p= 0.977$ ,  $W= 73$ ). However, the ability of the wild type strain to continue growing for longer than  $\Delta$ DB50 in initial growth phases results in a significantly higher area under the curve ( $p= 0.002$ ,  $W= 19$ ) and maximum OD ( $p= 0.002$ ,  $W= 18$ )(Figure 3.2E).

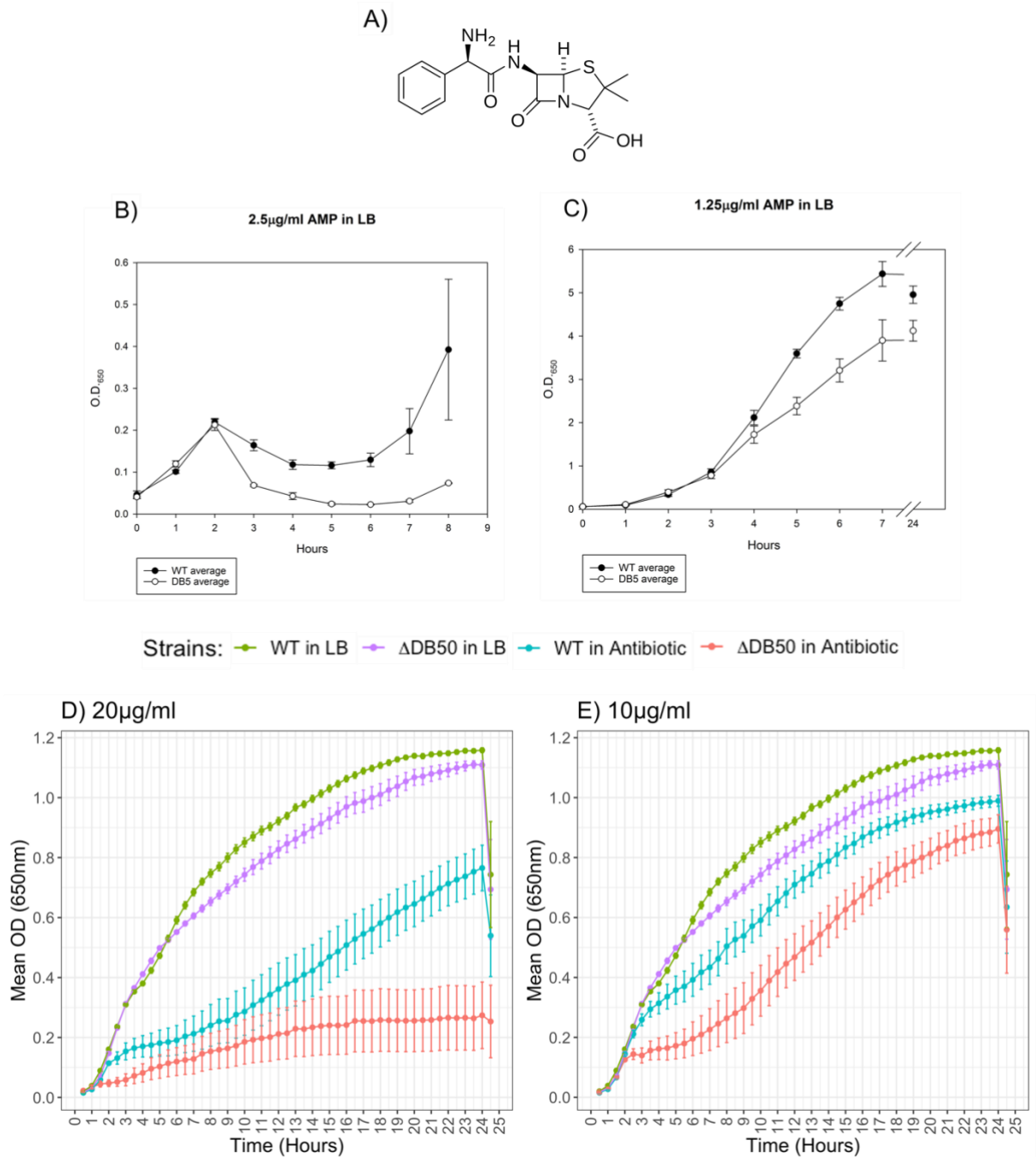


**Figure 3.2 – Growth comparison in ampicillin.** **A)** Skeletal structure of ampicillin (AMP). **B and C)** Growth experiments comparing wild type BW25113 *E. coli* (n=3)  $\Delta$ DB5 (n=3) in the presence of varying concentrations of AMP over a 24-hour period (up to 9 hours shown in C), performed by Injae Chung. Concentration of AMP: **B)** No AMP (LB only) **C)** 2.5µg/ml **D)** 1.25µg/ml. Error bars denote standard deviation. **D and E)** Growth experiments comparing wild type BW25113 *E. coli* (n=12) and  $\Delta$ DB50 (n=12) in the presence of varying concentrations of AMP over a 24-hour period. Concentration of AMP: **D)** 20µg/ml **E)** 10µg/ml. **20µg/ml:** area under the curve (WT:  $\bar{x}$  =48.2, SD=20.6, n=12 | DB50:  $\bar{x}$  = 0.36, SD=0.14, n=12), maximum OD (WT:  $\bar{x}$  =0.2, SD=0.09, n=12 | DB50:  $\bar{x}$  = $3.0 \times 10^{-4}$ , SD= $3.0 \times 10^{-4}$ , n=12), intrinsic growth rate (WT:  $\bar{x}$  =0.006, SD= $6.0 \times 10^{-4}$ , n=12 | DB50:  $\bar{x}$  = 0.002 SD= $6.0 \times 10^{-4}$ , n=12). **10µg/ml:** area under the curve (WT:  $\bar{x}$  =0.009, SD= $8.0 \times 10^{-4}$ , n=12 |

DB50:  $\bar{x} = 0.007$ ,  $SD=1.0 \times 10^{-4}$ ,  $n=12$ ), maximum OD (WT:  $\bar{x} = 0.009$ ,  $SD=8.0 \times 10^{-4}$ ,  $n=12$  | DB50:  $\bar{x} = 0.007$ ,  $SD=0.001$ ,  $n=12$ ), intrinsic growth rate (WT:  $\bar{x} = 0.009$ ,  $SD=8.0 \times 10^{-4}$ ,  $n=12$  | DB50:  $\bar{x} = 0.007$ ,  $SD=0.01$ ,  $n=12$ ). Error bars denote standard error, data generated in this study.

Therefore, the evidence shown here indicates that  $\Delta$ DB50 has a higher susceptibility to ampicillin than wild type *E. coli*. This recapitulates the results observed in  $\Delta$ DB5, and thus implies the observed phenotype is likely due to the loss of the POT transporters, rather than the presence of the genomic inversion. Furthermore, the ability of this method to effectively discriminate between  $\Delta$ DB50 and wild type *E. coli* on the basis of antibiotic susceptibility provides a reasonable proof of concept for the intrinsic resistance hypothesis, based on which future comparisons using novel antibiotics can be conducted. 20 $\mu$ g/ml and 10 $\mu$ g/ml ampicillin were the only concentrations which were discriminatory for susceptibility between the two strains.

### 3.1.3 Comparison of wild type *E. coli* and $\Delta$ DB50 susceptibility to Amoxicillin

Amoxicillin is another aminopenicillin beta-lactam antibiotic, formed from a penicillin backbone in which the substituent at position 6 of the penam ring is a 2-amino-2-(4hydroxyphenyl)acetamido group, differing from ampicillin which lacks the addition of a hydroxide group (Figure 3.3A, PubChem, 2004).

In the presence of 10 $\mu$ g/ml amoxicillin,  $\Delta$ DB50 undergoes a brief prolonged lag phase in the initial stages of growth which wild type *E. coli* does not. This again results in a smaller area under the curve ( $p=0.001$ ,  $W=128$ ), maximum OD ( $p=0.001$ ,  $W=127$ ) and growth rate ( $p=0.01$ ,  $W=30$ ) being generated by  $\Delta$ DB50 compared to the wild type (Figure 3.3C).

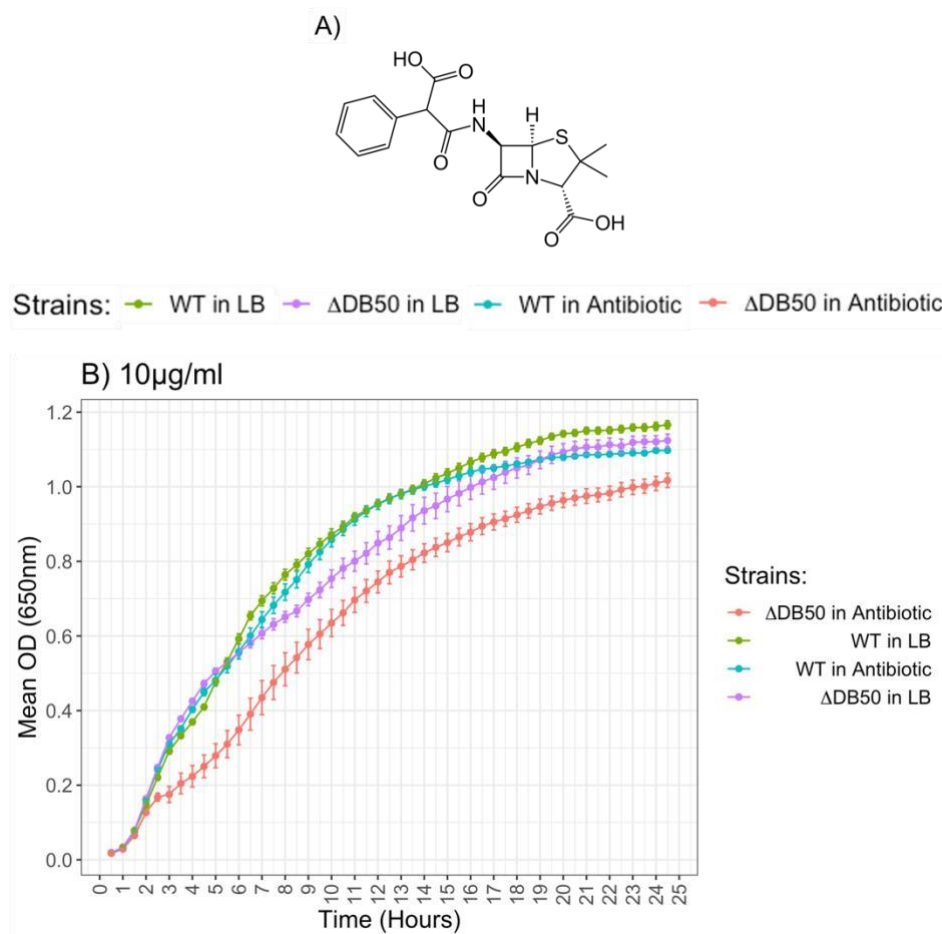


**Figure 3.3 – Growth comparison in amoxicillin.** A) Skeletal structure of amoxicillin . B) Growth experiments comparing wild type BW25113 *E. coli* (n=12) and  $\Delta$ DB50 (n=12) in the presence of 10 $\mu$ g/ml amoxicillin over a 24-hour period. Datapoints represent a mean of 12 OD measurements taken at 30-minute intervals, error bars denote standard error, data generated in this study. Area under the curve (WT:  $\bar{x}$  =63.5, SD=22.8 n=12 | DB50:  $\bar{x}$  = 35, SD=11.9, n=12), maximum OD (WT:  $\bar{x}$  =0.17, SD=0.07, n=12 | DB50:  $\bar{x}$  =3.0 x 10<sup>-4</sup>, SD=3.0 x 10<sup>-4</sup>, n=12), intrinsic growth rate (WT:  $\bar{x}$  =0.01, SD=0.005, n=12 | DB50:  $\bar{x}$  = 0.08, SD=0.04, n=12).

The evidence presented here thus implies that  $\Delta$ DB50 has a higher susceptibility to amoxicillin than wild type *E. coli*.

### 3.1.4 Comparison of wild type *E. coli* and $\Delta$ DB50 susceptibility to Carbenicillin

Carbenicillin is a beta-lactam antibiotic formed from a penicillin backbone with a 6-beta-2carboxy-2-phenylacetamido sidechain (PubChem, 2004)(Figure 3.4A), thus belonging to the carboxypenicillin sub-class.

In the presence of 10 $\mu$ g/ml carbenicillin, both strains initially grow normally. However, at approximately the 2.5-hour time point, growth of  $\Delta$ DB50 begins to stall with a decreasing OD. Simultaneously, the wild type is able to continue growing until the 5-hour time point, when growth begins to slow and fluctuate around an OD of 0.4, only increasing in growth rate towards the end of the time period. This likely represents a similar prolonged lag phase to that experienced by  $\Delta$ DB50, only occurring at a later time point. The delayed reaction of the wild type strain to the presence of the antibiotic results in a significantly larger area under the curve being generated through the time course ( $p=0$ ,  $W=4$ ) After passing through the prolonged lag phase, both strains follow a similar growth pattern, reaching an equivalent maximum OD by the end of the time course ( $p=0.58$ ,  $W=82$ ), despite the wild type strain having an overall higher growth rate ( $p=0.029$ ,  $W=0$ )(Figure 3.4B).

In the presence of 5 $\mu$ g/ml carbenicillin,  $\Delta$ DB50 experiences a much shorter prolonged lag phase at approximately 2.5 hours, but quickly recovers, growing for some time before reaching a premature stationary phase. The wild type strain does not undergo a similar prolonged lag phase and is able to continue growing past the point at which growth of  $\Delta$ DB50 has stalled entirely, resulting in a significantly larger area under the curve ( $p=0$ ,  $W=0$ ) and maximum OD ( $p=0.029$ ,  $W=0$ ). However, the wild type strain is still affected to some extent by the presence of the antibiotic, with a lower area under the curve ( $p=0$ ,  $W=2$ ) and maximum OD ( $p=0$ ,  $W=0$ ) than in LB alone (Figure 3.4C). A similar pattern of increased susceptibility was observed in 2.5 $\mu$ g/ml carbenicillin (supplementary figure 1), though all other concentrations did not discriminate between the two strains.

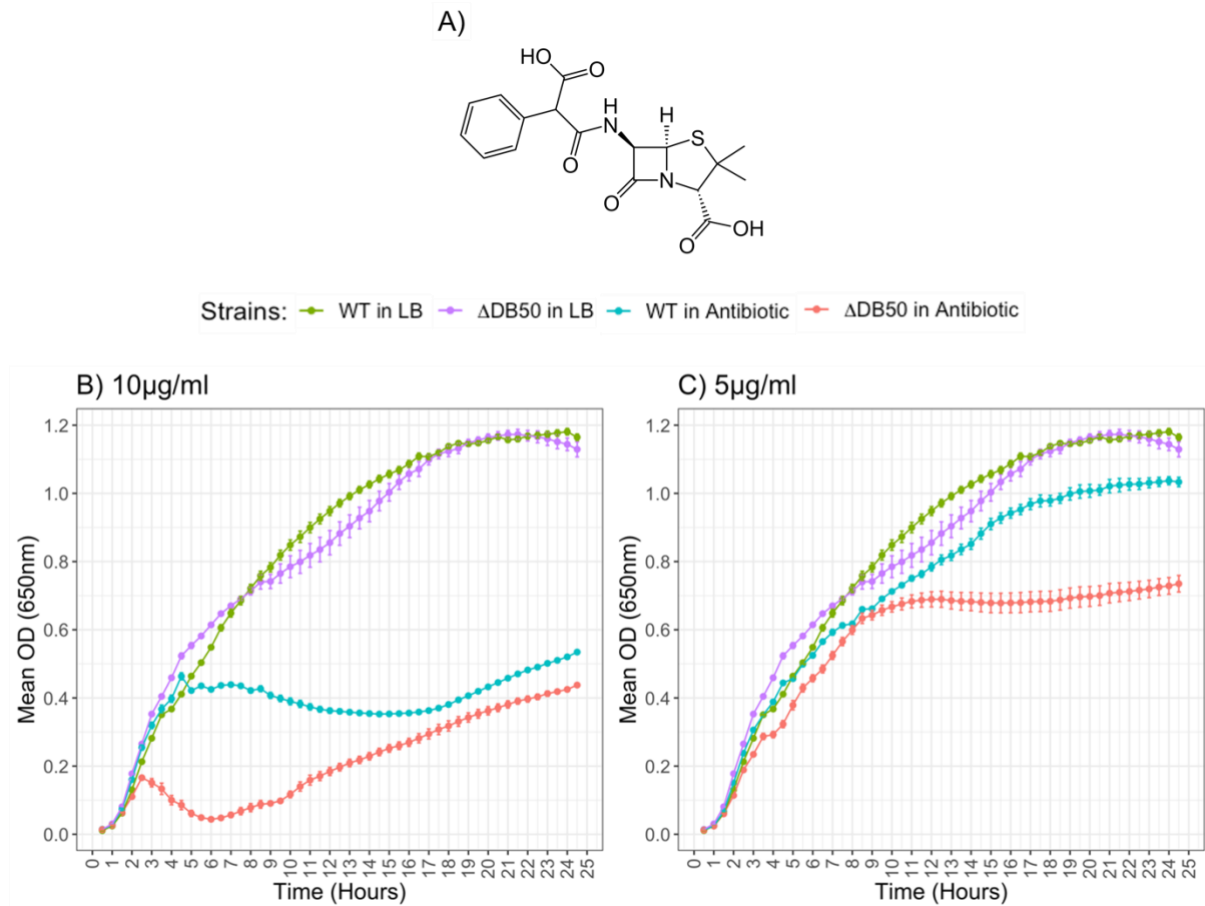


**Figure 3.4** – Growth comparison in carbenicillin. A) Skeletal structure of carbenicillin . B and C) Growth experiments comparing wild type BW25113 *E. coli* (n=12) and  $\Delta$ DB50 (n=12) in the presence of 10 $\mu$ g/ml (B) or 5 $\mu$ g/ml (C) carbenicillin over a 24-hour period. Datapoints represent a mean of 12 OD measurements taken at 30-minute intervals, error bars denote standard error, data generated in this study. **10 $\mu$ g/ml**: area under the curve (WT:  $\bar{x}$  =585.3, SD=61, n=12 | DB50:  $\bar{x}$  = 285.4, SD=160.3 n=12), maximum OD (WT:  $\bar{x}$  =295012.4, SD=613898, n=12 | DB50:  $\bar{x}$  =8546.4, SD=29603.9, n=12), intrinsic growth rate (WT:  $\bar{x}$  =0.02, SD=0.009, n=12 | DB50:  $\bar{x}$  = 0.004 SD=0.006, n=12). **5 $\mu$ g/ml**: area under the curve (WT:  $\bar{x}$  =1006.6, SD=43.6 , n=12 | DB50:  $\bar{x}$  = 848, SD=75.4 n=12), maximum OD (WT:  $\bar{x}$  =0.95, SD=0.07, n=12 | DB50:  $\bar{x}$  =0.72, SD=0.08, n=12).

Therefore, the evidence shown here indicates that  $\Delta$ DB50 has a higher susceptibility to carbenicillin than wild type *E. coli*.

### 3.1.5 Comparison of wild type *E. coli* and $\Delta$ DB50 susceptibility to Cefalexin and Cefadroxil

Cefalexin and cefadroxil represent a distinct class of beta-lactam antibiotics known as the cephalosporins (section 1.5.1), which differ in their core ring structure to the penam type antibiotics examined previously but are otherwise analogues of ampicillin and amoxicillin respectively (Figure 3.1A, 3.2A, 3.5A, 3.5B). These two antibiotics were tested to explore the effect of core ring structure in relation to the intrinsic resistance hypothesis.

In the presence of 6.25 $\mu$ g/ml cefalexin, growth of both strains is initially inhibited. At approximately the 7.5-hour mark, both strains begin to grow again, however wild type *E. coli* begins growing at a faster rate than  $\Delta$ DB50 ( $p=0.001$ ,  $W=18$ ). The growth of the wild type strain begins to slow by the end of the time course reaching a stationary phase, this allows  $\Delta$ DB50 to catch up, reaching an equivalent maximum OD ( $p=1$ ,  $W=72$ ). Despite this, the slower rate of growth of  $\Delta$ DB50 throughout the time course results in a smaller area under the curve being generated ( $p=0$ ,  $W=0$ )(Figure 3.5C).

A similar pattern is observed in 3 $\mu$ g/ml cefalexin, however in this case growth is not inhibited, instead growth of both strains is briefly stalled at the 3-hour period. This effect is shorter in the wild type strain, allowing growth to rapidly resume. Meanwhile in  $\Delta$ DB50 this phase lasts longer, leading to a decreased area under the curve being generated through the remainder of the time course ( $p=0.004$ ,  $W=23$ ). Despite the delayed start to growth,  $\Delta$ DB50 reaches a comparable growth rate to the wild type strain ( $p=0.068$ ,  $W=240$ ), allowing an equivalent maximum OD to be reached by the end of the time course ( $p=0.347$ ,  $W=55$ )(Figure 3.5D), in a similar fashion to that observed in 6.25 $\mu$ g/ml cefalexin (Figure 3.5C). A similar pattern was observed at 12.5 $\mu$ g/ml cephalexin (supplementary figure 3), but all other concentrations did not discriminate between the two strains.

Exposure to 12.5 $\mu$ g/ml cefadroxil elicits a similar reaction to in 3 $\mu$ g/ml cefalexin, with the wild type strain briefly stalling before growth resumes, while  $\Delta$ DB50 is more severely affected and takes longer for growth to recover. Whilst this results in a larger area under the curve being generated by the wild type strain ( $p=0.045$ ,  $W=37$ ),  $\Delta$ DB50 is again able to catch up reaching an equivalent OD by the end of the time course ( $p=0.486$ ,  $W=5$ ) (Figure 3.5E). Unlike the other beta-lactam antibiotics examined thus far, 12.5 $\mu$ g/ml cefadroxil was the only concentration in which a difference in response was present between  $\Delta$ DB50 and wild type *E. coli*.



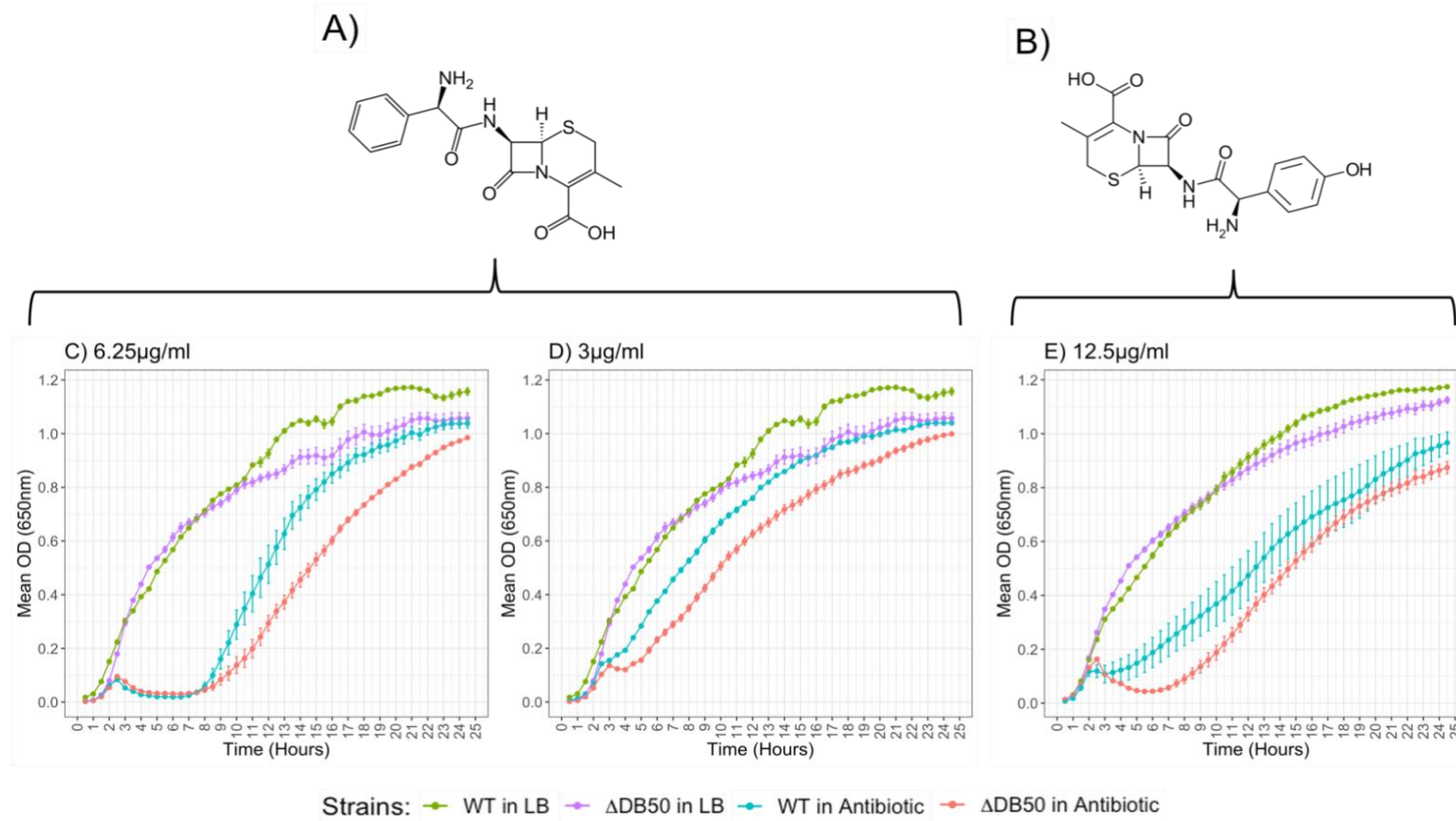


**Figure 3.5 – Growth phenotype comparison in cephalexin or cefadroxil. A and B) Skeletal structure of Cefalexin (A) and Cefadroxil (B). (CE) Growth experiments comparing wild type BW25113 E. coli (n=12) and ΔDB50 (n=12) in the presence of differing concentrations of cephalexin (C and D) or cefadroxil (E). C) 6.25µg/ml cephalexin:** area under the curve (WT:  $\bar{x}$  =48.2, SD=71.5, n=12 | DB50:  $\bar{x}$  = 0.36, SD=0.5 n=12), maximum OD (WT:  $\bar{x}$  =91.5, SD=316.4, n=12 | DB50:  $\bar{x}$  =0.003, SD=0.009, n=12), intrinsic growth rate (WT:  $\bar{x}$  =0.006, SD=0.005, n=12 | DB50:  $\bar{x}$  = 0.002, SD=0.002, n=12). **D) 3µg/ml cephalexin:** area under the curve (WT:  $\bar{x}$  =124.73, SD=68.4, n=12 | DB50:  $\bar{x}$

= 59.1, SD=86.8, n=12), maximum OD (WT:  $\bar{x}$ =0.42, SD=0.24, n=12 | DB50:  $\bar{x}$ =0.003, SD=0.25, n=12), intrinsic growth rate (WT:  $\bar{x}$ =0.009, SD=0.003, n=12 | DB50:  $\bar{x}$ =0.007, SD=0.004, n=12). **E) 12.5 $\mu$ g/ml cefadroxil:** area under the curve (WT:  $\bar{x}$ =711, SD=306.7, n=12 | DB50:  $\bar{x}$ =558.4, SD=84.4, n=12), maximum OD (WT:  $\bar{x}$ =0.94, SD=0.12, n=12 | DB50:  $\bar{x}$ =0.86, SD=0.07, n=12), intrinsic growth rate (WT:  $\bar{x}$ =0.008, SD=0.005, n=12 | DB50:  $\bar{x}$ =0.005, SD=7.0 x 10<sup>-4</sup>, n=12).

These results imply that  $\Delta$ DB50 has a higher susceptibility to both cefalexin and cefadroxil (albeit at a more limited range of concentrations in the latter). This conclusion would also imply that the core ring structure within a beta-lactam does not change the response of the POTs predicted under the intrinsic resistance hypothesis, thus indicating that the core betalactam structure does not affect the affinity of the POT transporters.

### 3.2 Comparison of wild type *E. coli* and $\Delta$ DB50 susceptibility to Kanamycin

Kanamycin is a bactericidal aminoglycoside antibiotic which targets the ribosome, inhibiting protein synthesis (Nishimura, Tanaka and Umezawa 1965). However, it does not contain a peptide bond within its structure (Figure 3.6A), and therefore would not be assumed to be a substrate of the POT transporters. For this reason, kanamycin was used as a negative control to test for non-specific transport of antibiotics by the POT transporters. The concentrations shown are closest to the reported MIC of approximately 30 $\mu$ g/ml (Guo et al., 2013).

In the presence of 40 $\mu$ g/ml kanamycin, growth of both strains is initially inhibited, but both eventually begin to grow at approximately 7 hours. Past this point, the two strains follow similar growth dynamics, with a similar growth rate when growth resumes ( $p=0.2$ ,  $W=3$ ), leading to an equivalent area under the curve ( $p=0.09$ ,  $W=42$ ), despite  $\Delta$ DB50 having a slightly reduced maximum OD ( $p=0.03$ ,  $W=0$ )(Figure 3.6B).

When exposed to 20 $\mu$ g/ml kanamycin, growth of both strains is limited compared to in LB alone, but not inhibited entirely. The growth dynamics of the wild type and  $\Delta$ DB50 fluctuate, but do not differ significantly, resulting in an equivalent area under the curve ( $W=58$   $n_1=12$ ,  $n_2=12$ ,  $p=0.44$ ), growth rate ( $p=0.34$ ,  $W=12$ ) and maximum OD ( $p=0.11$ ,  $W=2$ )(Figure 3.6C). The response of the two strains to any of the concentrations tested both above and below those shown here again do not differ significantly (supplementary figure 4).

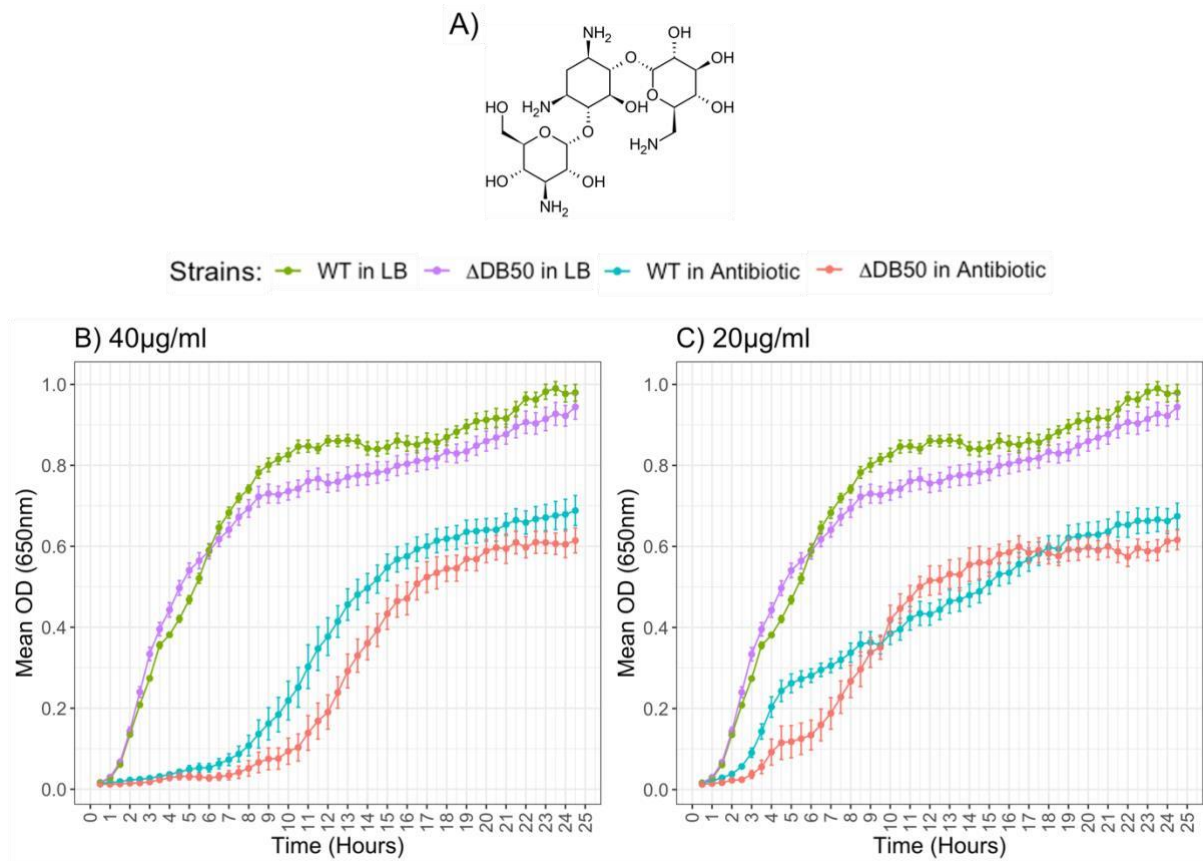


**Figure 3.6 – Growth comparison in kanamycin. A)** Skeletal structure of kanamycin . **B and C)** Growth experiments comparing wild type BW25113 *E. coli* (n=12) and  $\Delta$ DB50 (n=12) in the presence of **(B)** 10 $\mu$ g/ml or **(C)** 5 $\mu$ g/ml kanamycin over a 24-hour period. Datapoints represent a mean of 12 OD measurements taken at 30-minute intervals, error bars denote standard error. Data generated in this study. **40 $\mu$ g/ml:** area under the curve (WT:  $\bar{x}$  =500.3, SD=119.2, n=12 | DB50:  $\bar{x}$  = 400.19, SD=81.5, n=12), maximum OD (WT:  $\bar{x}$  =0.65, SD=0.12, n=12 | DB50:  $\bar{x}$  =0.6, SD=0.12, n=12), intrinsic growth rate (WT:  $\bar{x}$  =0.01, SD=0.004, n=12 | DB50:  $\bar{x}$  = 0.001, SD=0.005, n=12). **20 $\mu$ g/ml:** area under the curve (WT:  $\bar{x}$  =585.9, SD=108.1, n=12 | DB50:  $\bar{x}$  = 555.8, SD=91, n=12), maximum OD (WT:  $\bar{x}$  =0.69, SD=0.2, n=12 | DB50:  $\bar{x}$  =0.6, SD=0.07, n=12), intrinsic growth rate (WT:  $\bar{x}$  =0.04, SD=0.001, n=12 | DB50:  $\bar{x}$  = 0.01, SD=0.003, n=12).

These results imply that wild type *E. coli* and  $\Delta$ DB50 do not differ in their susceptibility to kanamycin. This implies that the increased susceptibility of  $\Delta$ DB50 to beta-lactams is specific to the peptidometric antibiotics, and not a generalised sensitivity to antibiotics.

### 3.2.1 Growth comparison of $\Delta$ DB51 and wild type *E. coli* in LB

Kasugamycin and blasticidin S are aminoglycoside antibiotics which target the ribosome, interfering with protein synthesis by disrupting translation (Takeuchi et al., 1958; Umezawa et al., 1965). There is existing evidence that they are substrates by the *E. coli* ABC peptide transporters (Shiver et al., 2016), however their affinity in relation to *E. coli* POT transporters has not been investigated. For this reason, the susceptibility of both  $\Delta$ DB50 and  $\Delta$ DB1 was tested.

To compare growth of  $\Delta$ DB1 and wild type *E. coli* in the presence of an antibiotic, it was first necessary to confirm the growth dynamics of the two strains do not differ in the LB alone, in a similar way to  $\Delta$ DB50 was examined (Figure 3.1).

Based on the growth pattern of the two strains across the 24-hour period, the two strains appear to share a similar growth dynamic. This is confirmed through a lack of statistically significant difference in maximum growth rate ( $p=0.798$ ,  $W=35$ ), area under the curve generated ( $p=0.105$ ,  $W=48$ ) or maximum OD reached ( $p=0.235$ ,  $W=44$ ). This implies that similarly to  $\Delta$ DB50,  $\Delta$ DB1 and wild type *E. coli* have equivalent growth dynamics in LB based on the parameters tested (Figure 3.7).

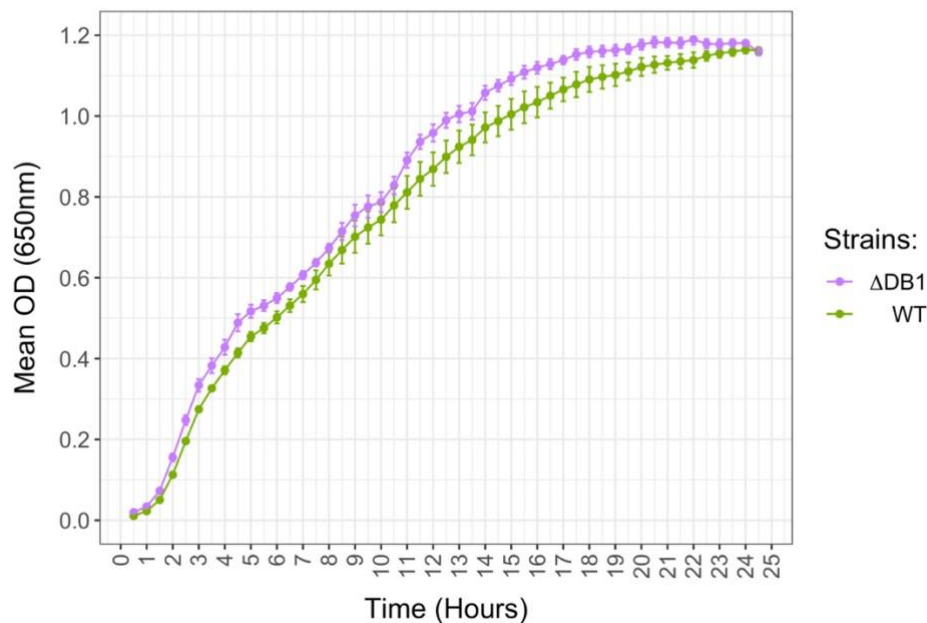


**Figure 3.7 – Growth dynamics of  $\Delta$ DB1 and wild type *E. coli*.** Comparison of growth dynamics of  $\Delta$ DB1 and wild type BW25113 *E. coli* in LB without antibiotic present. Data points represent a mean of 8 OD measurements, with readings taken at 30-minute intervals for a 24.5-hour period. Each mean is calculated from 2 sets of 4 technical repeats, in which

each set originated from a single biological sample. Error bars denote standard error. Data generated in this study. Area under the curve (WT:  $\bar{x}$  =1121.7, SD=85.6, n=8 | DB50:  $\bar{x}$  = 1190.9, SD=36.9, n=8), maximum OD (WT:  $\bar{x}$  =1.15, SD=0.04, n=8| DB50:  $\bar{x}$  = 1.17, SD=0.04, n=8), intrinsic growth rate (WT:  $\bar{x}$  =0.005, SD=0.001, n=8| DB50:  $\bar{x}$  = 0.005, SD=9.0 x 10<sup>-4</sup>, n=8). **n.b:** the equivalent data for Injae Chung's work is unavailable.

Therefore, similarly to  $\Delta$ DB50, any difference in growth in the presence of the antibiotic can likely be attributed to a difference in susceptibility between the two strains, rather than an intrinsic difference in growth.

### 3.2.2 Comparison of wild type *E. coli* and $\Delta$ DB50/ $\Delta$ DB1 susceptibility to Blastocidin S and Kasugamycin.

Despite not being beta-lactam antibiotics, both possess a peptide bond within their structure, making them peptidomimetic (Figure 3.8A and 3.8B). Due to their mode of action, if these antibiotics are substrates of the peptide transporters it would be disadvantageous for the bacteria, through transporting the antibiotic closer to its site of action (rather than outside of it, as in the case of the beta-lactam antibiotics). Therefore, in this case based on the intrinsic resistance hypothesis the peptide transporter knockout strains would be expected to be more resistant to the antibiotics.

#### **Comparison of susceptibility of wild type *E. coli* and $\Delta$ DB1 to and blastocidin S and kasugamycin.**

In the presence of 50 $\mu$ g/ml kasugamycin the growth rate of wild type *E. coli* is severely reduced compared to in LB alone, meanwhile growth of  $\Delta$ DB1 is limited compared to in LB but is comparatively much stronger than the wild type strain throughout the time course. This results in a significantly higher growth rate ( $p=0.029$ ,  $W= 0$ ), area under the curve ( $p=0.029$ ,  $W= 16$ ), and maximum OD ( $p=0.029$ ,  $W= 16$ ) in  $\Delta$ DB1 compared to wild type *E. coli* (Figure 3.8A). A similar pattern was observed in subsequent concentrations tested down to <0.4 $\mu$ g/ml (supplementary figure 5).

A similar pattern is observed in 12.5 $\mu$ g/ml blastocidin S, at which concentration growth of wild type *E. coli* is practically inhibited, while  $\Delta$ DB1 is able to grow to a much higher OD, albeit severely reduced from compared to in LB alone. This again results in  $\Delta$ DB1 having a significantly higher growth area under the curve ( $W= 16$ ,  $n_1=12$ ,  $n_2=12$ ,  $p=0.029$ ) and maximum OD ( $p=0.029$ ,  $W= 16$ ) compared to wild type *E. coli* (Figure 3.8B). A similar pattern was observed in subsequent concentrations tested down to <0.8 $\mu$ g/ml (supplementary figure 5).

This evidence therefore implies that wild type *E. coli* is more susceptible to blastocidin S and kasugamycin than  $\Delta$ DB1, thus implying the loss of the ABC peptide transporters is beneficial to resistance against these antibiotics. Under the intrinsic resistance hypothesis, this would imply that blastocidin S and kasugamycin are substrates of Dpp and Opp in *E. coli*, in agreement with previous findings (Shiver et al., 2016).

### **Comparison of susceptibility of wild type *E. coli* and $\Delta$ DB50 to blastacidin S and kasugamycin.**

When exposed to 25 $\mu$ g/ml kasugamycin, wild type *E. coli* and  $\Delta$ DB50 appear to follow similar growth dynamics, with a prolonged lag phase and lower OD at stationary phase than in LB alone. There was no significant difference in the growth rate ( $p=0.886$ ,  $W=7$ ), area under the curve generated ( $p=0.2$ ,  $W=3$ ) or maximum OD reached ( $p=0.343$ ,  $W=4$ ), between wild type *E. coli* and  $\Delta$ DB50 (Figure 3.8C).

In the presence of 3.125 $\mu$ g/ml blastacidin S, the two strains again follow similar growth dynamics, initially mirroring growth dynamics observed in the absence of the antibiotic, before entering stationary phase at an abnormally low OD. There is again no difference between the growth dynamics of the two strains based on the parameters tested, with an equivalent growth rate ( $p=0.686$ ,  $W=10$ ), area under the curve generated ( $p=0.886$ ,  $W=7$ ) and maximum OD ( $p=0.886$ ,  $W=7$ )(Figure 3.8D). A similar pattern was observed across all the tested concentrations of both antibiotics (supplementary figure 5).



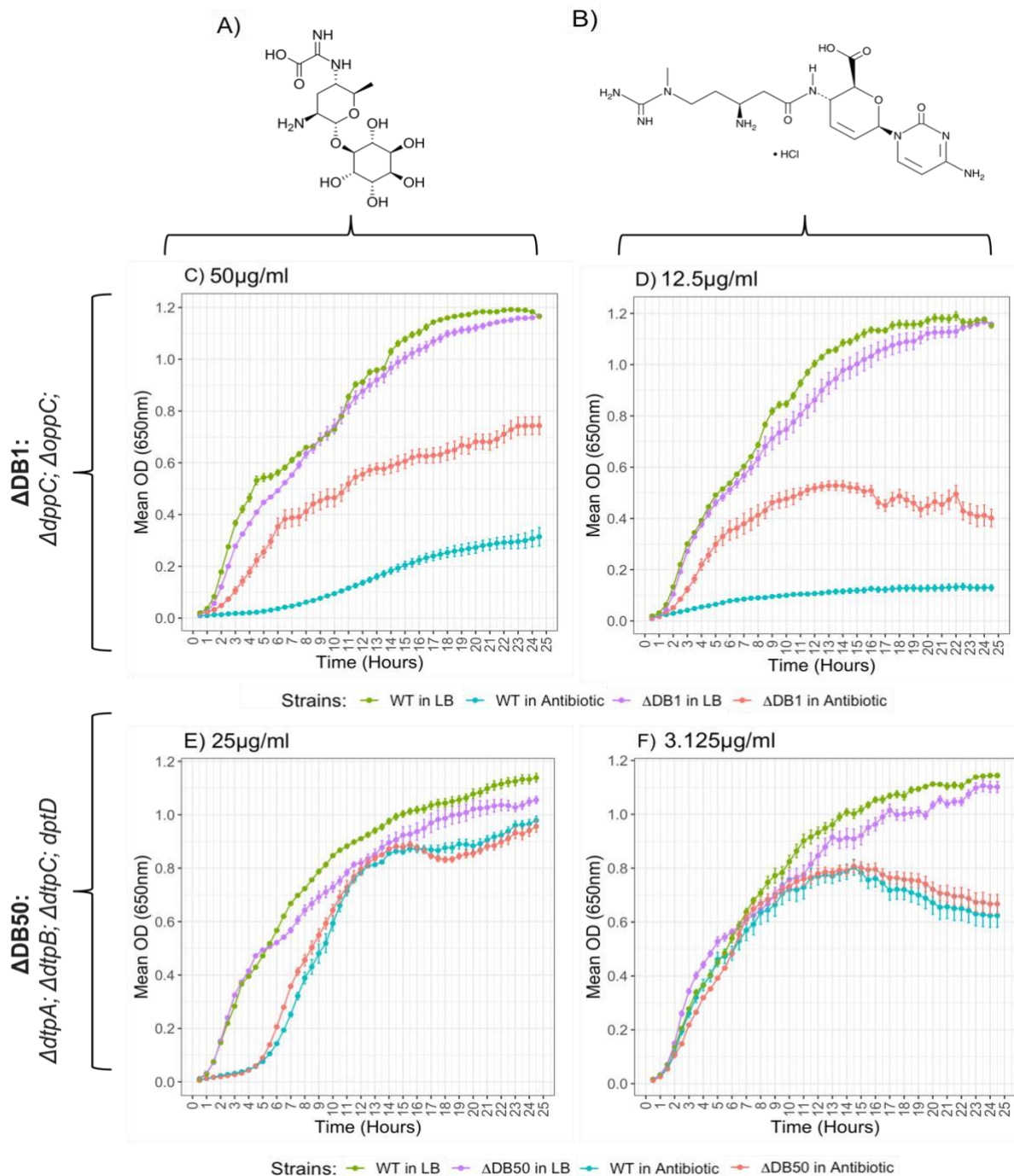


**Figure 3.8 – Growth phenotype comparison of  $\Delta DB50$  and  $\Delta DB1$  in kasugamycin and blasticidin S. A and B) Skeletal structure of kasugamycin (A) and blasticidin S (B). C and D) Growth phenotype experiments comparing wild type BW25113 *E. coli* and  $\Delta DB1$  in the presence of kasugamycin or blasticidin S. C)  $\Delta DB1$  in 50 μg/ml kasugamycin: Area under the curve (WT:  $\bar{x}$  =204.7, SD=58.3, n=4 | DB50:  $\bar{x}$  =674.7, SD=124.5, n=4), maximum OD (WT:  $\bar{x}$  =0.3, SD=0.1, n=4 | DB50:  $\bar{x}$  = 0.67, SD=0.12, n=4), intrinsic growth rate (WT:  $\bar{x}$  =0.005, SD=3.0 x 10<sup>-4</sup>, n=4 | DB50:  $\bar{x}$  = 0.006, SD=0.002, n=4). D)  $\Delta DB1$  in μg/ml 12.5 μg/ml blasticidin S: Area under the curve (WT:  $\bar{x}$  =118.8, SD=46.2, n=4 | DB50:  $\bar{x}$  =551.8, SD=38.1, n=4), maximum OD (WT:  $\bar{x}$  =0.11, SD=0.05, n=4 | DB50:  $\bar{x}$  = 0.48,**



SD=0.1, n=4), intrinsic growth rate (WT:  $\bar{x}$  =0.007, SD=0.003, n=4 | DB50:  $\bar{x}$  = 0.016, SD=0.006, n=4). **E and F**) Growth phenotype experiments comparing wild type BW25113 *E. coli* and  $\Delta$ DB50 in the presence of kasugamycin or Blastidicin S. **E)  $\Delta$ DB50 in 25 $\mu$ g/ml kasugamycin:** Area under the curve (WT:  $\bar{x}$  =844, SD=53.3, n=4 | DB50:  $\bar{x}$  =856.9, SD=43.5, n=4), maximum OD (WT:  $\bar{x}$  =0.9, SD=0.04, n=4| DB50:  $\bar{x}$  = 0.88, SD=0.03, n=4), intrinsic growth rate (WT:  $\bar{x}$  =0.01, SD=5.0 x 10<sup>-4</sup>, n=4| DB50:  $\bar{x}$  = 0.01, SD=0.001, n=4). **F)  $\Delta$ DB50 in 3.125 $\mu$ g/ml blastidicin S:** Area under the curve (WT:  $\bar{x}$  =833.9, SD=158.2, n=4 | DB50:  $\bar{x}$  =864.6, SD=91.2, n=4), maximum OD (WT:  $\bar{x}$  =0.07, SD=0.13, n=4 | DB50:  $\bar{x}$  = 0.74, SD=0.1, n=4), intrinsic growth rate (WT:  $\bar{x}$  =0.01, SD=0.001, n=4 | DB50:  $\bar{x}$  = 0.74, SD=0.087, n=4). Datapoints represent a mean of 4 OD measurements from technical repeats originating from a single biological sample taken at 30-minute intervals, error bars denote standard error. Data generated in this study. **N.B:** Concentrations shown here are those in which the pattern described is most clearly observed, direct comparisons between the two strains with antibiotics at equivalent concentrations are shown in supplementary figure 4 and 5.

Therefore, the evidence presented here indicates that  $\Delta$ DB50 does not differ from wild type *E. coli* in its susceptibility to either Blastidicin or Kasugamycin. In the context of the intrinsic resistance hypothesis this would imply that these antibiotics are not substrates for the *E. coli* POT transporters, like they are for the ABC transporters.

### 3.3 Toxic Peptide Inhibition Assay

An additional aim of this study is the further elucidation of the role of peptide transporters in *E. coli*. One aspect which is not fully understood is the specificity of different peptide transporters for different di- and tripeptides, and how this is impacted by the amino acid constituents which make up the peptide. This can be studied using peptides which are toxic to *E. coli* in which a binary phenotype is observed, with toxicity implying the peptide is transported into the cell, and resistance implies the peptide is not. This method was adapted to use both the multiple knockout strains generated by previous lab members, and the single gene KEIO collection knockouts, to observe how the loss of peptide transporters affected the toxicity/resistance phenotype of *E. coli* in the presence of a range of toxic di/tripeptides.

This method was previously utilised by Dr Daniel Bawdon, who investigated the effect of the tripeptide L-Val-Gly-Gly on a range of *E. coli* strains with altered peptide transporter complements (Bawdon 2014). L-Val-Gly-Gly is known to be toxic due to the presence of LValine, which is liberated from the tripeptide via peptidases within the cell. Valine exerts its toxic effect through feedback inhibition of acetohydroxy acid synthase, which normally catalyses the second reaction of the isoleucine biosynthetic pathway, thus leading to isoleucine starvation (Tuite, Fraser and O'Byrne 2005).

### 3.3.1 Dr Daniel Bawdon's Thesis Results

From this investigation, Dr Daniel Bawdon found that L-Val-Gly-Gly, was toxic to both wild type *E. coli* and  $\Delta$ DB1, but not to  $\Delta$ DB5. Based on this, it was concluded that L-Val-Gly-Gly is transported into the cell in strains where the 4 POT transporters are present (wild type *E. coli* and  $\Delta$ DB1) but not in strains in which they are deleted ( $\Delta$ DB5).

Following from this conclusion, KEIO collection strains in which single POT transporters are deleted were used to determine which of the 4 POT transporters were responsible for the transport of L-Val-Gly-Gly. This investigation found that strains lacking DtpB, DtpC and DtpD were still susceptible to the valine induced toxicity in a similar fashion to the wild type, indicating their loss did not confer the resistance observed in  $\Delta$ DB5. However, a strain lacking DtpA displayed the same resistance to L-Val-Gly-Gly observed in  $\Delta$ DB5, indicating DtpA is responsible for the transport of L-Val-Gly-Gly into the cell.

Meanwhile, the toxicity was still present in strains lacking either Dpp or Opp, albeit with a smaller zone of inhibition. This implies that L-Val-Gly-Gly is a weaker substrate of the *E. coli* ABC transporters.

Valine in its amino acid form is transported by a distinct mechanism from the POT or ABC transporters (Piperno, J.R. and Oxender 1968) and was found to be toxic to all strains, meanwhile H<sub>2</sub>O alone was not toxic to any of the strains, the combination of which verifies the methodology used (Figure 3.9).

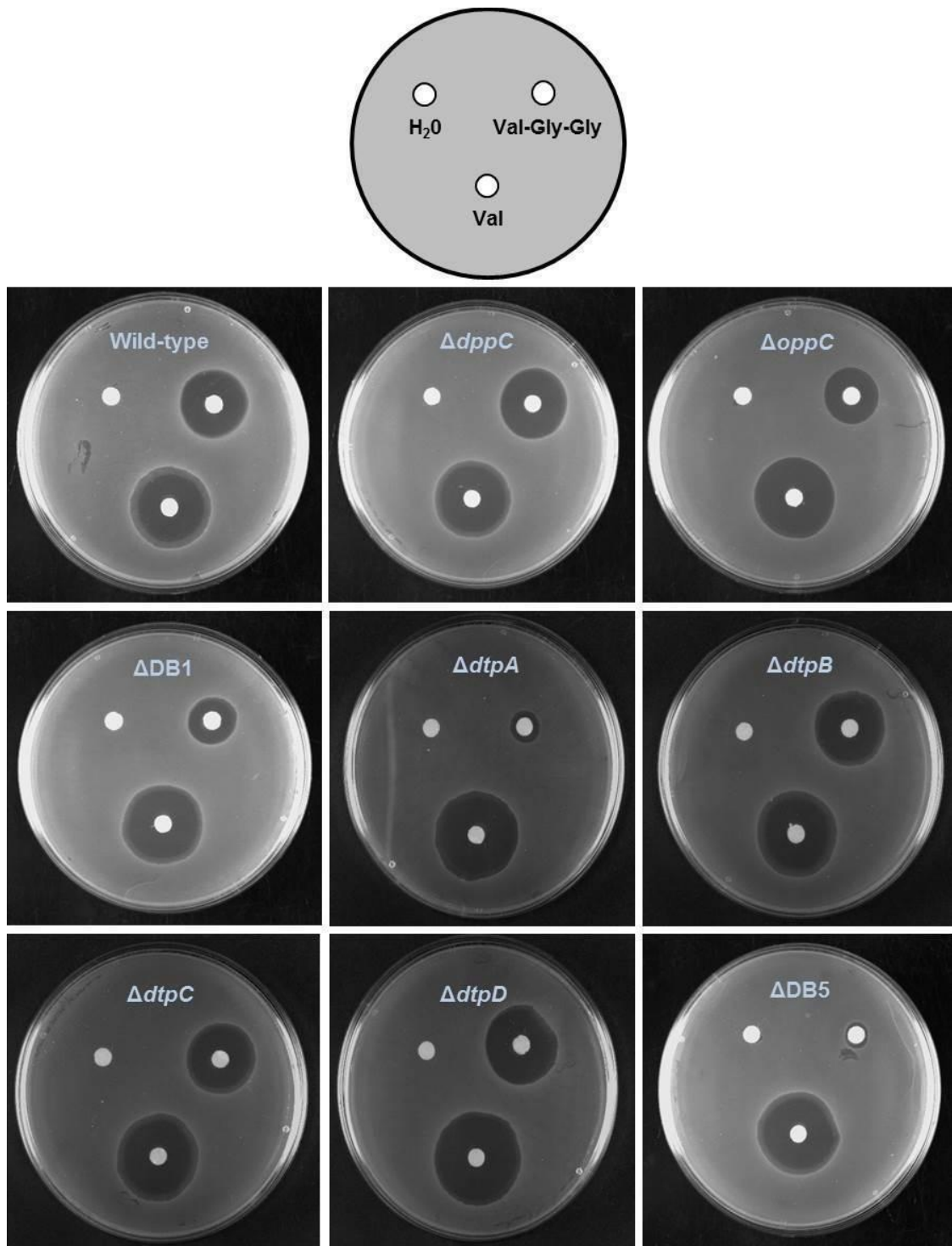


**Figure 3.9 – Toxic peptide inhibition assay performed by Dr Daniel Bawdon.** *E. coli* strains with differing peptide transporter genotypes grown on M9 minimal glucose agar plates with toxic peptide supplementation. A lawn of bacteria was spread onto each plate, allowed to dry, and filter paper discs added and saturated with the given compound. Top panel shows

layout of filter discs on each plate. Discs were saturated with equimolar concentrations of Val-Gly-Gly, L-Valine or H<sub>2</sub>O. Top panel shows layout of filter discs on each plate. Experiment performed by Dr Daniel Bawdon in 2014.

The original intention of this study was to recapitulate the results observed in  $\Delta$ DB5 with the newly developed  $\Delta$ DB50, however due to the original manufacturer which supplied the L-Val-Gly-Gly used in Dr Daniel Bawdon's experiment in 2014 discontinuing production, DL-Val-Gly-Gly (a mix of D and L stereoisomers) was used as an alternative in this work.

Despite this, in the time since Dr Daniel Bawdon's work a number of additional novel di/tripeptides thought to be toxic to *E. coli* had become available. These were used in additional experiments to further expand the range of substrates which can be attributed to the peptide transported investigated.

The new peptides included 3 leucine containing di-peptides (Phe-Leu, Leu-Gly, Ala-Leu) which are predicted to be toxic based on published studies. Leucine containing peptides exert their toxicity through the circumvention of normal Leucine uptake mechanisms, leading to an abnormally high intracellular leucine concentration, which interferes with the biosynthesis of isoleucine leading to the inhibition of growth (Tavori, Kimmel and Barak 1981).

Alongside peptides expected to be toxic, a series of peptides which are not expected to be toxic were included (Ala, Ala-Ala, Ala-Ala-Ala, Met, Met-Gly), acting as additional controls not included in the previous experiments conducted by Dr Daniel Bawdon (Vrajesh A. Karkhanis et al., 2007; Katsube et al., 2019).

### 3.3.2 Wild Type *E. coli*

In wild type *E. coli* single amino acid control tests gave the expected result, with only valine exerting a toxic effect, whilst all other single amino acids had no effect (Leucine alone is not expected to be toxic, due to the mechanism of toxicity). In addition, the control dipeptides Met-Gly and Ala-Ala along with the control tripeptide Ala-Ala-Ala did not exert a toxic effect. This indicates the toxicity observed is not a generalised response to additional peptide supplementation, alongside verifying the method used can effectively recapitulate the findings shown by Dr Daniel Bawdon (Figure 3.9, 3.10).

There appears to be weak inhibition incurred by Phe-Leu and to a lesser extent Leu-Gly and Ala-Leu. However, the same result is not displayed to the same extent as the Valine control, thus implying the affect is not complete toxicity. It is possible that the toxicity occurred in earlier time periods, but by the time the plates were examined the toxicity had been overcome, leading to weaker inhibition – this hypothesis was not examined due to time limitations.

Val-Tyr (a novel dipeptide not previously tested) and DL-Val-Gly-Gly both exerted a toxic affect due to the presence of Valine, indicating they are taken up into the cell. In this case, the results from DL-Val-Gly-Gly recapitulate the results found previously in the wild type *E. coli* (Figure 3.10).

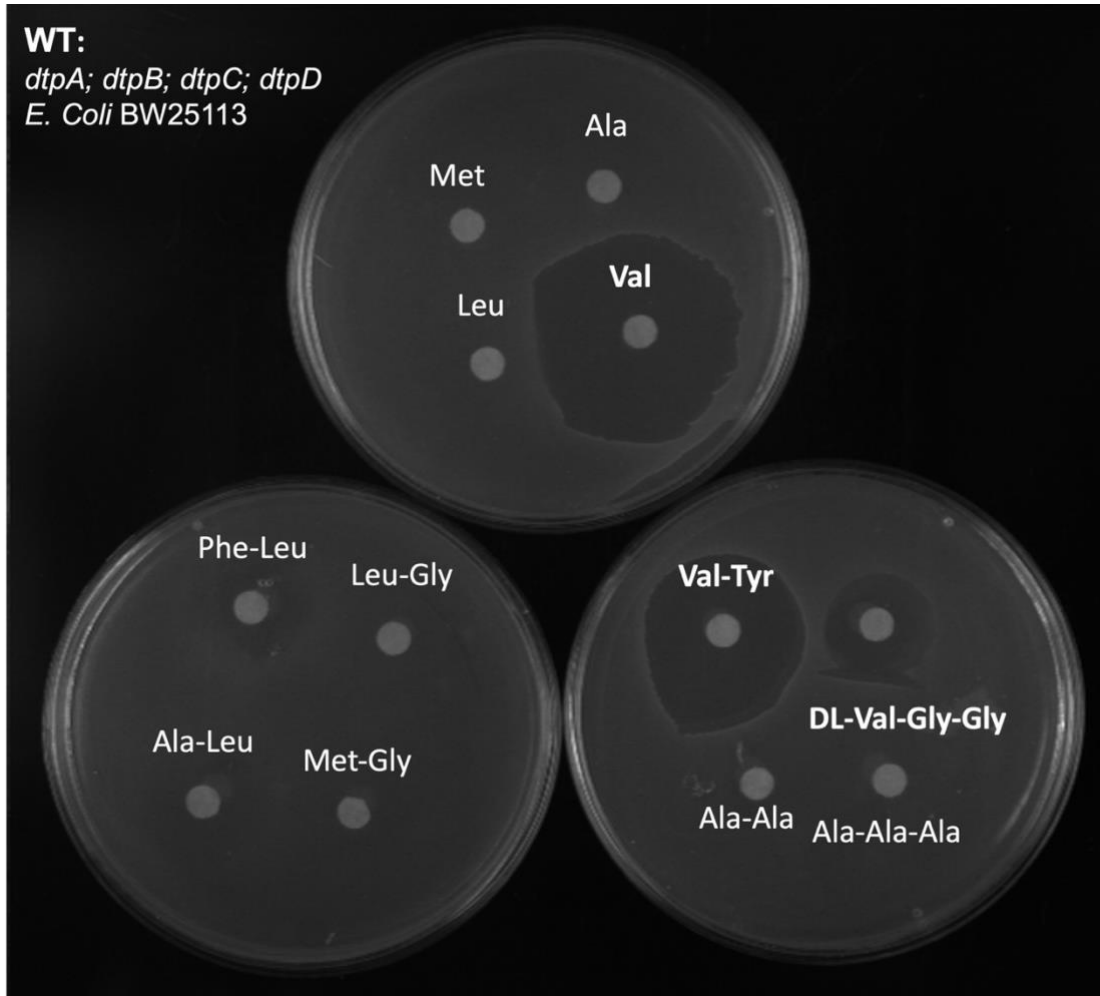


**Figure 3.10 - Toxic peptide inhibition assay (wild type *E. coli*).** Representative images of wild type BW25113 *E. coli* grown on M9 glucose minimal media plates. Filter paper disks are saturated with the relevant amino acid/peptide (see section 2.3.4). Work conducted in this study.

### 3.3.3 $\Delta$ DB50 and $\Delta$ DB5

When  $\Delta$ DB5 and  $\Delta$ DB50 were exposed to the leucine containing peptides, the weak inhibition previously observed in the wild type strain was lost. This could indicate that the POT transporters which are deleted in these strains are responsible for the transport of these dipeptides, and thus their loss leads to a loss of toxicity. However, as discussed previously there are concerns the toxicity of these peptides can be overcome through the duration of growth before the plates were examined, and thus it is impossible to definitively attribute transport of these peptides to the POT transporters.

The novel toxic dipeptide Val-Tyr exerted a toxic effect in both strains similar to that observed in the wild type strain, indicating the loss of the POTs did not lead to a loss of toxicity. This indicates that Val-Tyr is entering the cell through an alternative mechanism (Figure 3.11).

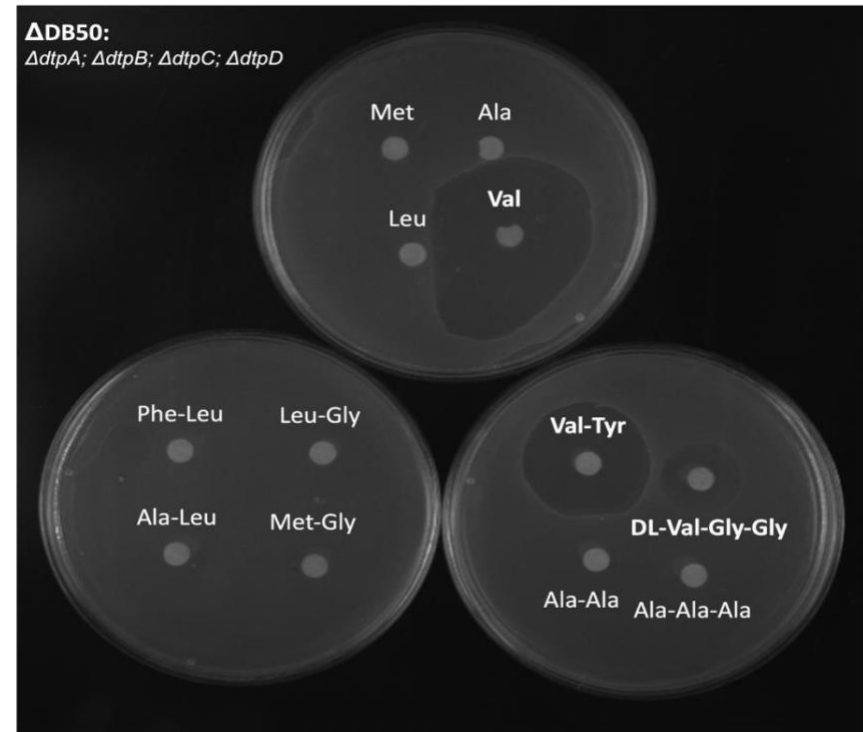
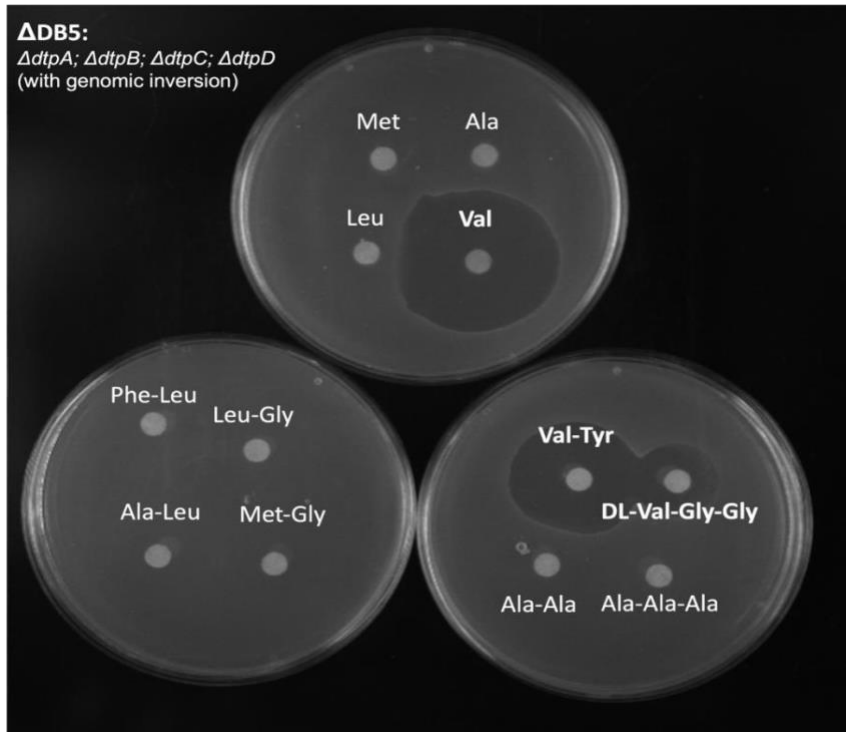


Figure 3.11 – Toxic peptide inhibition assay ( $\Delta$ DB5 and  $\Delta$ DB50). Representative images of  $\Delta$ DB5 and  $\Delta$ DB50 strains grown on M9 glucose minimal media plates. Filter paper disks are saturated with the relevant amino acid/peptide (see section 2.3.4). Work conducted in this study.



An additional aim of this line of enquiry was to recapitulate the results previously found in the (now obsolete) strain  $\Delta$ DB5, in the newly developed  $\Delta$ DB50 strain. However, DL-Val-GlyGly was toxic to both  $\Delta$ DB5 and  $\Delta$ DB50, despite Dr Daniel Bawdon previously finding that toxicity of L-Val-Gly-Gly was lost in these strains (Figure 3.9, 3.10).

The primary difference between the two is the presence of D-Val-Gly-Gly in the tripeptide used in this work, this could imply that while L-Val-Gly-Gly would appear to be exclusively transported by the POTs, D-Val-Gly-Gly is able to enter the cell through an alternative mechanism.

### 3.3.4 $\Delta$ DB1

When  $\Delta$ DB1 was exposed to the leucine containing peptides the weak toxicity observed in the wild type strain was again lost. This could indicate that these are substrates of the ABC transporters in addition to the POT transporters, but to the concerns raised previously this is impossible to attribute definitively.

Val-Tyr again exerts a toxic effect on the  $\Delta$ DB1 in a similar fashion to in  $\Delta$ DB5/50. This indicates that the neither the loss of the POT or ABC peptide transporters alone leads to a loss of toxicity, indicating that Val-Tyr is possible a substrate of both transporter types.

Meanwhile, toxicity of DL-Val-Gly-Gly seems to be lost completely (Figure 3.12). This result is unexpected, as based on the work of Dr Daniel Bawdon it would be expected that L-Val-GlyGly (which is present within the mix) is exclusively transported by the POT transporters (which are intact in  $\Delta$ DB1) and thus some toxicity should have been observed.

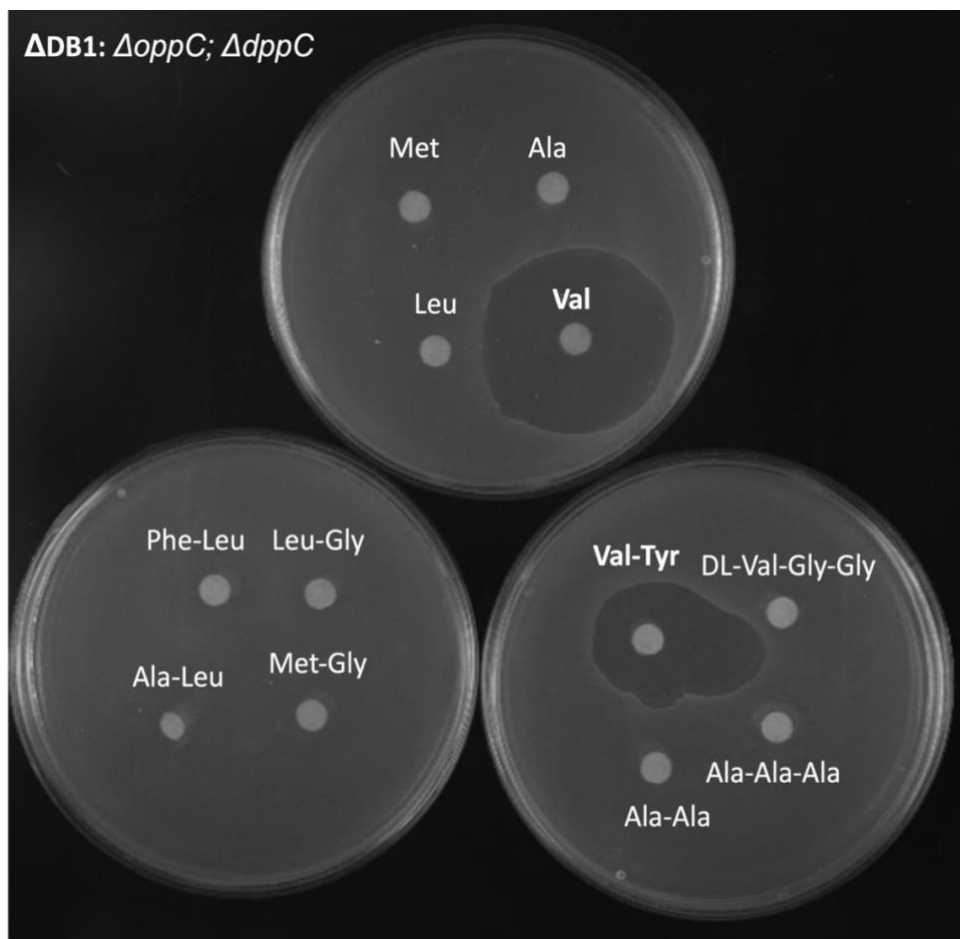


**Figure 3.12- Toxic peptide inhibition assay ( $\Delta$ DB1).** Representative images of wild type BW25113 *E. coli* grown on M9 glucose minimal media plates. Filter paper disks are saturated with the relevant amino acid/peptide (see section 2.3.4). Work conducted in this study.

The DL stereoisomer mix which was utilised as a substitute to L-Val-Gly-Gly used by Dr Daniel Bawdon did not report the exact composition of L- and D- components within the mix. It is therefore possible that the mix contained significantly more D- stereoisomers, thus explaining the lack of toxicity observed from L-Val-Gly-Gly. This conclusion is supported from the results of  $\Delta$ DB5/50 which implied that the D-Val-Gly-Gly stereoisomer was able to enter the cell through an alternative mechanism to the POTs (Figure 3.10). Taken alone this result could imply that the ABC transporters are responsible for this. Whilst this provides a plausible explanation for the results observed, it was not tested further due to time limitations.

### 3.3.5 $\Delta dppC$ and $\Delta oppC$

$\Delta DB1$  contains deletions in both *dppC* and *oppC*, and thus lacks the activity of both ABC peptide transporters within *E. coli*. Dpp is thought to primarily transport di-peptides, whilst Opp transports oligopeptides of 3-amino acids and above. Thus, using KEIO collections the role of the individual ABC transporters in the toxicity observed can be elucidated.

In the case of  $\Delta dppC$ , the toxicity of Val-Tyr was maintained, further implying Val-Tyr acts as a substrate for the POT transporters in addition to the ABCs. Meanwhile, when a  $\Delta oppC$  strain is exposed to DL-Val-Gly-Gly the toxicity is lost, whereas it was still present in  $\Delta dppC$ , thus implying that the loss of Opp was responsible for the lack of toxicity observed in  $\Delta DB1$  (Figure 3.12, 3.13).

Based on the explanation given for the difference in result seen between the results in this study and that of Dr Daniel Bawdon, this would imply that specifically D-Val-Gly-Gly is a substrate of OppC whilst L-Val-Gly-Gly is a substrate of the POT transporters (specifically DtpA) (Figure 3.10, 3.13).

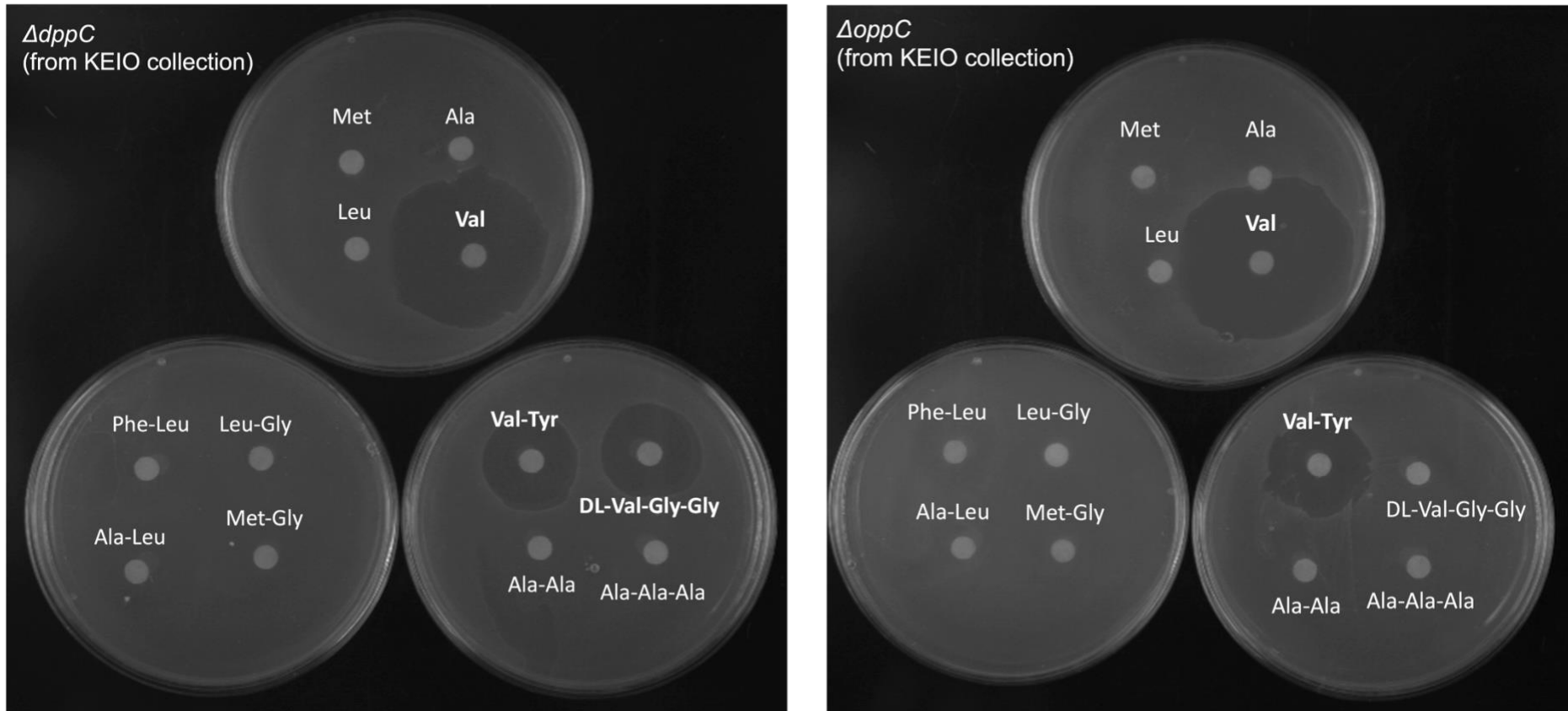


**Figure 3.13– Toxic peptide inhibition assay ( $\Delta DB5$  and  $\Delta DB50$ ).** Representative images of  $\Delta dppC$  and  $\Delta oppC$  strains originating from the KEIO collection (Baba, T. et al. 2006) grown on M9 glucose minimal media plates. Filter paper disks are saturated with the relevant amino acid/peptide (see section 2.3.4). Work conducted in this stu

### 3.4 Phylogenetic Analysis of POT transporters in pathogenic bacteria

The intrinsic resistance hypothesis postulates that peptide transporters such as the POTs contribute to bacterial resistance against antibiotics. Antibiotics are especially important in combatting pathogenic bacteria, in which resistance is becoming an increasingly important issue. Therefore, to understand the importance of POT transporters in resistance to antibiotics, it is also important to understand how widespread POT transporters are amongst pathogenic bacteria.

The pathogenic strains of the bacterial species chosen for inclusion in the analysis (section 2.4) were then examined using a database of bacterial transporter protein sequences to determine their POT transporter complement. Of the 52 species of bacteria included, 27 (52%) did not have any POT transporters, whilst the remaining 25 (48%) had at least one (supplementary table 2).

In the phylogeny created in this study, *E. coli* appears 4 times representing the 4 POT transporters (dtpA: , dptB, dtpC, dtpD: path25 pot 1) the species is known to have, this gives some evidence the coverage of the tree is comprehensive, encompassing all the POT transporters present within the species included.

Using the *E. coli* POT transporters as an illustrative example, the 4 transporters are split across two clades. This indicates there may have been an earlier duplication event which has led to the total number of transporters presently found in *E. coli*. This appears to be a universal pattern, with transporters from multiple species appearing across several clades, in which there are groups of POT transporters found within.

From this analysis it would also appear that there is substantial variation in the number of POT transporters found between species of the same genus. For example, within the *Clostridium* genus, *Clostridium botulinum* has 6 POT transporters, *Clostridium difficile* has 3, *Clostridium perfringens* has 1 whilst *Clostridium tetani* (not in figure) does not have any (Figure 3.14). This indicates that POT transporters can be gained (or lost) throughout the course of the evolution of a bacterial species.

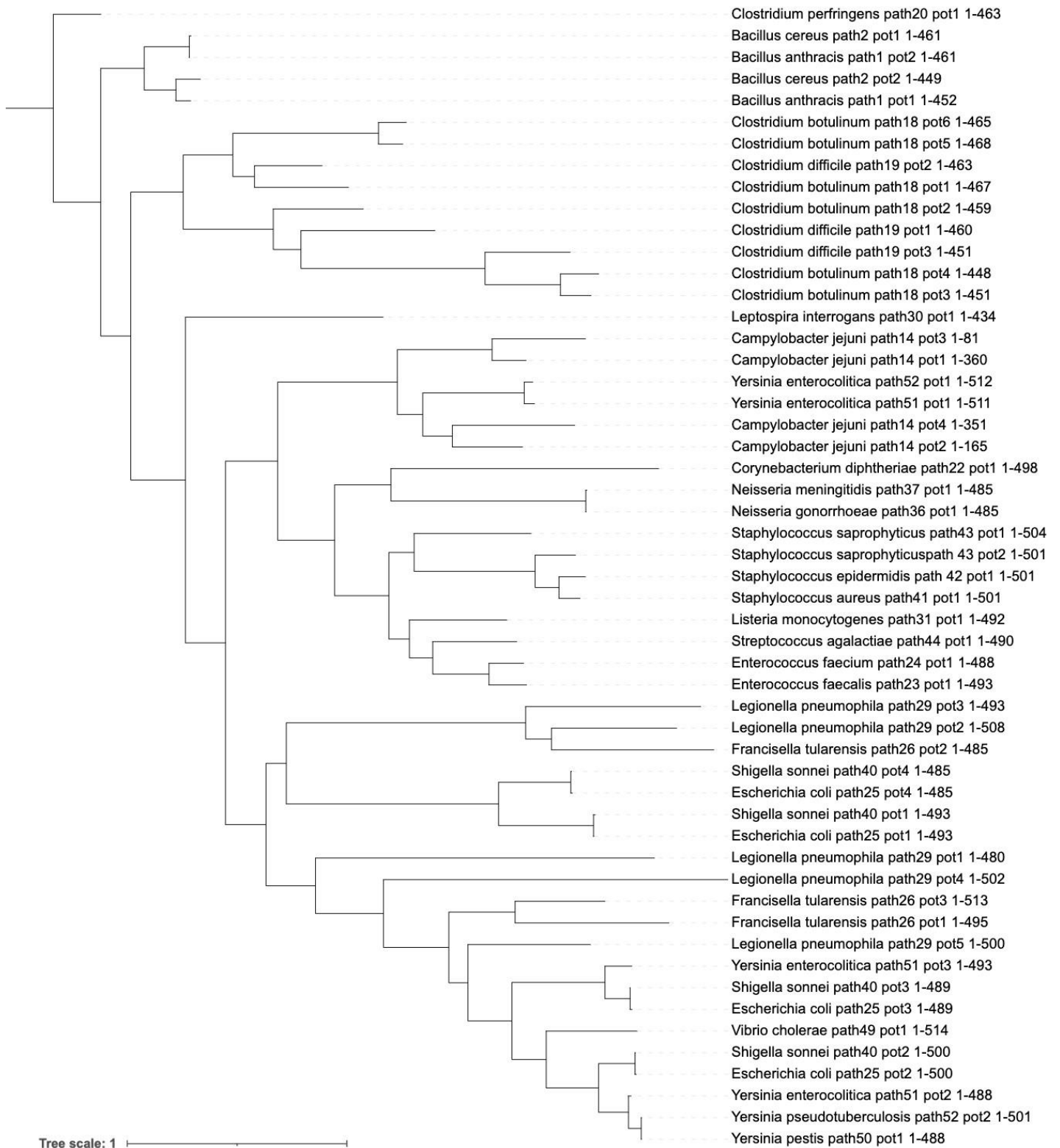


**Figure 3.14 – Phylogenetic tree displaying the relationship between POT transporters present in a selection pathogenic bacterial species.** 52 species were included in the analysis, only species in which POTs were found (n=25) are included, species which did not have POT transporters are listed in supplementary table 2. For tree creation method, see section 2.4.

From this analysis it can be concluded that POT transporters are widespread (but far from ubiquitous) amongst pathogenic bacteria. Amongst these bacteria, there is much diversity within the number of POT transporters each individual species carries, even varying within species of the same genus. This diversity could be due to the occurrence of duplication events increasing the complement of POT transporters carried by a species, but also possibly due to the acquisition of transporters from alternative sources such as horizontal gene transfer.

The species included in the phylogenetic analysis were purposely chosen to be representative of a range of biological characteristics, including oxygen requirement, environmental niche and gram staining (Section 2.4, Supplementary Table 1). In order to understand how these factors contribute to the number of POTs present in the genome of these species, the number of POTs identified were compared based on these characteristics. The resulting analysis found no difference in the number of POTs between gram negative and gram positive bacteria ( $X^2 = 0.87, p = 0.35$ ). However, there was a difference in the numbers of POTs identified in the two groups depending on their oxygen requirements ( $X^2 = 14.5, p = 0.001$ ) and environmental niche ( $X^2 = 19.95, p = 0.003$ ). This analysis concluded that amongst the species included those classed as anaerobic had a higher number ( $\bar{x} = 1.11$ ) than those classed as aerobic ( $\bar{x} = 0.74$ ), and those classed as extracellular having a higher number of POTs ( $\bar{x} = 0.96$ ) than those classed as intracellular (none of which had POTs) (Figure 3.15).





## 4 Discussion:

### 4.1 Creation of $\Delta$ DB5:

This project was based upon preliminary data generated utilising an *E. coli* strain lacking all 4 POT transporters known as  $\Delta$ DB5. One aim was to chronicle the methodology used to generate this strain, and the production of its later iteration  $\Delta$ DB50. The notes available in the lab regarding this process are summarised in this work. Section 3.1 describes the process by which Dr Daniel Bawdon generated  $\Delta$ DB5 using successive deletions of individual POT genes, utilising the methodology described in Datsenko and Wanner (2000), originating from a single deletion KEIO collection strain (Baba, T. et al. 2006)(Figure 1.14). However, later examinations performed by Emmanuele Severi discovered that an inversion had occurred within the genome of this strain between two of the deleted genes (*ntpB* and *ntpC*)(Figure 1.15). This was concluded to be due to the methodology by which the strains were created.

The basic strategy of the method developed by Datsenko and Wanner (2000) utilises an antibiotic resistance gene (in the case of  $\Delta$ DB5, kanamycin) flanked by FRT (FLP recognition target) sites and a homologous sequence to the gene of interest. The introduction and expression of a plasmid carrying the  $\lambda$ -red recombinase gene induces recombination that leads to the replacement of the gene of interest with the antibiotic resistance gene. The resistance gene can later be cured using a helper plasmid expressing FLP recombinase, which causes the excision of the resistance gene and thus deletion of the gene of interest, however this process leaves a single FRT scar sequence behind.

The successive deletions of POT genes conducted by Dr Daniel Bawdon would therefore have led to a FRT site being left after each deletion event, and thus by the time of the final deletion of *ntpC* there would have been three present (including that generated from the KEIO collection deletion). In order to cure the final kanamycin resistance gene inserted in place of *ntpC*, FLP recombinase would have been introduced to the final intermediate strain (in this case DB5)(Figure 1.14B). Therefore, it is likely that the genomic inversion event which occurred during the creation of  $\Delta$ DB5 occurred as a result of inadvertent targeting of the FRT sites remaining from previous deletion events in the site of *ntpC* and *ntpD* by the FLP introduced to cure the final kanamycin resistance gene. Whilst this inversion did not occur in all the strains generated from this step, allowing the strain  $\Delta$ DB50 (which lacks the inversion) to be produced, this provides a cautionary note in the use of  $\lambda$ -Red mediated deletion of multiple genes within a single genome. The possibility of such an inversion occurring was not discussed in the original Datsenko and Wanner (2000) paper, possibly as the methodology was originally designed for the deletion of single genes within a chromosome rather than successive deletions within a single genome.

In the years since the creation of  $\Delta$ DB5, multiple methods have been developed to overcome this problem. Two examples include “CRISPR-FRT” and “no-SCAR”, both of which utilise CRISPR-Cas9 mediated deletion of the FRT scar sites to improve efficiency of gene deletion using the existing  $\lambda$ -Red mediated deletion method (Reisch and Prather, 2015; Swings et al.,

2018). Whilst neither of these methods were available at the time  $\Delta$ DB5 was created, this provides a mechanism for use in future work to efficiently remove the FRT sequences generated by successive gene deletions within a single genome, the importance of which is highlighted in the results described in this study.

## 4.2 Antibiotic Susceptibility Comparison

### 4.2.1 Growth comparisons in the absence of antibiotic:

The central aim of this project was to determine the experimental evidence for the proposed intrinsic resistance hypothesis, which postulates that the bacterial peptide transporters contribute to the level of intrinsic resistance to peptide-like antibiotics in bacteria by transporting them outside their site of action. Therefore, the primary method by which the intrinsic resistance hypothesis was investigated was through comparing the growth of a wild type *E. coli* BW25113 strain and mutant *E. coli* strains which lack either POT ( $\Delta$ DB50) or ABC ( $\Delta$ DB1) peptide transporters, in the presence of peptide-like antibiotics.

However, in order to compare the growth of these strains in the presence of antibiotics, it was first necessary to determine if the loss of the peptide transporters had any adverse effect on growth in LB in the absence of the antibiotic. Injae chung previously compared the growth of the progenitor strain to  $\Delta$ DB50 (known as  $\Delta$ DB5) and wild type *E. coli* in the presence of LB alone. From this, Injae Chung found a “growth defect” in  $\Delta$ DB5 compared to wild type *E. coli* (Figure 3.7A). However, as previously discussed this strain was known to carry a genomic inversion, which was hypothesised to be the cause of the weaker growth phenotype, through causing mis-regulation of the motility phenotype of  $\Delta$ DB5. Specifically, the inversion of the genomic section between *ntpB* and *ntpC* was thought to have altered the regulation of genes such as those within the *flhDC* operon, which are responsible for flagella production (Gauger et al. 2007). Flagella production and thereby motility in bacteria is an energy expensive process, and thus is normally tightly controlled. However, the loss of repression could have led to an aberrant motility phenotype in  $\Delta$ DB5, causing greater ATP expenditure and thus explaining the reduced growth phenotype. Evidence for this hypothesis was based on the fact that  $\Delta$ DB5 displayed a “hyper-motile” phenotype when grown in motility agar (Kearns 2010), showing a swarming phenotype which was not present in wild type *E. coli* BW25113.

However, a later study which was not available at the time this work was conducted later provided an explanation for the motility phenotype present in  $\Delta$ DB5. As chronicled previously,  $\Delta$ DB5 originated from a KEIO collection  $\Delta$ *ntpB* strain (Figure 1.14B). The work of Parker et al (2019) describes how the methodology used to generate the KEIO collection strains selected for the rapid evolution of motility, resulting in a significant number of KEIO collection strains having an increased motility phenotype which was not present in the original wild type strain. In this study, the source of the motility was determined to be due to the upregulation of motility activating genes, as a result of the growth method utilised during the creation of the strains, resulting in 69% of KEIO collection strains having an increased motility phenotype relative to the parental line. While the strains utilized in this

study were not specifically tested in the work by Parker et al (2019), since  $\Delta$ DB5 originated from this collection, this likely explains the hypomotile phenotype observed in the strain. However, since  $\Delta$ DB50 shares the same origin, it would therefore be expected that it would share the motility phenotype. Despite this, findings produced in this work demonstrate that  $\Delta$ DB50 and a wild type BW25113 *E. coli* strain do not differ in their growth phenotype (Figure 3.7B). Whilst this is beneficial for comparing the growth of the two strains, as any difference in growth in the presence of antibiotic is not due to an intrinsic difference in growth, it does not explain the difference previously observed in  $\Delta$ DB5.

Two possible explanations are proposed for this, the first of which is a result of differences in methodology used to generate the data. Whilst this work utilised a 96-well plate-based approach, the data generated by Injae Chung utilised a flask culture. Bacteria within the flask culture will unavoidably have a greater oxygen supply than those in a plate, *E. coli* utilises oxygen in aerobic respiration, which is known to be the preferable metabolic mode due to its high energy efficiency allowing the greatest growth rate (Jones, S.A. et al. 2007). Meanwhile, multiple studies have demonstrated that oxygen availability can become a limiting growth factor in 96-well plate cultures (Cotter et al., 2009; Fisher et al., 2021). Therefore, it is possible that the differences in growth between the two strains only become apparent at a growth rate which is not achievable within a 96-well plate, thus hiding a potential difference between wild type *E. coli* and  $\Delta$ DB50.

Another possible explanation for this is intrinsic differences in the wild type *E. coli* strains used to compare growth to  $\Delta$ DB5 and  $\Delta$ DB50. The Thomas lab in which all work discussed in this report was conducted holds a number of wild type BW25113 *E. coli* strains, all of which have independent origins. The wild type strain used in this study was obtained directly from the Mori lab (Table 2.2), in which the KEIO collection was created, and thus originates from the same ancestral strain as the  $\Delta$ dtpB line from which both  $\Delta$ DB5 and  $\Delta$ DB50 were originally developed - it is therefore logical that the two strains do not differ in their growth phenotype. However, from the records available it is unknown which of the available BW25113 *E. coli* strains was utilised in the work conducted by Injae Chung, it is therefore impossible to determine if the same strain originating from the Mori lab was used in both comparisons. Whilst nominally both being wild type BW25113 *E. coli* strains, other studies have raised concerns regarding the divergence of laboratory *E. coli* strains from its ancestral state (Hobman, Penn and Pallen 2007), therefore if the strain used in Injae Chung's work had an independent origin, the accumulation of genetic differences could account for the difference in growth pattern observed in comparisons with  $\Delta$ DB5 but not  $\Delta$ DB50. Despite the lack of a definitive explanation for the difference in phenotype observed in  $\Delta$ DB5, the most important conclusion for this study is that in the conditions used there is no difference in growth phenotype between  $\Delta$ DB50 and the wild type *E. coli* strain utilised.

Whilst only  $\Delta$ DB5 was investigated by Injae Chung, this study also utilised an ABC mutant line termed  $\Delta$ DB1 (also generated by Dr Daniel Bawdon). Whilst this strain also originated from the KEIO collection, and thus may share the hypermotility phenotype (not tested), there was similarly no difference in growth phenotype between this strain and wild type BW25113 *E. coli* observed in LB (Figure 3.7). Taken together, these results are beneficial for

testing the intrinsic resistance hypothesis in the manner proposed previously, as any difference in antibiotic susceptibility between the two strains can more definitively be attributed to the activity of the peptide transporters.

#### 4.2.2 Susceptibility to penam beta-lactam antibiotics:

Having confirmed the two strains to be compared had equivalent growth in LB, it was possible to compare growth dynamics in the presence of antibiotics. The first antibiotic tested was ampicillin (a penam type beta-lactam) as this had been tested by Injae Chung in relation to  $\Delta$ DB5. The findings presented here utilising  $\Delta$ DB50 are broadly in agreement with those found previously, with both studies showing a clear increased susceptibility to ampicillin in the mutant strain compared to the wild type strain (Figure 3.). The only difference is the susceptibility phenotype in this study was found at a higher concentration of antibiotic than was previously found, this is concluded to be due to the difference in methodology used to generate the growth phenotype data (section 2.3.2). In Injae's work, the flask culture utilized in the growth experiments conducted would have had greater oxygen availability than the plate reader used in this work, this would have resulted in different growth dynamics (primarily growth rate). These differing growth dynamics likely led to the range of antibiotic concentrations in which the difference in susceptibility becomes apparent shifting upwards.

In the case of  $\Delta$ DB50, the increased susceptibility phenotype was also confirmed using analysis from the growthcurver R package (Sprouffske and Wagner 2016). The difference in growth dynamics observed in the plate reader experiments confirmed that the outputs generated by growthcurver were plausible despite the novel application of this package, whilst comparisons of the outputs for the parameters themselves confirmed that the difference in growth observed in the two strains in response to the antibiotic is statistically significant.

Under the intrinsic resistance hypothesis this finding implies that ampicillin may be a substrate of the *E. coli* POT transporters. This conclusion agrees with a previous study by Prabhala et al (2017) which concluded that ampicillin is transported by both the human POT transporter hPEPT1 and its equivalent in *E. coli* YdgR (DtpA). However, this study was limited to DtpA alone, and thus it is unknown if ampicillin is also a substrate of the other three Dtp transporters present in *E. coli*, and whether their loss is contributing further to the increased susceptibility observed in  $\Delta$ DB50. Taken with the empirical evidence produced in this project, this provided a reasonable proof of concept to continue with additional antibiotics.

As ampicillin was the only antibiotic which had been tested previously by Injae Chung, the future antibiotics to be tested were chosen based on published studies implying they may be substrates of either the POT or ABC transporters. A study by Stauffer et al (2021) implied that two additional penam beta-lactam antibiotics (carbenicillin and amoxicillin), were substrates of a POT transporter found within *Yersinia enterocolitica*. When tested in the context of  $\Delta$ DB50, the strain displayed an increased susceptibility to both antibiotics compared to wild type *E. coli*. This implies that the ability of POTs to transport beta-lactam

antibiotics is cross-species, and also provides additional evidence for the intrinsic resistance hypothesis in the context of novel beta-lactam antibiotics.

A reoccurring theme throughout all three beta-lactams tested is the initial growth period for the first 2-3 hours in which both strains seem to be unaffected by the presence of the antibiotic. At this point, a common theme is for growth  $\Delta$ DB50 to stall, and decrease in OD before entering a prolonged lag phase. Meanwhile, growth of wild type *E. coli* continues growing for longer before entering the prolonged lag phase (e.g: Figure 3.2B) or does not enter it at all (e.g: Figure 3.2C). This difference in initial growth dynamic between the two strains has a lasting effect throughout the remainder of the growth course, with many examples of the wild type strain generating a greater area under the curve and reaching a higher maximum OD than  $\Delta$ DB50 (Figure 3.1, 3.2, 3.4). The similarity between the growth dynamic generated across all three antibiotics despite their differing structural modifications (Figure 3.1A, 3.2A, 3.4A), implies a common mechanism across all the betalactams through which the difference in susceptibility becomes apparent.

As discussed previously, the beta-lactam antibiotics exert their mode of action through inhibiting the synthesis of peptidoglycan, which is a core component of the bacterial cell wall (section 1.5.2). A typical bacterial growth course begins with a lag phase, whilst the bacteria adapt to the growth conditions, this is followed by a phase of exponential growth during which rapid growth occurs (Madigan et al., 2017). This growth phase requires the formation of new bacterial cells through binary fission, and thus rapid formation of new bacterial cell walls - which requires peptidoglycan.

Therefore, since the beta-lactam antibiotics inhibit the synthesis of peptidoglycan, the sensitivity of bacteria to their mode of action is proportional to the growth rate. This explains the lack of an effect observed in the first few hours of the time course, in which the growth rate is very slow. It also explains the sudden loss of growth observed, which coincides with the entry into exponential phase in the absence of the antibiotic. This dynamic has also been observed in multiple published studies, and its causes are well understood (Tuomanen et al., 1986; Balaban et al., 2004; Lee et al., 2018). However, in the growth courses observed in this study the effect of the beta-lactam during the entry to exponential phase (the period of greatest sensitivity) appears to be exaggerated in  $\Delta$ DB50 across all dynamics examined. This indicates that in wild type *E. coli*, the POT transporters are likely contributing to the level of growth, which is achievable despite the presence of the antibiotic, an effect which is not present in  $\Delta$ DB50. This therefore indicates that the POT transporters play a role in the basal level of resistance to antibiotics – as the intrinsic resistance hypothesis predicts.

Under the proposed hypothesis, this is due to the transport of the antibiotics away from their site of action. For this to be possible, the beta-lactam antibiotics need to act as substrates for the POT transporters, for which the natural substrate is peptides. As discussed previously, the POT transporters operate through an alternating access mechanism, a core aspect of which is the ability to transport a diverse range of possible peptide substrates with differing side chains (section 1.3.2). To date, a structure of a bacterial POT transporter in

complex with a beta-lactam antibiotic has not been obtained and thus transport can only be inferred. Despite this, the mechanism by which the POT transporters may recognise beta-lactam antibiotics can be predicted using existing understanding of the specificity towards peptides. In this case, the amide bond within the beta-lactam antibiotic provides the initial target for recognition (Figure 1.9), whilst the binding pocket accommodates the wider beta-lactam structure in a way analogous to peptide side chains. Furthermore, the additions to the core penicillin structure (Figure 1.8) from which new beta-lactam antibiotics are made resemble side chains already present in amino acids, and thus fit within this mechanism and explain the lack of difference observed between different beta-lactams.

#### 4.2.3 Susceptibility to cephalosporin beta-lactam antibiotics:

The study performed by Stauffer et al (2021) also included two additional cephalosporin beta-lactam antibiotics: cefalexin and cefadroxil. These antibiotics are analogues of ampicillin and amoxicillin respectively but possess an altered beta-lactam ring structure (but still possess an amide bond) (Figure 3.5A/B). Stauffer et al (2021) presented evidence that cefadroxil, but not cefalexin, were substrates of the *Yersinia enterocolitica* POT transporters. These antibiotics were therefore included in this study to determine the effect of the core ring structure of the beta-lactam antibiotic introduced on the susceptibility phenotype observed, and also determine any possible species-specific differences in the transport of the beta-lactam antibiotics.

In contrast to the previous study described, the results presented here imply that  $\Delta$ DB50 has a greater susceptibility to both cefalexin and cefadroxil (Figure 3.5), thus inferring that both antibiotics are substrates of the *E. coli* POT transporters. This would indicate that the core ring structure has no effect on the transport of the beta-lactam antibiotics. This can be explained using the working theory for POT recognition of beta-lactam antibiotics discussed previously, as both antibiotic types contain a peptide bond, whilst the wider structure (including the beta-lactam ring) is accommodated by the pocket whilst not contributing to the specificity. Furthermore, this implies that cefadroxil is a substrate of the *E. coli* POTs whilst not being a substrate for those in *Yersinia*. However, it is notable that in the tests performed for cefadroxil there was only 1 concentration in which a difference in susceptibility was observed, whilst all other antibiotics had at least 2. This could imply that although cefadroxil is transported by the POT transporters, it may be with a lower affinity.

#### 4.2.4 Non-specific transport of antibiotics:

The evidence presented thus far implies that  $\Delta$ DB50 has a greater susceptibility to beta-lactam antibiotics than wild type *E. coli*, whilst the hypothesis proposed postulates this is due to the activity of the POT transporters, this is only logical if the beta-lactam antibiotics are indeed acting as substrates. An alternative hypothesis would imply that  $\Delta$ DB50 simply has a greater susceptibility to all antibiotics, with the POTs playing either no or an indirect role in the effect. To control against this, growth of the two strains was compared in the presence of kanamycin. Kanamycin has no peptide bond, and thus would not be expected to be a substrate of the POT transporters. Therefore, the two strains would be expected to

have similar susceptibilities. Analysis performed in this study concludes this prediction is correct, with no difference in susceptibility between the two strains across a range of kanamycin concentrations (Figure 3.6), thus implying that kanamycin is indeed not a substrate of the *E. coli* POT transporters. Thereby, this indicates that the results previously observed are specific to the beta-lactam antibiotics, and thus is likely due to the peptide bond making them a substrate of the POT transporters.

#### 4.2.5 Susceptibility to aminoglycoside antibiotics:

There are also examples of non-beta-lactam antibiotics acting as substrates for peptide transporters, namely the transport of Kasugamycin and Blastidicin S by *E. coli* and *Erwinia amylovora* ABC transporters (Shiver et al., 2016; Ge et al., 2018). Kasugamycin and Blastidicin S are two aminoglycoside antibiotics which contain a peptide bond within their structure. Both antibiotics target the ribosome, and thus under the proposed hypothesis it would be expected that the loss of the peptide transporters would be beneficial (through an opposite mechanism to the beta-lactams). This is because in the wild type state the peptide transporters function to move the antibiotic closer to its site of action

Alongside  $\Delta$ DB50, Dr Daniel Bawdon also generated  $\Delta$ DB1 (a mutant *E. coli* strain which lacks both ABC peptide transporters). In this study,  $\Delta$ DB1 was therefore used to confirm the findings of the previous studies which concluded that Kasugamycin and Blastidicin S were substrates of the ABC transporters. The results presented in this study agree with this conclusion, with  $\Delta$ DB1 exhibiting a greater resistance to both antibiotics compared to wild type *E. coli* (Figure 3.8C/D). Notably, this difference in both cases is greater than that observed in any of the tests performed using  $\Delta$ DB50, implying that the ABC transporters may have a greater affinity for these antibiotics than the POT transporters do the betalactam antibiotics. Due to time limitations, the susceptibility of  $\Delta$ DB1 to beta-lactam antibiotics was not tested, though it is possible that the ABC transporters are also contributing the baseline level of resistance in addition to the POT transporters.

Whilst the aforementioned studies have examined the response of ABC peptide transporter mutants to the presence of Kasugamycin and Blastidicin S, an equivalent study has not been performed for *E. coli* mutants lacking POT transporters. The ABC transporters share some overlap in specificity with the POT transporters, and thus it would be logical to predict that the POT transporters may also have a role in transporting these antibiotics. However, the results presented in this study imply there is no difference in susceptibility in  $\Delta$ DB50 compared to wild type *E. coli* in the presence of either antibiotic (Figure 3.8F)(displaying a similar result to that observed in kanamycin – Figure 3.6), implying that the POT transporters have no affinity for them.

One possible explanation for the transport of Kasugamycin and Blastidicin S by the ABC transporters but not the POT transporters can be understood through their mechanism of action. As previously described (section 1.4.2), ABC transporters utilise substrate binding proteins (SBPs) to confer peptide specificity. In the proposed model, the SBP binds to the backbone region of the antibiotic in which the peptide bond is found (mimicking a peptide),



the remainder of the structure is then held within the water filled cavity, which gives the promiscuity required. Meanwhile, the POT transporters confer substrate specificity through the existence of regions within the peptide binding pocket from which electrostatic interactions with the substrate can be formed (rather than a water filled cavity)(section 1.3.2). From the structures of Kasugamycin and Blasticidin S, it can be seen that both are much larger than a typical beta-lactam antibiotic (Figure 1.8, 1.11), with a more complex wider structure (analogous to peptide side chains). Therefore, it is possible that these antibiotics are only transported by the ABC transporters as the water filled cavity within the SBP confers the promiscuity required for transport, whilst the regions within the POT transporters which confer specificity to peptides do not allow for such promiscuity.

#### 4.2.6 Implications for antibiotic resistance:

The evidence presented thus far implies that peptide transporters within *E. coli* contribute to the resistance (and in the case of the aminoglycosides, the sensitivity) to peptide-like antibiotics such as the beta-lactams. This represents a distinct mechanism of resistance from those which have been previously described (section 1.5.3). Although this effect is relatively minor, and their loss does not result in total susceptibility, the peptide transporters can be described as contributing to the baseline level of resistance to antibiotics in wild type *E. coli*. Despite existing research demonstrating the ability of antibiotics to act as substrates for peptide transporters (e.g Prabhala et al., 2017) and evidence for the ABC transporters playing a role in susceptibility to aminoglycoside antibiotics (e.g Shiver et al., 2016), to date this is the first known study linking the POT transporters to beta-lactam antibiotic resistance.

As previously discussed, the beta-lactams represent an extremely successful class of antibiotics, despite suffering from the development of resistance (section 1.5). The findings of this study therefore have important implications for the possible future of beta-lactam usage. For example, if the activity of bacterial POT transporters could be inhibited, this could increase the sensitivity of bacterial infections to antibiotic treatment, thereby increasing their potency. A proof of concept is provided for this by multiple studies describing inhibitors of the human POT transporters PEPT1 and PEPT2 (Knütter et al. 2001; Stauffer et al. 2022). An equivalent in bacteria has not yet been described, though if found to exclusively target bacterial POT transporters whilst not affecting those of the host (thereby preventing potential toxicity) this could inform future drug design strategies. Conversely, for antibiotics in which the site of action is within the cytoplasm, the activity of the peptide transporters is beneficial in the context of antibiotic usage by bringing the antibiotic closer to their site of action. In addition to the aminoglycosides described in this study which are substrates of the ABC transporters, a similar concept applies to chloramphenicol, which also targets the ribosome and has been demonstrated to be a substrate of YgdR/DtpA (Prabhala et al. 2018). The potency of such antibiotics could theoretically be improved by increasing their uptake by peptide transporters. A similar approach is widely used to design drugs which target the human peptide transporters to aid in drug absorption (Brodin et al. 2002; Rubio-Aliaga and Daniel 2002; Groneberg et al. 2004). Therefore, although a similar drug design methodology has not been developed for the equivalent bacterial transporters, this provides a proof of

concept for the future design of antibiotics which target the bacterial peptide transporters in order to improve their efficacy.

#### 4.2.7 Limitations:

Although the results presented here seem comprehensively in favour of the hypothesis, there are a number of limitations associated with this conclusion. Firstly, to date the structure of an *E. coli* peptide transporters in complex with a beta-lactam antibiotic has not been resolved. For this reason, the transport of the beta-lactam antibiotics by the peptide transporters, and thus the precise binding mechanism of the POT transporters to antibiotics is unknown. Such a mechanism could also explain why the POT transporters appear unable to transport antibiotics such as kasugamycin and Blastocidin S which are substrates of the ABC transporters.

Other studies in this field of research have utilised alternative methods to demonstrate the transport of beta-lactam antibiotics by peptide transporters. One such example is an uptake competition assay such as that performed in Stauffer et al (2021), in which the affinity of antibiotics as a substrate for POT transporters is inferred by their ability to compete with uptake of a known substrate (in this case, Ala-Ala). Whilst the scope of the aforementioned study is limited to *Yersinia* POT transporters, a similar technique could be utilised in the context of the *E. coli* POT transporters, whilst possibly being expanded to the ABC transporters, in order to provide additional evidence of the affinity of *E. coli* peptide transporters for peptidometric antibiotics. An alternative method which could further strengthen the evidence that peptide transporters contribute to antibiotic resistance utilises an overexpression-plasmid based approach to increase expression of peptide transporters (such as in Prabhala et al (2018)). A similar method to that used in this study could then be utilised to compare a wild type and overexpression strain, after which based on the proposed hypothesis it would be expected that overexpression would result in increased levels of resistance. Therefore, whilst the evidence presented in this study remains circumstantial, the methodologies employed by similar studies in the field could be used in future to provide further evidence for the transport of antibiotics by *E. coli* peptide transporters, and thus elucidate their role in the proposed mechanism of resistance.

Furthermore, an open question not answered by the existing hypothesis is the fate of the beta-lactam antibiotics after they enter the cytoplasm. Multiple possibilities are plausible, one example being their direct export from the cytoplasm out of the cell. *E. coli* is known to have evolved elevated resistance to a range of antibiotics through the use AcrAB-TolC efflux pump, which traditionally exports antibiotics from the cytoplasm outside of the cell (Du et al. 2014). The periplasmic nature of their targets means the beta-lactams are not obvious targets of such a transporter, however multiple studies have described the ability of betalactam antibiotics to interact with similar efflux pump systems, contributing to intrinsic resistance in *E. coli* (Chetri et al. 2019), *S. typhimurium* (Bernal et al. 2021) and *Pseudomonas aeruginosa* (Srikumar, Li, X.Z. and Poole 1997). Whilst no studies to date have examined the ability of beta-lactams to interact with such a pump starting from a cytoplasmic origin within *E. coli*, it is possible that after entering the cytoplasm as a result of

peptide transporter activity, the beta-lactams could be removed by the activity of an efflux pump. A second possibility is the breakdown of the beta-lactam antibiotics within the cytoplasm by intracellular peptidases, which traditionally digest peptides within the cell but could potentially recognise beta-lactam antibiotics due to the presence of the amide bond (Miller 1975).

A second limitation stems from the analysis used to determine if differences in the growth dynamics between bacterial strains were statistically significant. The growthcurver R package utilised has been extensively tested and has been found to produce a robust analysis for a range of growth curve datasets (Sprouffske and Wagner 2016). However, a study performed by Concepción-Acevedo et al (2015) describes substantial variation in the measurements generated from automated microplate-based approaches to monitoring bacterial growth - such as that used in this study. The study also highlights examples in which clear differences in fitness phenotypes observed in pairwise competition experiments are not identified in identical comparisons performed in a microplate reader. Therefore, this provides an important caveat for this study, in which examples of a lack of difference in growth may exist but were not detected due to the methodology used, and also that in examples in which a difference is found, this may not occur outside of such an artificial environment. The second is particularly important in the context of antibiotic usage, as although there is a clear difference in susceptibility between wild type *E. coli* and peptide transporter deficient mutants in microplate experiments, it is impossible to conclude this difference would still be apparent in the native environment of pathogenic *E. coli* (the human gut) in which the antibiotics would be used in a clinical setting. This limitation could be examined through the use of a mouse model system, in which an infection with a wild type pathogenic strain of *E. coli* is compared with a strain lacking peptide transporters (such as  $\Delta$ DB50/ $\Delta$ DB1) in the presence of beta-lactam antibiotic treatment. The effectiveness of the antibiotic could then be compared (possibly measured by monitoring CFUs isolated from the intestine over time) in the two lines, allowing the clinical importance of the POT transporters in antibiotic susceptibility to be assayed.

### 4.3 Determination of peptide transporter specificities:

An additional aim of this study was the further elucidation of the role of peptide transporters in *E. coli*. One aspect of this system which is not fully understood is the differing specificities of peptide transporters. In the research presented here, this was investigated using a toxic peptide assay, utilising peptide transporter deficient mutants to understand the role of individual transporters in the uptake of peptides with differing amino acid constituents.

The abundance of peptides in LB medium allows for rapid growth of an *E. coli* culture, however this also makes it unsuitable for this assay as the high number of possible peptides to uptake would dilute the contribution of the toxic peptides and limit their effect. For this reason, M9 Glucose minimal media was used, which contains all the essential substances needed for growth of *E. coli* but no peptides (section 2.1.4) – this means that the only peptides taken up by the transporters are those which are supplemented.

Supplementation of toxic peptides to *E. coli* mutants in this way allows uptake to be monitored through observing a binary phenotype, in which toxicity is present or not depending on the ability of the bacteria to take up the peptide. This ability is governed by the peptide transporter complement of the strain assayed, with mutants lacking the transporters responsible for the uptake of the peptide appearing resistant, whilst growth of wild type *E. coli* is inhibited.

The toxic effect of a peptide is dependent upon its amino acid constituents. After the peptide enters the cell, it's broken down by peptidases within the cytoplasm, releasing the amino acids with a potentially toxic effect. Two amino acids with predicted toxicity are used in this study: Leucine and Valine. Leucine toxicity is conferred through the circumvention of leucine transport, which is normally regulated by amino acid transporters, thus leading to abnormally high concentrations of free leucine within the cell. The leucine within the cell then interferes with the biosynthesis of isoleucine, thus inhibiting the growth of the bacteria (Tavori, Kimmel and Barak 1981). Whilst Valine works through a similar mechanism through inhibiting the biosynthesis of isoleucine, it does not require to circumvent the existing transport mechanism to do so and is thus toxic in its free form (Tuite, Fraser and O'Byrne 2005).

The toxic peptide assay performed in was based upon previous work conducted by Dr Daniel Bawdon, however some of the results observed in this study show conflicting results. One example is the loss of toxicity of L-Val-Gly-Gly in  $\Delta$ DB5 (utilised by Dr Daniel Bawdon) which is not observed in the presence of DL-Val-Gly-Gly (DL mix) in  $\Delta$ DB50 (utilised in this study)(Figure 3.9, 3.10). In contrast, the toxicity of DL-Val-Gly-Gly was lost in  $\Delta$ DB1 (which was found to be due to the activity of the Opp transporter), whereas L-Val-Gly-Gly remained toxic to  $\Delta$ DB1 in Dr Daniel Bawdon's work (Figure 3.9, 3.18, 3.19). Whilst these results would initially appear contradictory, they are limited by the fact that different stereoisomer forms were used in the two studies. Whereas Dr Daniel Bawdon's work used the L form of Val-Gly-Gly alone, this study utilised a mix of D and L forms of Val-Gly-Gly in unknown proportions. One possible explanation for the results observed in this study is that the mix used in this study contains a higher proportion of D than L forms, leading to the conclusion that the L forms are substrates of the POT transporters whilst the D forms are substrates of the ABC transporters – thus explaining the difference in results observed. This is consistent with previous studies demonstrating a preference of PEPT1 (a mammalian POT transporter) for L-stereoisomers with relatively little affinity for the equivalent D form (Lister et al. 1995; Meredith, D. and Boyd 1995). However, no studies have specifically examined the relative preference towards D and L forms of Val-Gly-Gly specifically. Meanwhile, a similar stereoisomeric preference for the ABC peptide transporters has not been demonstrated. Therefore, additional research would be required to determine if this is the true explanation for the observed result, chiefly the isolation of D and L forms of Val-Gly-Gly alone, and their re-exposure to  $\Delta$ DB1.

A second valine containing peptide (Val-Tyr) expected to be toxic through the same mechanism as Val-Gly-Gly was also examined. Val-Tyr was toxic to strains lacking both the

POT transporters ( $\Delta$ DB5/50) and those lacking the ABC peptide transporters ( $\Delta$ DB1)(Figure 3.1, 3.18). The explanation given for this is that Val-Tyr is transported by both transporters.

A set of leucine containing peptides which were found in a study by Tavori et al. (1981) were also examined, however none of these were toxic to the same extent as those containing valine. Despite this, there was an indication that weak inhibition may have occurred in the wild type strain. One possible explanation for this, is that the peptides are initially toxic, but this effect is overcome over the course of growth before the plates are examined (which in this case was approximately 17+ hours). Therefore, a future study could examine the effect of leucine containing peptide supplementation over a shorter time period (e.g 8 hours) to determine if the toxic effect was initially present, and thus elucidate which transporters they are substrates for.

As part of this study, 4 strains of *E. coli* each complemented with a single Dtp transporter were developed. Whilst they were not used in the experiments described in this report due to time limitations, they could in future be used to determine any potential differences in the specificities of different peptides between the different Dtp transporters, which could be further complemented by comparison with single Dtp KEIO collection deletion strains. A proof of concept is provided for this in Dr Daniel Bawdon's work, in which L-Val-Gly-Gly is toxic to all Dtp KEIO collection strains but not  $\Delta$ *dtpA*, indicating that *dtpA* is responsible for transport of Val-Gly-Gly whereas the other *dtp* transporters are not.

#### 4.4 Phylogenetic analysis:

In bacteria, one role performed by the POT transporters is nutrient acquisition, by aiding in peptide scavenging from the environment. Meanwhile, many bacteria also have ABC peptide transporters which can perform the same function. There is therefore a degree of redundancy between the two transporters. For this reason, the POT transporters are not ubiquitous across all bacterial species - including those which are pathogenic. While one aim of this project was to further elucidate the role of POT in bacteria, another aim was to determine the experimental evidence in favour of the intrinsic resistance hypothesis. This hypothesis postulates a link between bacterial peptide transporters and antibiotics - which are primarily used to combat pathogenic bacterial species. Therefore, it is important to understand how widespread the peptide transporters are amongst pathogenic bacterial species. In this study a sample of pathogenic bacterial strains were selected using a criteria designed to be representative of a wide range of biological attributes (section 2.4), these strains were then examined for their POT transporter complement. Approximately half (52%) of the strains examined did not have those that did have POT transporters, whilst within the strains selected that did have POT transporters there was diversity in both the number of transporters present (even at the genus level) and the protein sequence of the transporters themselves. This indicates that POT transporters could have been both gained and lost throughout the evolutionary course of these bacterium, and also that a significant amount of diversity has evolved within the transporter family (section 3.2).

This could coincide with changes in environmental conditions, such as greater peptide availability, or conversely a need for greater peptide scavenging capabilities. This is particularly relevant for pathogenic species for which colonisation of the gut is an important factor in determining pathogenicity, such as *E. coli* and *V. cholerae* (section 1.1). Within this context, it is notable that the *E. coli* POT transporter *ntpA* shares significant both functional and sequence similarity with the peptide transporter protein (PEPT1) found in mammals. The shared functionality has been demonstrated through the high degree of similarity in the substrate recognition pattern between the two strains (Weitz et al. 2007). Through locus analysis, there is also a high degree sequence homology identified between *ntpA* and the POT transporter family present in humans (Daniel et al. 2006.). This demonstrates the presence of evolutionary conservation acting within the transporter class.

In addition to their role in nutrition, there are many examples of both POT and ABC transporters having a more direct role in virulence (Garai, Chandra and Chakravorty 2016). For example, in *Salmonella* the POT genes *cstA* and *yjiY* contribute directly to virulence, with mutant strains lacking the transporters showing reduced colonisation capacity in *Caenorhabditis elegans* and mouse intestine models respectively (Tenor et al. 2004; Garai et al. 2016). Meanwhile, ABC peptide transporters are also known to play a diverse range of roles in virulence across multiple species, such as adhesion to host cells (McNab and Jenkinson 1998; Moraes et al. 2014), chemotaxis (Abouhamad et al. 1991) and sporulation (Edwards, Nawrocki and McBride 2014) amongst many others. The contribution to the virulence of bacterial pathogens could explain some of the diversity in POT transporters seen in this study, with the nature and number of POT transporters present in each species determined by a combination of nutrient requirement (possibly coinciding with environmental conditions) and pathogenicity. To date, this is the first known phylogenetic examination of the POT transporters focusing exclusively on pathogenic bacterial strains.

Alongside a phylogenetic comparison of the POTs identified, a comparison of the POT complement based on biological characteristics was also conducted (Figure 3.7). This analysis found no difference in the number of POTs based on gram staining, indicating that the composition of the cell wall has no bearing on the number of POTs a bacterial species possesses. This result is not unexpected, as the cell wall is thought to be largely permissive to the passage of substances the size of peptides (Demchick and Koch 1996), and therefore would have no bearing on the number of POT transporters required for protein uptake. The same analysis also concluded that anaerobic bacteria had a significantly higher number of POT transporters, this implies that a greater number of POT transporters may be beneficial in such conditions. A study by X found that anaerobic conditions were linked with upregulation of peptide transporters in *Salmonella typhimurium*. In this case this upregulation was hypothesized to assist in scavenging peptides lost as a result of nutrient starvation, which is likely to be more commonly experienced in anaerobic conditions (Jamieson and Higgins 1984). This provides an example in which POT transporters are highly beneficial in anaerobic conditions, possibly selecting for a higher number of POT transporters in this group, further driven by the pathogenic nature of the species chosen, many of which will occupy anaerobic niches such as the human gut. Furthermore, it was also found that of the bacterial species

Included only those which were extracellular had POT transporters. Intracellular pathogenic bacteria are able to exploit the free amino acids generated within a cell as part of normal protein turnover (Kwaik and Bumann 2015), this comparative abundance of amino acids within an intracellular environment may mean that POT transporters are not required, as the amino acids requirements can be fulfilled by the activity of non-POT amino acid transporters (Figure 3.15). Whilst this analysis yields two novel results, it is limited by the sample size with only 52 species included in the original analysis, with this being further reduced by the exclusion of species classed as 'facultative' aerobic or intracellular. Future analyses could also include non-pathogenic bacterial species, to determine if the perceived differences are pathogenic specific.

## 5 Conclusion

This study chronicles the creation and verification of three mutant strains of *E. coli* created by previous lab members termed  $\Delta$ DB5,  $\Delta$ DB50 and  $\Delta$ DB1. This provides provenance for these strains which have the potential to be used in a variety of contexts to further elucidate the role of peptide transporters in *E. coli*, whilst also highlighting the phenomenon of a genomic inversion which is possible as a result of  $\lambda$ -red mediated gene deletion. Peptide transporters have been observed in multiple contexts to be capable of transporting various drug molecules including beta-lactam antibiotics, this led to the proposal of the intrinsic resistance hypothesis which postulates a role of peptide transporters in the basal level of bacterial resistance to these drugs. The creation of mutant strains lacking these transporters allows this hypothesis to be tested, in this context by comparing the growth dynamics of mutant strains in the presence of various peptide-like antibiotics to that of wild type *E. coli*. This revealed a comparatively higher susceptibility to beta-lactam antibiotics in strains lacking POT transporters, manifesting through examples of decreased growth rate, lower maximum OD and lower area under the curve generated. This conclusion is supported by the lack of difference observed in the presence of antibiotics which lack the peptide bond. However, this difference was only present at a subset of the total concentrations tested, revealing a key “window” in which this difference in susceptibility is apparent. Although the difference in susceptibility was observable it was relatively minor, raising the question as to whether this difference would be relevant in a more complex in-vivo setting. Therefore, whilst providing a “proof of concept” for the role of peptide transporters in antibiotic susceptibility, additional work would be needed to establish a definitive role of peptide transporters in this context and establish the feasibility of exploiting this process in a clinical setting. This study also recapitulated the previously described role of bacterial ABC transporters in resistance to two aminoglycoside antibiotics, whilst demonstrating that the same antibiotics are not substrates of POT transporters, revealing a key difference in the specificity towards antibiotics associated with the transporter mechanism of action.

The importance of understanding the role of peptide transporters in antibiotic resistance is emphasised by the widespread distribution and diversity of POT transporters amongst pathogenic bacterial species. Further research will be required to understand why this diversity exists and uncover any possible correlation between biological attributes and POT transporter complement. In addition to genetic diversity, there is also considerable diversity in substrate specificity observed within peptide transporters. This is demonstrated in this study, which includes examples of both substrates which are common across POT and ABC transporters, in addition to substrates which are specific to one depending on their stereochemistry whilst otherwise identical in amino acid content.

In conclusion, this study has revealed a potential mechanism of antibiotic resistance facilitated by bacterial peptide transporters which has not been previously described, in addition to elucidating the role of peptide transporters in bacteria more widely. This information can be used as a basis for future studies to further understand the diversity of peptide transporters, whilst assessing them as a possible target for combatting the growing threat of antibiotic resistance.



## 6 Supplementary Information

### 6.1 Supplementary Methods:

**Table 1** – Pathogenic bacterial species examined for their POT complement. Species (strains not shown here) were chosen based on known pathogenicity, and then to be representative of a range of biological attributes (section 2.4). Continued on next page.

Genus	Species	Gram staining	Shape	Oxygen requirement	Intra/Extracellular
<i>Bacillus</i>	<i>Bacillus anthracis</i>	Positive	Rods	Facultative anaerobic	Extracellular
	<i>Bacillus cereus</i>				
<i>Bartonella</i>	<i>Bartonella henselae</i>	Negative	Rods	Aerobic	Facultative intracellular
	<i>Bartonella quintana</i>				
<i>Bordetella</i>	<i>Bordetella pertussis</i>	Negative	Small coccobacilli	Aerobic	Extracellular
<i>Borrelia</i>	<i>Borrelia burgdorferi</i>	Negative	Spirochete	Anaerobic	Extracellular
	<i>Borrelia garinii</i>				
	<i>Borrelia afzelii</i>				
	<i>Borrelia recurrentis</i>				
<i>Brucella</i>	<i>Brucella abortus</i>	Negative	Coccobacilli	Aerobic	Intracellular
	<i>Brucella canis</i>				
	<i>Brucella melitensis</i>				
	<i>Brucella suis</i>				
<i>Campylobacter</i>	<i>Campylobacter jejuni</i>	Negative	Spiral rods	Microaerophilic	Extracellular
			coccoid in older cultures		
<i>Chlamydia and Chlamydophila</i>	<i>Chlamydia pneumoniae</i>	(none)	Small, round, ovoid	Facultative or strictly aerobic	Obligate intracellular
	<i>Chlamydia trachomatis</i>				
	<i>Chlamydophila psittaci</i>				
<i>Clostridium</i>	<i>Clostridium botulinum</i>	Positive	Large, blunt-ended rods	Obligate anaerobic	Extracellular
	<i>Clostridium difficile</i>				
	<i>Clostridium perfringens</i>				
	<i>Clostridium tetani</i>				
<i>Corynebacterium</i>	<i>Corynebacterium diphtheriae</i>	Positive	Rods	Mostly facultative anaerobic	Extracellular
<i>Enterococcus</i>	<i>Enterococcus faecalis</i>	Positive	Cocci	Facultative Anaerobic	Extracellular
	<i>Enterococcus faecium</i>				
<i>Escherichia</i>	<i>Escherichia coli</i>	Negative	Rods	Facultative anaerobic	Extracellular or Intracellular
<i>Francisella</i>	<i>Francisella tularensis</i>	Negative	Coccobacillus	Strictly aerobic	Facultative intracellular
Haemophilus	<i>Haemophilus influenzae</i>	Negative	Coccobacilli to long and slender filaments	Facultative anaerobic	Extracellular

<i>Helicobacter</i>	<i>Helicobacter pylori</i>	Negative	Spiral rod	Microaerophile	Extracellular
<i>Legionella</i>	<i>Legionella pneumophila</i>	Negative	Cocobacilli	Aerobic	Facultative intracellular
<i>Leptospira</i>	<i>Leptospira interrogans</i>	Negative	Spirochete	Strictly aerobic	Extracellular
	<i>Leptospira santarosai</i>				
	<i>Leptospira weilii</i>				
	<i>Leptospira noguchii</i>				
<i>Listeria</i>	<i>Listeria monocytogenes</i>	Positive	Slender, short rods	Facultative Anaerobic	Facultative intracellular
<i>Mycobacterium</i>	<i>Mycobacterium leprae</i>	(none)	Long, slender rods	Aerobic	Intracellular
	<i>Mycobacterium tuberculosis</i>				
	<i>Mycobacterium ulcerans</i>				
<i>Mycoplasma</i>	<i>Mycoplasma pneumoniae</i>	(none)	Indistinct 'fried egg' appearance, no cell wall	Mostly facultative anaerobic	Extracellular
<i>Neisseria</i>	<i>Neisseria gonorrhoeae</i>	Negative	Kidney bean-shaped	Aerobic	<i>Gonococcus</i> : facultative intracellular
	<i>Neisseria meningitidis</i>				<i>N. meningitidis</i> : extracellular
<i>Pseudomonas</i>	<i>Pseudomonas aeruginosa</i>	Negative	Rods	Obligate aerobic	Extracellular
<i>Rickettsia</i>	<i>Rickettsia rickettsii</i>	Negative	Small, rod-like coccobacillary	Aerobic	Obligate intracellular
<i>Salmonella</i>	<i>Salmonella typhi</i>	Negative	Rods	Facultative anaerobic	Facultative intracellular
	<i>Salmonella typhimurium</i>				
<i>Shigella</i>	<i>Shigella sonnei</i>	Negative	Rods	Facultative anaerobic	Extracellular
<i>Staphylococcus</i>	<i>Staphylococcus aureus</i>	Positive	Round cocci	Facultative anaerobic	Extracellular, facultative intracellular
	<i>Staphylococcus epidermidis</i>				
	<i>Staphylococcus saprophyticus</i>				
<i>Streptococcus</i>	<i>Streptococcus agalactiae</i>	Positive	Ovoid to spherical	Facultative anaerobic	Extracellular
	<i>Streptococcus pneumoniae</i>				
	<i>Streptococcus pyogenes</i>				
<i>Treponema</i>	<i>Treponema pallidum</i>	Negative	Spirochete	Aerobic	Extracellular
<i>Ureaplasma</i>	<i>Ureaplasma urealyticum</i>	(none)	Indistinct, 'fried egg' appearance, no cell wall	Anaerobic	Extracellular
<i>Vibrio</i>	<i>Vibrio cholerae</i>	Negative	Spiral with single polar flagellum	Facultative anaerobic	Extracellular
<i>Yersinia</i>	<i>Yersinia pestis</i>	Negative	Small rods	Facultative anaerobe	Intracellular
	<i>Yersinia enterocolitica</i>				
	<i>Yersinia pseudotuberculosis</i>				

## 6.2 Supplementary Data:

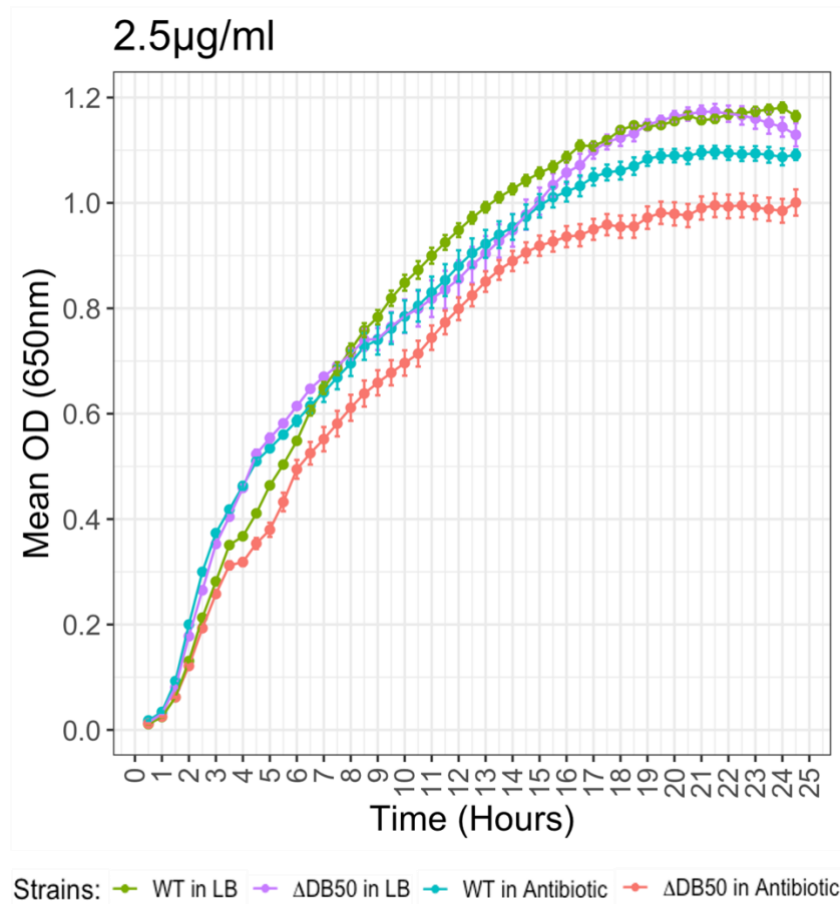
**Table 2** – POT transporter proteins identified from TransportDB. Known pathogenic strains of bacteria from the species included in table 1 were examined for their POT transporter complement using the database TransportDB. Pathogen number and POT number are terms used only in the analysis conducted within this report. The protein name and NCBI (National Centre for Biotechnology Information) code are both obtained from TransportDB, strains which had no POT transporters are designated as such. Table is continued on the next page.

Genus	Pathogen Number	POT Number	Species	Strain	Protein Name	NCBI Protein Code
Bacillus	Path1	POT1	Bacillus anthracis	Ames Ancestor	GBAA_0614	ZP_04287703.1
	Path1	POT2			GBAA_0689	YP_002444152.1
	Path2	POT1	Bacillus cereus	G9842	BCG9842_B4615	ZP_04105514.1
	Path2	POT2			BCG9842_B4686	P_04100481.1
Bartonella	Path3	NO POT	Bartonella henselae	No pots		
	Path4	NO POT	Bartonella quintana	No pots		
Bordetella	Path5	NO POT	Bordetella pertussis	No pots		
Borrelia	Path6	NO POT	Borrelia burgdorferi	No POTs		
	Path7	NO POT	Borrelia garinii	No POTs		
	Path8	NO POT	Borrelia afzelii	No POTs		
	Path9	NO POT	Borrelia recurrentis	No POTs		
Brucella	Path10	NO POT	Brucella abortus	No POTs		
	Path11	NO POT	Brucella canis	No POTs		
	Path12	NO POT	Brucella melitensis	No POTs		
	Path13	NO POT	Brucella suis	No POTs		
Campylobacter	Path14	POT1	Campylobacter jejuni	81176	CJJ81176_0682	ZP_06371589.1
	Path14	POT2			CJJ81176_0683	YP_001398387.1
	Path14	POT3			CJJ81176_0684	ZP_06056135.1
	Path14	POT4			CJJ81176_0685	YP_004066172.1
Chlamydia and Chlamydia	Path15	NO POT	Chlamydia pneumoniae	No POTs		
	Path16	NO POT	Chlamydia trachomatis	No POTs		
	Path17	NO POT	Chlamydia psittaci	No POTs		
Clostridium	Path18	POT1	Clostridium botulinum	A2strKyo to	CLM_1774	ZP_08695724.1
	Path18	POT2			CLM_1924	ZP_05272324.1
	Path18	POT3			CLM_2243	YP_001781591.1
	Path18	POT4			CLM_2244	ZP_02614399.1
	Path18	POT5			CLM_2372	YP_001787643.1

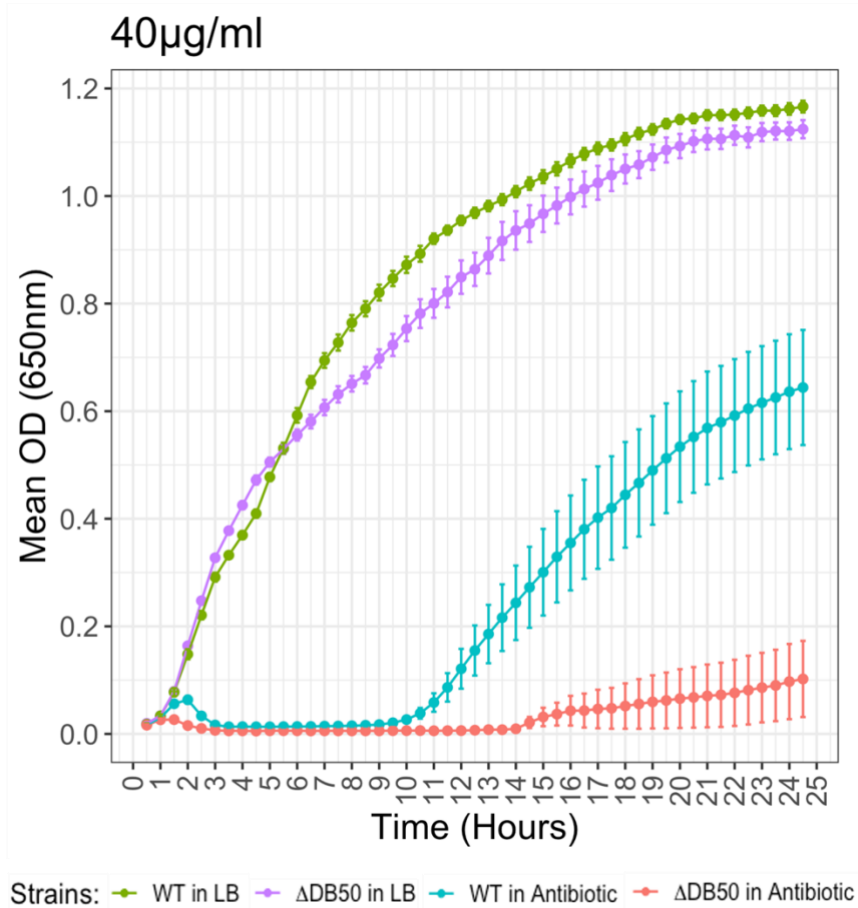
	Path18	POT6			CLM_2473	ZP_02995545.1
	Path19	POT1	Clostridium difficile	BI1	CDBI1_10945	ZP_06892078.1
	Path19	POT2			CDBI1_10955	YP_001254657.1
	Path19	POT3			CDBI1_14600	YP_002804413.1
	Path20	POT1	Clostridium perfringens	ATCC13124	CPF_0523	ZP_04105514.1
	Path21	NO POT	Clostridium tetani	No POTs		
Corynebacterium	Path22	POT1	Corynebacterium diphtheriae	PW8	CDPW8_1169	ZP_08517411.1
Enterococcus	Path23	POT1	Enterococcus faecalis	OG1RF	OG1RF_10326	ZP_05664375.1
	Path24	POT1	Enterococcus faecium	Aus0004	EFAU004_01045	ZP_06701569.1
Escherichia	Path25	POT1	Escherichia coli	0157	Z0860	NP_415237.1
	Path25	POT2			Z2646	ZP_08373971.1
	Path25	POT3			Z4896	ZP_08366004.1
	Path25	POT4			Z5733	YP_313035.1
Francisella	Path26	POT1	Francisella tularensis	OSU18	FTH_0693	ZP_04990148.1
	Path26	POT2			FTH_0940	YP_004648058.1
	Path26	POT3			FTH_1228	ZP_05249810.1
Haemophilus	Path27	NO POT	Haemophilus influenzae	No POTs		
Helicobacter	Path28	NO POT	Helicobacter pylori	No POTs		
Legionella	Path29	POT1	Legionella pneumophila	Corby	LPC_0794	ZP_01946494.1
	Path29	POT2			LPC_0954	ZP_06189647.1
	Path29	POT3			LPC_1662	ZP_06189647.1
	Path29	POT4			LPC_2546	ZP_03246771.1
	Path29	POT5			LPC_3091	ZP_04613082.1
Leptospira	Path30	POT1	Leptospira interrogans	IPAV	LIF_A1976	ZP_04124929.1
Listeria	Path31	POT1	Listeria monocytogenes	EGD	LMON_0555	YP_002351029.1
Mycobacterium	Path32	NO POT	Mycobacterium leprae	No POTs		
	Path33	NO POT	Mycobacterium tuberculosis	No POTs		
	Path34	NO POT	Mycobacterium ulcerans	No POTs		
Mycoplasma	Path35	NO POT	Mycoplasma pneumoniae	No POTs		
Neisseria	Path36	POT1	Neisseria gonorrhoeae	FA1090	NGO1954	YP_001600179.1
	Path37	POT1	Neisseria meningitidis	MC58	NMB2136	YP_002341762.1
Pseudomonas	Path38	NO POT	Pseudomonas aeruginosa	No POTs		
Rickettsia	Path39	NO POT	Rickettsia rickettsii	No POTs		
Shigella	Path40	POT1	Shigella sonnei	53G	SSON53_03535	ZP_03029039.1

	Path40	POT2			SSON53_08835	ZP_02775572.1
	Path40	POT3			SSON53_20915	ZP_07450296.1
	Path40	POT4			SSON53_24910	ZP_07140379.1
Staphylococcus	Path41	POT1	Staphylococcus aureus	MRSA USA300	SAUSA300_0712-sa367830	ABD21982.1
	Path42	POT1	Staphylococcus epidermidis	ATCC1222	SE0509	ZP_06334220.1
	Path43	POT1	Staphylococcus saprophyticus	ATCC15305	SSP1990	ZP_01169775.1
	Path43	POT2			SSP1991	YP_003472320.1
Streptococcus	Path44	POT1	Streptococcus agalactiae	NEM316	gbs1513	ZP_07641110.1
Streptococcus	Path45	NO POT	Streptococcus pneumoniae	No POTs		
	Path46	NO POT	Streptococcus pyogenes	No POTs		
	Path47	NO POT	Treponema pallidum	No POTs		
Ureaplasma	Path48	NO POT	Ureaplasma urealyticum	No POTs		
Vibrio	Path49	POT1	Vibrio cholerae	EITorstrN16961	VC0988	ZP_04419307.1
Yersinia	Path50	POT1	Yersinia pestis	Angola	YpAngola_A2548	YP_001006373.1
	Path51	POT1	Yersinia enterocolitica	8081	YE1609	ZP_04615720.1
	Path51	POT2			YE2133	ZP_04614966.1
	Path51	POT3			YE2391	ZP_02660247.1
	Path52	POT1	Yersinia pseudotuberculosis	IP31758	YpsIP31758_1555	ZP_08499094.1
	Path52	POT2			YpsIP31758_1778	ZP_04623488.1



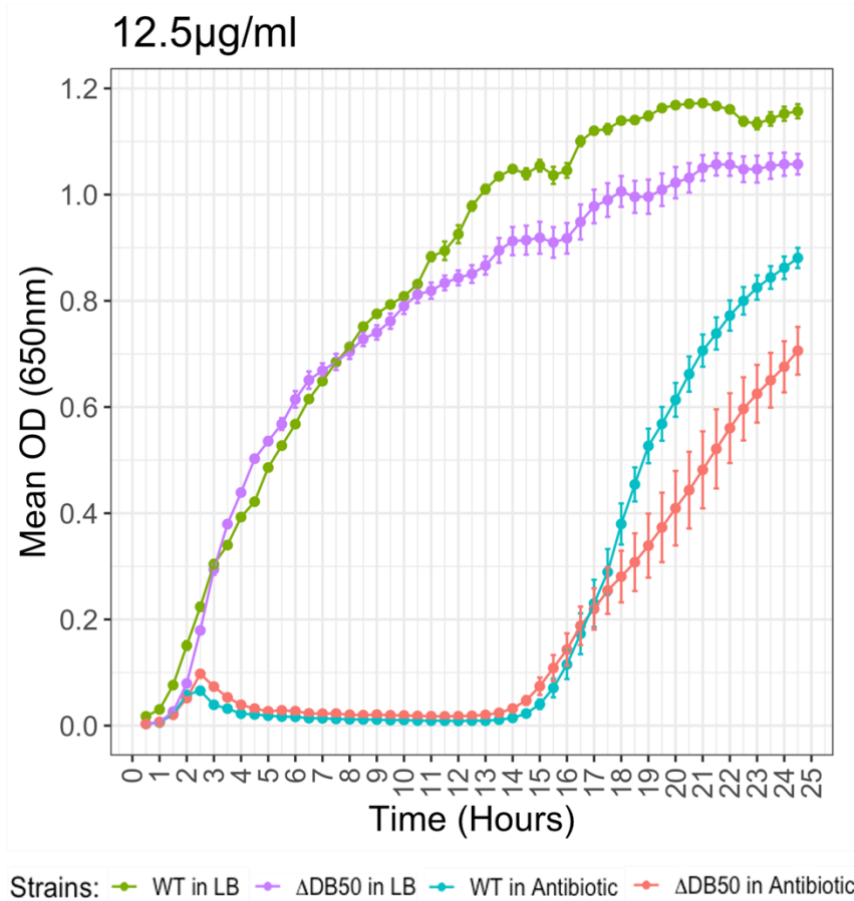


**Supplementary Figure 1 – Growth comparison in 2.5µg/ml carbenicillin.** The difference at this concentration was relatively minor compared to those shown in the main text, though the difference in max OD ( $W= 38, n_1=12, n_2=12, p= 0.053$ ) and area under the curve ( $W= 39, n_1=12, n_2=12, p= 0.06$ ) generated by wild type *E. coli* was borderline significantly higher than in  $\Delta$ DB50. 2.5µg/ml was the only additional concentration at which a difference in susceptibility between the two strains was present.

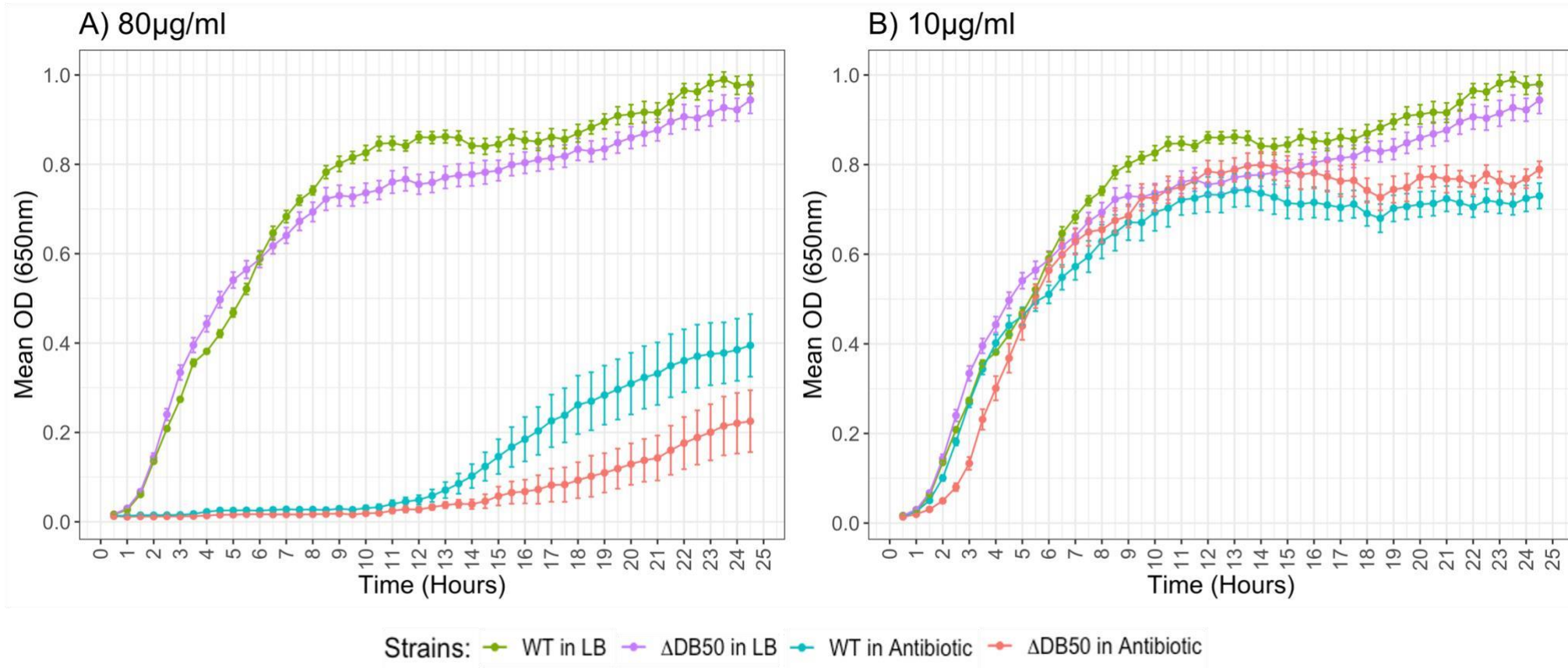


**Supplementary Figure 2 – Growth comparison in 12.5µg/ml amoxicillin.** The growth dynamic pictured here differs from that in the report, but the ability of wild type to achieve a significantly higher growth rate ( $W= 32, n_1=12, n_2=12, p= 0.018$ ) and generate a larger area under the curve ( $W= 20, n_1=12, n_2=12, p= 0.002$ ) after relief from the antibiotic pressure (at approximately 10 hours) indicates a greater susceptibility in  $\Delta$ DB50.

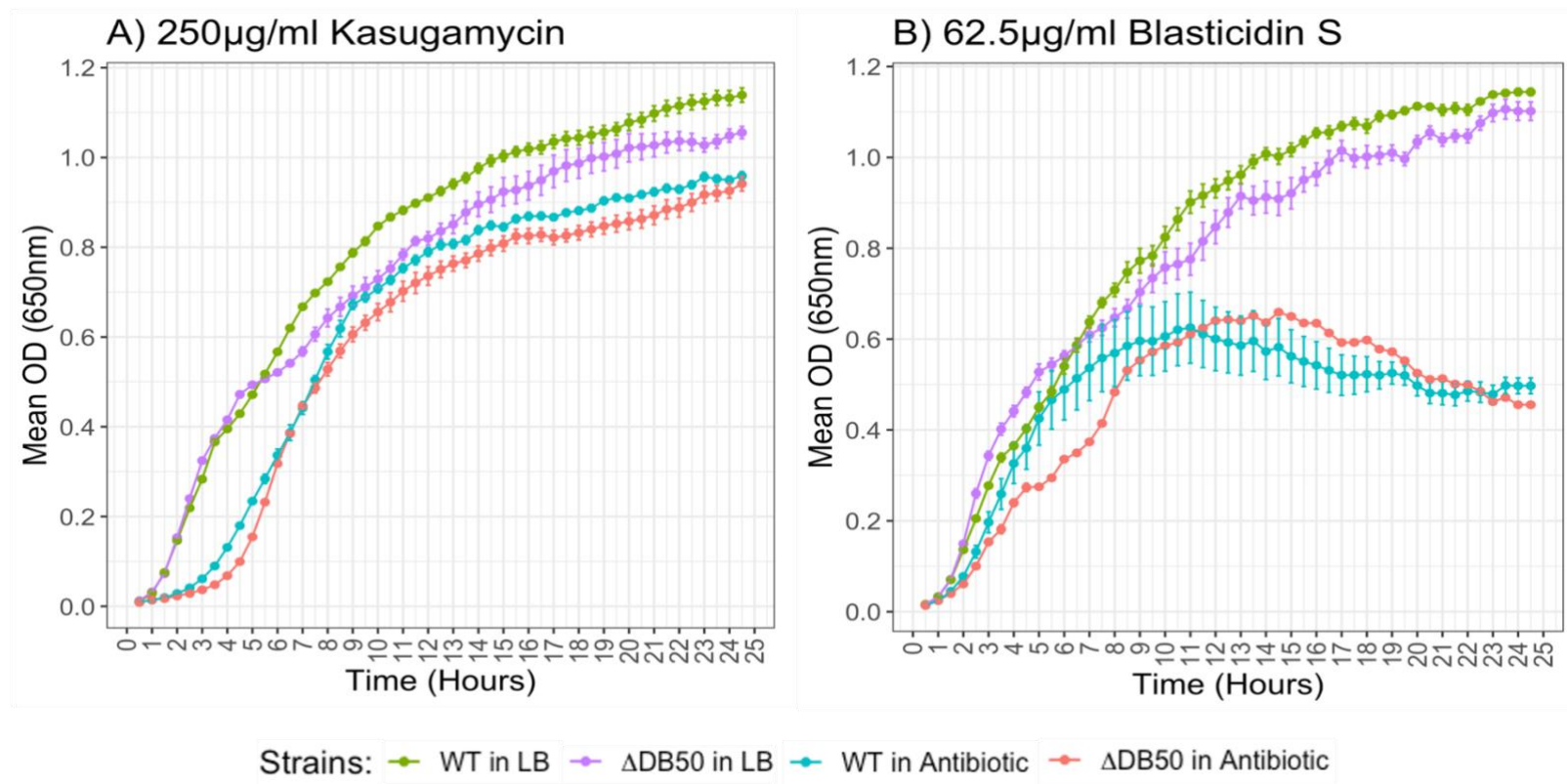




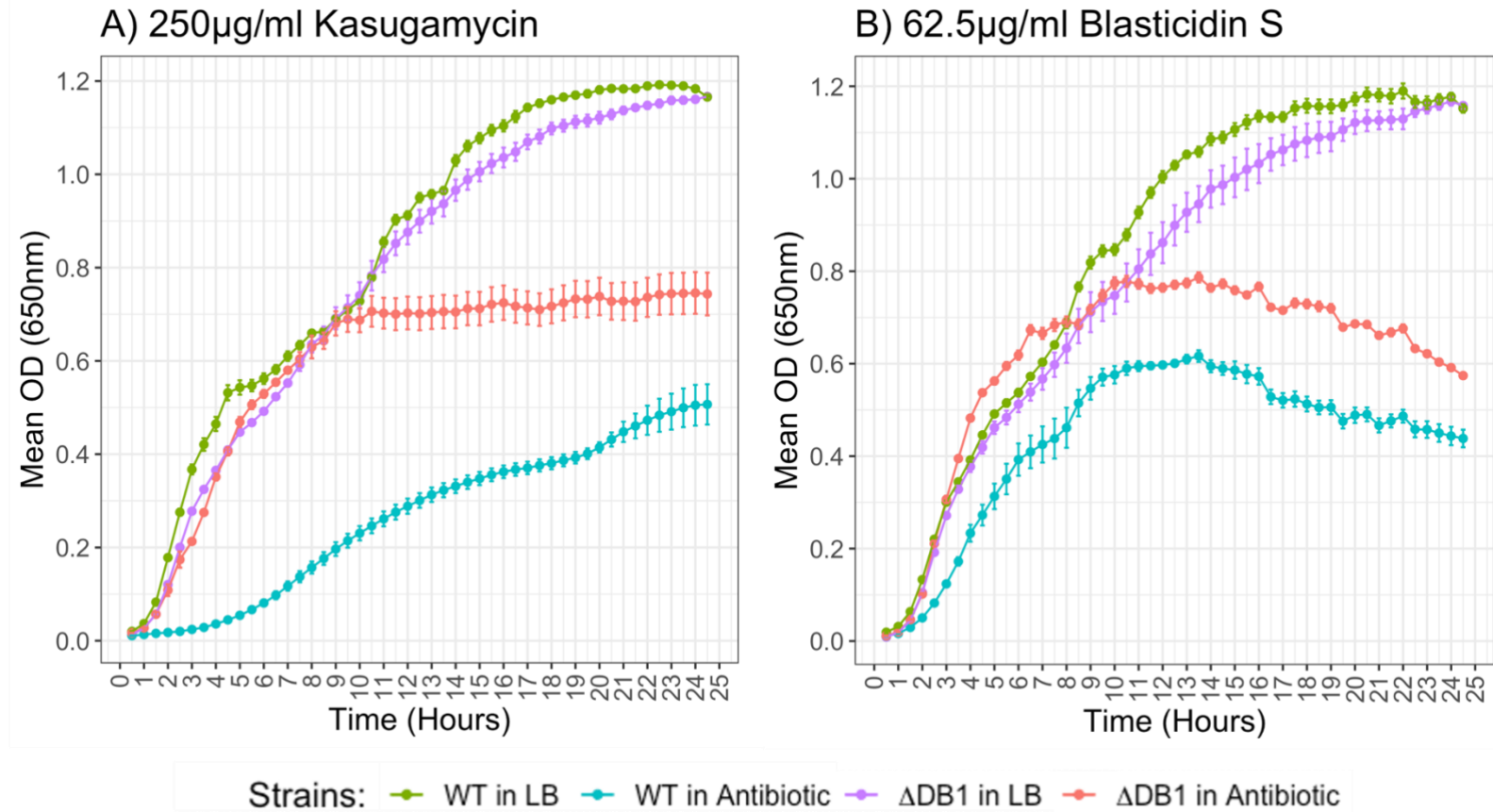
**Supplementary Figure 3 – Growth comparison in 12.5µg/ml cephalixin.** The growth dynamic pictured here differs from that in the report, but the ability of wild type to achieve a significantly higher growth rate ( $W= 36$ ,  $n_1=12$ ,  $n_2=12$ ,  $p= 0.039$ ) after relief from the antibiotic pressure (at approximately 14 hours) indicates a greater susceptibility in  $\Delta$ DB50.



**Supplementary Figure 4 – Growth comparison in kanamycin.** Additional concentrations above and below those presented in the report in which the same pattern of no difference in susceptibility is observed between the two strains. At 80µg/ml, there is no difference between growth of the two strains based on the three parameters tested, including the maximum OD ( $W=2$ ,  $n_1=12$ ,  $n_2=12$ ,  $p=0.114$ ), area under the curve ( $W=41.5$ ,  $n_1=12$ ,  $n_2=12$ ,  $p=0.083$ ) or growth rate ( $W=5$ ,  $n_1=12$ ,  $n_2=12$ ,  $p=0.486$ ). At 10µg/ml, there is also no difference between growth of the two strains based on the three parameters tested, including the maximum OD ( $W=6$ ,  $n_1=12$ ,  $n_2=12$ ,  $p=0.686$ ), area under the curve ( $W=88$ ,  $n_1=12$ ,  $n_2=12$ ,  $p=0.378$ ) or growth rate ( $W=14$ ,  $n_1=12$ ,  $n_2=12$ ,  $p=0.114$ ). There was also no difference in susceptibility across all the remaining concentrations tested above and below this range (not shown).



**Supplementary Figure 5 – Growth comparison in  $\Delta$ DB50 and wild type *E. coli* in Kasugamycin and Blasticidin S.** Additional concentrations outside the range of those shown in the main text which also show no difference in susceptibility for  $\Delta$ DB50 in the presence of either aminoglycoside antibiotic. **A)** In 250μg/ml kasugamycin there is no difference in maximum OD ( $W=4$ ,  $n_1=6$ ,  $n_2=6$ ,  $p=0.343$ ), area under the curve ( $W=3$ ,  $n_1=6$ ,  $n_2=6$ ,  $p=0.2$ ) and growth rate ( $W=7$ ,  $n_1=6$ ,  $n_2=6$ ,  $p=0.886$ ) between wild type *E. coli* and  $\Delta$ DB50. **B)** In 62.5μg/ml Blasticidin S there is no difference in maximum OD ( $W=1$ ,  $n_1=6$ ,  $n_2=6$ ,  $p=0.114$ ), area under the curve ( $W=4$ ,  $n_1=6$ ,  $n_2=6$ ,  $p=0.343$ ) and growth rate ( $W=4$ ,  $n_1=6$ ,  $n_2=6$ ,  $p=0.343$ ) between wild type *E. coli* and  $\Delta$ DB50.



**Supplementary Figure 6 – Growth comparison in  $\Delta$ DB1 and wild type *E. coli* in Kasugamycin and Blasticidin S.** Additional concentrations outside the range of those shown in the main text which also show no difference in susceptibility for  $\Delta$ DB1 in the presence of either aminoglycoside antibiotic. **A)** In 250 $\mu$ g/ml kasugamycin  $\Delta$ DB1 displays a higher area under the curve ( $W= 16, n_1=6, n_2=6, p= 0.029$ ) and growth rate ( $W= 16, n_1=6, n_2=6, p= 0.029$ ) than wild type *E. coli*. **B)** In 62.5 $\mu$ g/ml Blasticidin S  $\Delta$ DB1 displays a higher maximum OD ( $W= 16, n_1=6, n_2=6, p= 0.029$ ) and area under the curve ( $W= 16, n_1=6, n_2=6, p= 0.029$ ) than wild type *E. coli*.

## 7 References

- Abouhamad, W.N., Manson, M., Gibson, M.M. and Higgins, C.F. (1991). Peptide transport and chemotaxis in *Escherichia coli* and *Salmonella typhimurium*: characterization of the dipeptide permease (Dpp) and the dipeptide-binding protein. *Molecular microbiology*, 5(5), pp.1035-1047.
- Abu Kwaik, Y. and Bumann, D. (2015). Host delivery of favorite meals for intracellular pathogens. *PLoS pathogens*, 11(6), p.e1004866.
- Adibi, S.A. (1997). The oligopeptide transporter (Pept-1) in human intestine: biology and function. *Gastroenterology*, 113(1), pp.332-340.
- Agarwal, S., Boddu, S.H.S., Jain, R., Samanta, S., Pal, D. and Mitra, A.K. (2008). Peptide prodrugs: improved oral absorption of lopinavir, a HIV protease inhibitor. *International journal of pharmaceutics*, 359(1-2), pp.7-14.
- Ames, B.N., Ames, G.F.L., Young, J.D., Tsuchiya, D. and Lecocq, J. (1973). Illicit transport: the oligopeptide permease. *Proceedings of the National Academy of Sciences*, 70(2), pp.456458.
- Baba, T., Ara, T., Hasegawa, M., Takai, Y., Okumura, Y., Baba, M., Datsenko, K.A., Tomita, M., Wanner, B.L. and Mori, H. (2006). Construction of *Escherichia coli* K-12 in-frame, single-gene knockout mutants: the Keio collection. *Molecular systems biology*, 2(1), pp.2006-0008.
- Balaban, N.Q., Merrin, J., Chait, R., Kowalik, L. and Leibler, S. (2004). Bacterial persistence as a phenotypic switch. *Science*, 305(5690), pp.1622-1625.
- Barrick Lab (2018) :: ProtocolsRecipesM9 [Internet]. Available from <https://barricklab.org/twiki/bin/view/Lab/ProtocolsRecipesM9>. [Accessed 15th August 2022].
- Bawdon, D., 2014. Identification of bacterial transporters for hydroxyalkylcysteinylglycines (Doctoral dissertation, University of York).
- Beck, J.C. and Rosen, B.P. (1979) Cation/proton antiport systems in *Escherichia coli*: Properties of the sodium/proton antiporter. *Archives of Biochemistry and Biophysics*, 194 (1), pp. 208–214.
- Behrens, O.K., Corse, J., Edwards, J.P., Garrison, L., Jones, R.G., Soper, Q.F., Van Abeele, F.R. and Whitehead, C.W. (1948). Biosynthesis of penicillins: IV. New crystalline biosynthetic penicillins. *Journal of Biological Chemistry*, 175(2), pp.793-809.
- Berger, E.A. and Heppel, L.A. (1974) Different Mechanisms of Energy Coupling for the Shocksensitive and Shock-resistant Amino Acid Permeases of *Escherichia coli*. *Journal of Biological Chemistry*, 249 (24), pp. 7747–7755.

- Berntsson, R.P.A., Smits, S.H., Schmitt, L., Slotboom, D.J. and Poolman, B. (2010). A structural classification of substrate-binding proteins. *FEBS letters*, 584(12), pp.2606-2617.
- Blattner, F.R., Plunkett III, G., Bloch, C.A., Perna, N.T., Burland, V., Riley, M., Collado-Vides, J., Glasner, J.D., Rode, C.K., Mayhew, G.F. and Gregor, J. (1997). The complete genome sequence of *Escherichia coli* K-12. *science*, 277(5331), pp.1453-1462
- Blount, Z.D. (2015). The natural history of model organisms: The unexhausted potential of *E. coli*. *Elife*, 4, p.e05826.
- Blumberg, P.M. and Strominger, J.L. (1974). Interaction of penicillin with the bacterial cell: penicillin-binding proteins and penicillin-sensitive enzymes. *Bacteriological reviews*, 38(3), pp.291-335.
- Boggavarapu, R., Jeckelmann, J.M., Harder, D., Ucurum, Z. and Fotiadis, D. (2015). Role of electrostatic interactions for ligand recognition and specificity of peptide transporters. *BMC biology*, 13(1), pp.1-10.
- Boyle, J. (2005) *Lehninger principles of biochemistry* (4th ed.): Nelson, D., and Cox, M. *Biochemistry and Molecular Biology Education*, 33 (1).
- Brodin, B., Nielsen, C.U., Steffansen, B. and Frøkjær, S. (2002). Transport of peptidomimetic drugs by the intestinal di/tri-peptide transporter, PepT1. *Pharmacology & toxicology*, 90(6), pp.285-296.
- Chalova, V.I., Sirsat, S.A., O'Bryan, C.A., Crandall, P.G. and Ricke, S.C. (2009). *Escherichia coli*, an intestinal microorganism, as a biosensor for quantification of amino acid bioavailability. *Sensors*, 9(9), pp.7038-7057.
- Chesnel, L., Pernot, L., Lemaire, D., Champelovier, D., Croizé, J., Dideberg, O., Vernet, T. and Zapun, A. (2003). The structural modifications induced by the M339F substitution in PBP2x from *Streptococcus pneumoniae* further decreases the susceptibility to  $\beta$ -lactams of resistant strains. *Journal of Biological Chemistry*, 278(45), pp.44448-44456.
- Cochrane, S.A. and Lohans, C.T. (2020). Breaking down the cell wall: strategies for antibiotic discovery targeting bacterial transpeptidases. *European journal of medicinal chemistry*, 194, p.112262.
- Collins, B., Curtis, N., Cotter, P.D., Hill, C. and Ross, R.P. (2010). The ABC transporter AnrAB contributes to the innate resistance of *Listeria monocytogenes* to nisin, bacitracin, and various  $\beta$ -lactam antibiotics. *Antimicrobial agents and chemotherapy*, 54(10), pp.4416-4423.
- Concepción-Acevedo, J., Weiss, H.N., Chaudhry, W.N. and Levin, B.R. (2015). Malthusian parameters as estimators of the fitness of microbes: A cautionary tale about the low side of high throughput. *PloS one*, 10(6), p.e0126915.
- Cotter, J.J., O'Gara, J.P. and Casey, E. (2009). Rapid depletion of dissolved oxygen in 96-well microtiter plate *Staphylococcus epidermidis* biofilm assays promotes biofilm development

and is influenced by inoculum cell concentration. *Biotechnology and bioengineering*, 103(5), pp.1042-1047.

Daniel, H., Spanier, B., Kottra, G. and Weitz, D. (2006). From bacteria to man: archaic proton-dependent peptide transporters at work. *Physiology*, 21(2), pp.93-102.

Dantzig, A.H. (1997). Oral absorption of  $\beta$ -lactams by intestinal peptide transport proteins. *Advanced drug delivery reviews*, 23(1-3), pp.63-76.

Datsenko, K.A. and Wanner, B.L. (2000). One-step inactivation of chromosomal genes in *Escherichia coli* K-12 using PCR products. *Proceedings of the National Academy of Sciences*, 97(12), pp.6640-6645.

Demchick, P. and Koch, A.L. (1996). The permeability of the wall fabric of *Escherichia coli* and *Bacillus subtilis*. *Journal of bacteriology*, 178(3), pp.768-773.

Demain, A.L. and Elander, R.P. (1999). The  $\beta$ -lactam antibiotics: past, present, and future. *Antonie Van Leeuwenhoek*, 75(1), pp.5-19.

Detmers, F.J., Lanfermeijer, F.C. and Poolman, B. (2001). Peptides and ATP binding cassette peptide transporters. *Research in Microbiology*, 152(3-4), pp.245-258.

Doki, S., Kato, H.E., Solcan, N., Iwaki, M., Koyama, M., Hattori, M., Iwase, N., Tsukazaki, T., Sugita, Y., Kandori, H. and Newstead, S. (2013). Structural basis for dynamic mechanism of proton-coupled symport by the peptide transporter POT. *Proceedings of the National Academy of Sciences*, 110(28), pp.11343-11348.

Edwards, A.N., Nawrocki, K.L. and McBride, S.M. (2014). Conserved oligopeptide permeases modulate sporulation initiation in *Clostridium difficile*. *Infection and immunity*, 82(10), pp.4276-4291.

Elbourne, L.D., Tetu, S.G., Hassan, K.A. and Paulsen, I.T. (2017). TransportDB: a database for exploring membrane transporters in sequenced genomes from all domains of life. *Nucleic acids research*, 45(D1), pp.D320-D324.

Erni, B. (1992). Group translocation of glucose and other carbohydrates by the bacterial phosphotransferase system. *International review of cytology*, 137, pp.127-148.

Ernst, H.A., Pham, A., Hald, H., Kastrup, J.S., Rahman, M. and Mirza, O. (2009). Ligand binding analyses of the putative peptide transporter YjdL from *E. coli* display a significant selectivity towards dipeptides. *Biochemical and biophysical research communications*, 389(1), pp.112-116.

Fernández, M. and Zúñiga, M. (2006). Amino acid catabolic pathways of lactic acid bacteria. *Critical reviews in microbiology*, 32(3), pp.155-183.

Fisher, J.T., Gurney, T.O., Mason, B.M., Fisher, J.K. and Kelly, W.J. (2021). Mixing and oxygen transfer characteristics of a microplate bioreactor with surface-attached microposts.

Biotechnology Journal, 16(5), p.2000257.

Foley, D.W., Rajamanickam, J., Bailey, P.D. and Meredith, D. (2010). Bioavailability through PepT1: the role of computer modelling in intelligent drug design. *Current computer-aided drug design*, 6(1), pp.68-78.

Ganapathy, M.E., Brandsch, M., Prasad, P.D., Ganapathy, V. and Leibach, F.H. (1995). Differential Recognition of  $\beta$ -Lactam Antibiotics by Intestinal and Renal Peptide Transporters, PEPT 1 and PEPT 2 (\*). *Journal of Biological Chemistry*, 270(43), pp.2567225677.

Garai, P., Chandra, K. and Chakravorty, D. (2017). Bacterial peptide transporters: Messengers of nutrition to virulence. *Virulence*, 8(3), pp.297-309.

Garai, P., Lahiri, A., Ghosh, D., Chatterjee, J. and Chakravorty, D. (2016). Peptide-utilizing carbon starvation gene *yjiY* is required for flagella-mediated infection caused by *Salmonella*. *Microbiology*, 162(1), pp.100-116.

Gauger, E.J., Leatham, M.P., Mercado-Lubo, R., Laux, D.C., Conway, T. and Cohen, P.S. (2007). Role of motility and the *flhDC* operon in *Escherichia coli* MG1655 colonization of the mouse intestine. *Infection and immunity*, 75(7), pp.3315-3324.

Ge, Y., Lee, J.H., Hu, B. and Zhao, Y. (2018). Loss-of-function mutations in the *Dpp* and *Opp* permeases render *Erwinia amylovora* resistant to kasugamycin and blasticidin S. *Molecular Plant-Microbe Interactions*, 31(8), pp.823-832.

Geertsma, E.R. and Poolman, B. (2007). High-throughput cloning and expression in recalcitrant bacteria. *Nature methods*, 4(9), pp.705-707.

Goh, E.B., Siino, D.F. and Igo, M.M. (2004). The *Escherichia coli* *tppB* (*ydgR*) gene represents a new class of *OmpR*-regulated genes. *Journal of bacteriology*, 186(12), pp.4019-4024.

Groneberg, D.A., Fischer, A., Chung, K.F. and Daniel, H. (2004). Molecular mechanisms of pulmonary peptidomimetic drug and peptide transport. *American journal of respiratory cell and molecular biology*, 30(3), pp.251-260.

Guettou, F., Quistgaard, E.M., Raba, M., Moberg, P., Löw, C. and Nordlund, P. (2014). Selectivity mechanism of a bacterial homolog of the human drug-peptide transporters *PepT1* and *PepT2*. *Nature structural & molecular biology*, 21(8), pp.728-731.

Guo, X., Murray, M., Xiong, C. and Zhu, S., 2013. Treatment of *Escherichia coli* BW25113 with subinhibitory levels of kanamycin results in antibiotic cross-resistance and *TolC* upregulation. *J Exp Microbiol Immun*, 17, pp.19-23.

Harder, D. (2009). Characterization of the PTR peptide transporter family of *Escherichia coli* (Doctoral dissertation, Technische Universität München).

Harvey, R.A., Champe, P.C. and Fisher, B.D. (2007). *Lippincott's illustrated reviews: microbiology*. Philadelphia: Lippincott Williams & Wilkins.



Hobman, J.L., Penn, C.W. and Pallen, M.J. (2007). Laboratory strains of *Escherichia coli*: model citizens or deceitful delinquents growing old disgracefully?. *Molecular microbiology*, 64(4), pp.881-885.

Hollenstein, K., Dawson, R.J. and Locher, K.P. (2007). Structure and mechanism of ABC transporter proteins. *Current opinion in structural biology*, 17(4), pp.412-418.

Iseki, K., Iemura, A., Sato, H., Sunada, K., Miyazaki, K. and Arita, T. (1984) Intestinal absorption of several beta-lactam antibiotics. V. Effect of amino beta-lactam analogues and dipeptides on the absorption of amino beta-lactam antibiotics. *Journal of pharmacobiodynamics*, 7 (10), pp. 768–775.

Ito, K., Hikida, A., Kawai, S., Lan, V.T.T., Motoyama, T., Kitagawa, S., Yoshikawa, Y., Kato, R. and Kawarasaki, Y. (2013). Analysing the substrate multispecificity of a proton-coupled oligopeptide transporter using a dipeptide library. *Nature communications*, 4(1), pp.1-10.

Izaki, K., Matsushashi, M. and Strominger, J.L. (1966). Glycopeptide transpeptidase and Dalanine carboxypeptidase: penicillin-sensitive enzymatic reactions. *Proceedings of the National Academy of Sciences*, 55(3), pp.656-663.

Izaki, K., Matsushashi, M. and Strominger, J.L. (1968). Biosynthesis of the peptidoglycan of bacterial cell walls: XIII. Peptidoglycan transpeptidase and D-alanine carboxypeptidase: Penicillin-sensitive enzymatic reaction in strains of *Escherichia coli*. *Journal of Biological Chemistry*, 243(11), pp.3180-3192.

Jamieson, D.J. and Higgins, C.F. (1984). Anaerobic and leucine-dependent expression of a peptide transport gene in *Salmonella typhimurium*. *Journal of bacteriology*, 160(1), pp.131-136.

Jeckelmann, J.M. and Erni, B. (2019). Carbohydrate transport by group translocation: the bacterial phosphoenolpyruvate: sugar phosphotransferase system. *Bacterial cell walls and membranes*, pp.223-274.

Jiang, W., Yang, W., Zhao, X., Wang, N. and Ren, H. (2020). *Klebsiella pneumoniae* presents antimicrobial drug resistance for  $\beta$  lactam through the ESBL/PBP signaling pathway. *Experimental and therapeutic medicine*, 19(4), pp.2449-2456.

Jones, P.M. and George, A.M. (2002). Mechanism of ABC transporters: a molecular dynamics simulation of a well characterized nucleotide-binding subunit. *Proceedings of the National Academy of Sciences*, 99(20), pp.12639-12644.

Jones, S.A., Chowdhury, F.Z., Fabich, A.J., Anderson, A., Schreiner, D.M., House, A.L., Autieri, S.M., Leatham, M.P., Lins, J.J., Jorgensen, M. and Cohen, P.S. (2007). Respiration of *Escherichia coli* in the mouse intestine. *Infection and immunity*, 75(10), pp.4891-4899.

Jurtshuk, P. (1996). Bacterial metabolism. *Medical microbiology*, 4.

Karkhanis, V.A., Mascarenhas, A.P. and Martinis, S.A. (2007). Amino acid toxicities of *Escherichia coli* that are prevented by leucyl-tRNA synthetase amino acid editing. *Journal of bacteriology*, 189(23), pp.8765-8768.

Katsube, S., Ando, T. and Yoneyama, H. (2019). L-alanine exporter, AlaE, of *Escherichia coli* functions as a safety valve to enhance survival under feast conditions. *International journal of molecular sciences*, 20(19), p.4942.

Kearns, D.B. (2010). A field guide to bacterial swarming motility. *Nature Reviews Microbiology*, 8(9), pp.634-644.

Kerr, I.D. (2002). Structure and association of ATP-binding cassette transporter nucleotidebinding domains. *Biochimica et Biophysica Acta (BBA)-Biomembranes*, 1561(1), pp.47-64.

Kessel, D. and Lubin, M. (1963). On the distinction between peptidase activity and peptide transport. *Biochimica et biophysica acta*, 71, pp.656-663.

Kitchen, C.M. (2009). Nonparametric vs parametric tests of location in biomedical research. *American journal of ophthalmology*, 147(4), pp.571-572.

Klepsch, M.M., Kovermann, M., Löw, C., Balbach, J., Permentier, H.P., Fusetti, F., de Gier, J.W., Slotboom, D.J. and Berntsson, R.A. (2011). *Escherichia coli* peptide binding protein OppA has a preference for positively charged peptides. *Journal of molecular biology*, 414(1), pp.75-85.

Knütter, I., Theis, S., Hartrodt, B., Born, I., Brandsch, M., Daniel, H. and Neubert, K. (2001). A novel inhibitor of the mammalian peptide transporter PEPT1. *Biochemistry*, 40(14), pp.4454-4458.

Kong, K.F., Schneper, L. and Mathee, K. (2010). Beta-lactam antibiotics: from antibiosis to resistance and bacteriology. *Apmis*, 118(1), pp.1-36.

Lee, A.J., Wang, S., Meredith, H.R., Zhuang, B., Dai, Z. and You, L. (2018). Robust, linear correlations between growth rates and  $\beta$ -lactam-mediated lysis rates. *Proceedings of the National Academy of Sciences*, 115(16), pp.4069-4074.

Letunic, I. and Bork, P. (2021). Interactive Tree Of Life (iTOL) v5: an online tool for phylogenetic tree display and annotation. *Nucleic acids research*, 49(W1), pp.W293-W296.

Lin, Y., O'Malley, D. and Vesselinov, V.V. (2016). A computationally efficient parallel Levenberg-Marquardt algorithm for highly parameterized inverse model analyses. *Water Resources Research*, 52(9), pp.6948-6977.

Linton, K.J. and Higgins, C.F. (2007). Structure and function of ABC transporters: the ATP switch provides flexible control. *Pflügers Archiv-European Journal of Physiology*, 453(5), pp.555-567.

Lister, N., Sykes, A.P., Bailey, P.D., Boyd, C.A. and Bronk, J.R. (1995). Dipeptide transport and hydrolysis in isolated loops of rat small intestine: effects of stereospecificity. *The Journal of physiology*, 484(1), pp.173-182.

Llarrull, L.I., Testero, S.A., Fisher, J.F. and Mobashery, S. (2010). The future of the  $\beta$ -lactams. *Current opinion in microbiology*, 13(5), pp.551-557.

Locher, K.P. (2004). Structure and mechanism of ABC transporters. *Current opinion in structural biology*, 14(4), pp.426-431.

Lyons, J.A., Parker, J.L., Solcan, N., Brinth, A., Li, D., Shah, S.T., Caffrey, M. and Newstead, S. (2014). Structural basis for polyspecificity in the POT family of proton-coupled oligopeptide transporters. *EMBO reports*, 15(8), pp.886-893.

Macheboeuf, P., Contreras-Martel, C., Job, V., Dideberg, O. and Dessen, A. (2006). Penicillin binding proteins: key players in bacterial cell cycle and drug resistance processes. *FEMS microbiology reviews*, 30(5), pp.673-691.

Madigan, M.T., Martinko, J.M. and Parker, J. (2006). *Brock biology of microorganisms* (Vol. 11, p. 136). Upper Saddle River, NJ: Pearson Prentice Hall.

Madigan, MT; Bender, KS; Buckley, DH; Sattley, WM; Stahl, DA. (2017) *Brock Biology of Microorganisms*, Global Edition. 15th edition. pp. 1–2.

Mainardi, J.L., Villet, R., Bugg, T.D., Mayer, C. and Arthur, M. (2008). Evolution of peptidoglycan biosynthesis under the selective pressure of antibiotics in Gram-positive bacteria. *FEMS microbiology reviews*, 32(2), pp.386-408.

Mao, B., Pear, M.R., McCammon, J.A. and Quioco, F.A., (1982). Hinge-bending in Larabinose-binding protein. The "Venus's-flytrap" model. *Journal of Biological Chemistry*, 257(3), pp.1131-1133.

McNab, R. and Jenkinson, H.F. (1998). Altered adherence properties of a *Streptococcus gordonii* hppA (oligopeptide permease) mutant result from transcriptional effects on cshA adhesin gene expression. *Microbiology*, 144(1), pp.127-136.

Meredith, D. and Boyd, C.A.R. (1995). Oligopeptide transport by epithelial cells. *The Journal of membrane biology*, 145(1), pp.1-12.

Meredith, D., Temple, C.S., Guha, N., Sword, C.J., Boyd, C.R., Collier, I.D., Morgan, K.M. and Bailey, P.D., (2000). Modified amino acids and peptides as substrates for the intestinal peptide transporter PepT1. *European Journal of Biochemistry*, 267(12), pp.3723-3728.

Miller, C.G. (1975). Peptidases and proteases of *Escherichia coli* and *Salmonella typhimurium*. *Annual review of microbiology*, 29(1), pp.485-504.

Minsky, A., Summers, R.G. and Knowles, J.R. (1986). Secretion of beta-lactamase into the periplasm of *Escherichia coli*: evidence for a distinct release step associated with a

conformational change. *Proceedings of the National Academy of Sciences*, 83(12), pp.4180-4184.

Miyoshi, S.I. (2013). Extracellular proteolytic enzymes produced by human pathogenic *Vibrio* species. *Frontiers in microbiology*, 4, p.339.

Montville, T.J. and Bruno, M.E.C., (1994). Evidence that dissipation of proton motive force is a common mechanism of action for bacteriocins and other antimicrobial proteins. *International journal of food microbiology*, 24(1-2), pp.53-74.

Moraes, P.M., Seyffert, N., Silva, W.M., Castro, T.L., Silva, R.F., Lima, D.D., Hirata, R., Silva, A., Miyoshi, A. and Azevedo, V. (2014). Characterization of the Opp peptide transporter of *Corynebacterium pseudotuberculosis* and its role in virulence and pathogenicity. *BioMed research international*, 2014.

Moussatova, A., Kandt, C., O'Mara, M.L. and Tieleman, D.P., (2008). ATP-binding cassette transporters in *Escherichia coli*. *Biochimica et Biophysica Acta (BBA)-Biomembranes*, 1778(9), pp.1757-1771.

Newstead, S. (2011). Towards a structural understanding of drug and peptide transport within the proton-dependent oligopeptide transporter (POT) family. *Biochemical Society Transactions*, 39(5), pp.1353-1358.

Newstead, S. 2017(b) Symmetry and Structure in the POT Family of Proton Coupled Peptide Transporters. *Symmetry*, 9 (6), p. 85.

Newstead, S., 2017(a). Recent advances in understanding proton coupled peptide transport via the POT family. *Current opinion in structural biology*, 45, pp.17-24.

Newstead, S., Drew, D., Cameron, A.D., Postis, V.L., Xia, X., Fowler, P.W., Ingram, J.C., Carpenter, E.P., Sansom, M.S., McPherson, M.J. and Baldwin, S.A. (2011). Crystal structure of a prokaryotic homologue of the mammalian oligopeptide-proton symporters, PepT1 and PepT2. *The EMBO journal*, 30(2), pp.417-426.

Nguyen, T.T., Myrold, D.D. and Mueller, R.S. (2019). Distributions of extracellular peptidases across prokaryotic genomes reflect phylogeny and habitat. *Frontiers in microbiology*, 10, p.413.

Nishimura, T., Tanaka, N. and Umezawa, H. (1965) Inhibition of Protein Synthesis by Kanamycin. *The Journal of Antibiotics, Ser. A*, 15 (5).

Okano, T., Inui, K.L., Maegawa, H., Takano, M. and Hori, R. (1986). H<sup>+</sup> coupled uphill transport of aminocephalosporins via the dipeptide transport system in rabbit intestinal brush-border membranes. *Journal of Biological Chemistry*, 261(30), pp.14130-14134.

Oldham, M.L. and Chen, J. (2011). Snapshots of the maltose transporter during ATP hydrolysis. *Proceedings of the National Academy of Sciences*, 108(37), pp.15152-15156.

Pao, S.S., Paulsen, I.T. and Saier Jr, M.H. (1998). Major facilitator superfamily. *Microbiology and molecular biology reviews*, 62(1), pp.1-34.

Parker, D.J., Demetci, P. and Li, G.W. (2019). Rapid accumulation of motility-activating mutations in resting liquid culture of *Escherichia coli*. *Journal of bacteriology*, 201(19), pp.e00259-19.

Pernot, L., Chesnel, L., Le Gouellec, A., Croizé, J., Vernet, T., Dideberg, O. and Dessen, A. (2004). A PBP2x from a clinical isolate of *Streptococcus pneumoniae* exhibits an alternative mechanism for reduction of susceptibility to  $\beta$ -lactam antibiotics. *Journal of Biological Chemistry*, 279(16), pp.16463-16470.

Piperno, J.R. and Oxender, D.L. (1968). Amino acid transport systems in *Escherichia coli* K12. *Journal of Biological Chemistry*, 243(22), pp.5914-5920.

Poole, K. (2005). Efflux-mediated antimicrobial resistance. *Journal of Antimicrobial Chemotherapy*, 56(1), pp.20-51.

Prabhala, B.K., Aduri, N.G., Iqbal, M., Rahman, M., Gajhede, M., Hansen, P.R. and Mirza, O. (2017). Several hPepT1-transported drugs are substrates of the *Escherichia coli* proton-coupled oligopeptide transporter YdgR. *Research in microbiology*, 168(5), pp.443-449.

Prabhala, B.K., Aduri, N.G., Sharma, N., Shaheen, A., Sharma, A., Iqbal, M., Hansen, P.R., Brasen, C., Gajhede, M., Rahman, M. and Mirza, O. (2018). The prototypical proton-coupled oligopeptide transporter YdgR from *Escherichia coli* facilitates chloramphenicol uptake into bacterial cells. *Journal of Biological Chemistry*, 293(3), pp.1007-1017.

Reisch, C.R. and Prather, K.L. (2015). The no-SCAR (Scarless Cas9 Assisted Recombineering) system for genome editing in *Escherichia coli*. *Scientific reports*, 5(1), pp.1-12.

Rismondo, J. and Schulz, L.M. (2021). Not just Transporters: alternative functions of ABC transporters in *Bacillus subtilis* and *Listeria monocytogenes*. *Microorganisms*, 9(1), p.163.

Rubio-Aliaga, I. and Daniel, H. (2002). Mammalian peptide transporters as targets for drug delivery. *Trends in pharmacological sciences*, 23(9), pp.434-440.

Sato, A.K., Viswanathan, M., Kent, R.B. and Wood, C.R. (2006). Therapeutic peptides: technological advances driving peptides into development. *Current opinion in biotechnology*, 17(6), pp.638-642.

Sauvage, E. and Terrak, M. (2016). Glycosyltransferases and transpeptidases/penicillin-binding proteins: valuable targets for new antibacterials. *Antibiotics*, 5(1), p.12.

Sauvage, E., Kerff, F., Terrak, M., Ayala, J.A. and Charlier, P. (2008). The penicillin-binding proteins: structure and role in peptidoglycan biosynthesis. *FEMS microbiology reviews*, 32(2), pp.234-258.

- Sezonov, G., Joseleau-Petit, D. and d'Ari, R. (2007). *Escherichia coli* physiology in Luria-Bertani broth. *Journal of bacteriology*, 189(23), pp.8746-8749.
- Shapiro, S.S. and Wilk, M.B. (1965). An analysis of variance test for normality (complete samples). *Biometrika*, 52(3/4), pp.591-611.
- Sharpe, A., Blumberg, P.M. and Strominger, J.L. (1974). D-Alanine carboxypeptidase and cell wall cross-linking in *Bacillus subtilis*. *Journal of Bacteriology*, 117(2), pp.926-927.
- Sheehan, J.C. and Logan, K.R.H. (1959). A general synthesis of the penicillins. *Journal of the American Chemical Society*, 81(21), pp.5838-5839.
- Shiver, A.L., Osadnik, H., Kritikos, G., Li, B., Krogan, N., Typas, A. and Gross, C.A. (2016). A chemical-genomic screen of neglected antibiotics reveals illicit transport of kasugamycin and blasticidin S. *PLoS genetics*, 12(6), p.e1006124.
- Sleigh, S.H., Tame, J.R., Dodson, E.J. and Wilkinson, A.J., (1997). Peptide binding in OppA, the crystal structures of the periplasmic oligopeptide binding protein in the unliganded form and in complex with lysyllysine. *Biochemistry*, 36(32), pp.9747-9758.
- Solcan, N., Kwok, J., Fowler, P.W., Cameron, A.D., Drew, D., Iwata, S. and Newstead, S., (2012). Alternating access mechanism in the POT family of oligopeptide transporters. *The EMBO journal*, 31(16), pp.3411-3421.
- Song, X., Lorenzi, P.L., Landowski, C.P., Vig, B.S., Hilfinger, J.M. and Amidon, G.L. (2005). Amino acid ester prodrugs of the anticancer agent gemcitabine: synthesis, bioconversion, metabolic bioevasion, and hPEPT1-mediated transport. *Molecular pharmaceutics*, 2(2), pp.157-167.
- Sprouffske, K. and Wagner, A. (2016). Growthcurver: an R package for obtaining interpretable metrics from microbial growth curves. *BMC bioinformatics*, 17(1), pp.1-4.
- Stauffer, M., Jeckelmann, J.M., Ilgü, H., Ucurum, Z., Boggavarapu, R. and Fotiadis, D. (2022). Peptide transporter structure reveals binding and action mechanism of a potent PEPT1 and PEPT2 inhibitor. *Communications Chemistry*, 5(1), pp.1-10.
- Stauffer, M., Ucurum, Z., Harder, D. and Fotiadis, D. (2021). Engineering and functional characterization of a proton-driven  $\beta$ -lactam antibiotic translocation module for bionanotechnological applications. *Scientific reports*, 11(1), pp.1-10.
- Steiner, H.Y., (1995). Naider F, Becker JM. The PTR family: a new group of peptide transporters. *Mol Microbiol*, 16, pp.825-834.
- Sturme, M.H., Kleerebezem, M., Nakayama, J., Akkermans, A.D., Vaughan, E.E. and De Vos, W.M., (2002). Cell to cell communication by autoinducing peptides in gram-positive bacteria. *Antonie Van Leeuwenhoek*, 81(1), pp.233-243.

Swings, T., Marciano, D.C., Atri, B., Bosserman, R.E., Wang, C., Leysen, M., Bonte, C., Schalck, T., Furey, I., Van den Bergh, B. and Verstraeten, N. (2018). CRISPR-FRT targets shared sites in a knock-out collection for off-the-shelf genome editing. *Nature communications*, 9(1), pp.110.

Takeuchi, S. (1958). Hirayama, K; Ueda, K.; Sakai, H.; Yonehara, H. Blastocidin S. A new antibiotic. *J. Antibiot*, 11, pp.1-5.

Tam, R.O.L.A.N.D. and Saier Jr, M.H., (1993). Structural, functional, and evolutionary relationships among extracellular solute-binding receptors of bacteria. *Microbiological reviews*, 57(2), pp.320-346.

Tame, J.R., Dodson, E.J., Murshudov, G., Higgins, C.F. and Wilkinson, A.J., (1995). The crystal structures of the oligopeptide-binding protein OppA complexed with tripeptide and tetrapeptide ligands. *Structure*, 3(12), pp.1395-1406.

Tavori, H., Kimmel, Y. and Barak, Z. (1981). Toxicity of leucine-containing peptides in *Escherichia coli* caused by circumvention of leucine transport regulation. *Journal of Bacteriology*, 146(2), pp.676-683.

Tavori, H., Kimmel, Y. and Barak, Z. (1981). Toxicity of leucine-containing peptides in *Escherichia coli* caused by circumvention of leucine transport regulation. *Journal of Bacteriology*, 146(2), pp.676-683.

Tenor, J.L., McCormick, B.A., Ausubel, F.M. and Aballay, A. (2004). *Caenorhabditis elegans* based screen identifies *Salmonella* virulence factors required for conserved host-pathogen interactions. *Current Biology*, 14(11), pp.1018-1024.

Thoendel, M. and Horswill, A.R., (2010). Biosynthesis of peptide signals in gram-positive bacteria. *Advances in applied microbiology*, 71, pp.91-112.

Thomas, G.H. (2010). Homes for the orphans: utilization of multiple substrate-binding proteins by ABC transporters. *Molecular microbiology*, 75(1), pp.6-9.

Tooke, C.L., Hinchliffe, P., Bragginton, E.C., Colenso, C.K., Hirvonen, V.H., Takebayashi, Y. and Spencer, J. (2019).  $\beta$ -Lactamases and  $\beta$ -Lactamase Inhibitors in the 21st Century. *Journal of molecular biology*, 431(18), pp.3472-3500.

Trifinopoulos, J., Nguyen, L.T., von Haeseler, A. and Minh, B.Q. (2016). W-IQ-TREE: a fast online phylogenetic tool for maximum likelihood analysis. *Nucleic acids research*, 44(W1), pp.W232-W235.

Tsuji, A., Tamai, I., Hirooka, H. and Terasaki, T. (1987).  $\beta$ -Lactam antibiotics and transport via the dipeptide carrier system across the intestinal brush-border membrane. *Biochemical pharmacology*, 36(4), pp.565-567.

Tuite, N.L., Fraser, K.R. and O'byrne, C.P. (2005). Homocysteine toxicity in *Escherichia coli* is

caused by a perturbation of branched-chain amino acid biosynthesis. *Journal of bacteriology*, 187(13), pp.4362-4371.

Tuomanen, E., Cozens, R., Tosch, W., Zak, O. and Tomasz, A. (1986). The rate of killing of *Escherichia coli* by  $\beta$ -lactam antibiotics is strictly proportional to the rate of bacterial growth. *Microbiology*, 132(5), pp.1297-1304.

Typas, A., Banzhaf, M., Gross, C.A. and Vollmer, W. (2012). From the regulation of peptidoglycan synthesis to bacterial growth and morphology. *Nature Reviews Microbiology*, 10(2), pp.123-136.

Umezawa, H., Hamada, M., Suhara, Y., Hashimoto, T. and Ikekawa, T. (1965). Kasugamycin, a new antibiotic. *Antimicrobial agents and chemotherapy*, 5, pp.753-757.

Umezawa, H., Hamada, M., Suhara, Y., Hashimoto, T. and Ikekawa, T. (1965). Kasugamycin, a new antibiotic. *Antimicrobial agents and chemotherapy*, 5, pp.753-757.

Ural-Blimke, Y., Flayhan, A., Strauss, J., Rantos, V., Bartels, K., Nielsen, R., Pardon, E., Steyaert, J., Kosinski, J., Quistgaard, E.M. and Löw, C. (2019). Structure of prototypic peptide transporter DtpA from *E. coli* in complex with valganciclovir provides insights into drug binding of human PepT1. *Journal of the American Chemical Society*, 141(6), pp.2404-2412.

van Heijenoort, J. (2010). Biosynthesis of bacterial peptidoglycan. In *Microbial Glycobiology* (pp. 285-304). Academic Press.

Verbeke, F., De Craemer, S., Debunne, N., Janssens, Y., Wynendaele, E., Van de Wiele, C. and De Spiegeleer, B. (2017). Peptides as quorum sensing molecules: measurement techniques and obtained levels in vitro and in vivo. *Frontiers in neuroscience*, 11, p.183.

Waterhouse, A.M., Procter, J.B., Martin, D.M., Clamp, M. and Barton, G.J. (2009). Jalview Version 2—a multiple sequence alignment editor and analysis workbench. *Bioinformatics*, 25(9), pp.1189-1191.

Weitz, D., Harder, D., Casagrande, F., Fotiadis, D., Obrdlik, P., Kelety, B. and Daniel, H. (2007). Functional and structural characterization of a prokaryotic peptide transporter with features similar to mammalian PEPT1. *Journal of biological chemistry*, 282(5), pp.2832-2839.

Weldhagen, G.F. (2004). Integrons and  $\beta$ -lactamases—a novel perspective on resistance. *International journal of antimicrobial agents*, 23(6), pp.556-562.

Wilkens, S. (2015). Structure and mechanism of ABC transporters. *F1000prime reports*, 7.

Zhao, Y., Mao, G., Liu, M., Zhang, L., Wang, X. and Zhang, X.C. (2014). Crystal structure of the *E. coli* peptide transporter YbgH. *Structure*, 22(8), pp.1152-1160.